

Master Thesis

# Influence of Remote Fluorine-Metal Interactions on Dynamics of Diene Complexes and $\eta^6$ -Arene Tungsten(0) Complexes

carried out in the research group of Prof. Dr. Antonio Togni

by **Lukas Pascal Sigrist**

under the supervision of Barbara Czarniecki

**ETH**

Eidgenössische Technische Hochschule Zürich  
Swiss Federal Institute of Technology Zurich

*Ich habe keine besondere Begabung, sondern bin nur leidenschaftlich neugierig.* - Albert Einstein

In memoriam Stefan Walther († 25.01.2011), der seine Begeisterung für die Chemie auf mich übertragen konnte und damit maßgeblich dafür mitverantwortlich ist, dass ich den Weg in dieses spannende Wissenschaftsfeld gefunden habe.

## Acknowledgements

Amongst many others, I wish to thank...

- ... *Prof. Dr. Antonio Togni* for giving me the opportunity to carry out another project in his research group. Also, I am grateful for all the suggestions and advice on tungsten chemistry.
- ... *Barbara Czarniecki* for the project idea which suited my expectations perfectly. I was joining her to achieve in-depth-knowledge on NMR and even though I ended this project knowing more about what I do not know, I still feel like I could enhance my knowlegde a lot thanks to her great experience and ability to explain. Also, I want to thank her for all the nice scientific and non-scientific conversations we had, sometimes sitting in the NMR-room until late in the evening.
- ... *Raphael Aardoom* for introducing me to the group in my first semester project and now being my "backup"-assistant in the lab. He did not only support me from chemical view but I also enjoyed less productive moments with him. And, of course, I want to thank him very much for measuring the crystals and all - successful as well as failed - refinement attempts.
- ... *Raphaël Rochat* for his assistance and support whenever needed and for sharing his profound knowledge on phosphine chemistry. And of course for not losing his humor at any time.
- ... *PD Dr. Hans-Peter Lüthi* for his outstanding support and effort on doing the quantum chemical calculations for me which helped me a lot in the course of this thesis.
- ... *Dr. René Verel* for his assistance in measuring NMR spectra, whenever Barbara was not around or when we both seemed unable. Also, I thank him for his efforts concerning the simulation program.
- ... *Dominikus Heift* and *Georgina Müller* for showing me how to and letting me use the UV lamps and advising me concerning photochemistry.
- ... The trifluoromethyl-phosphine specialists *Jonas Bürgler* and *Rino Schwenk* for all the useful information and advice they gave me concerning this topic and for supply with the respective chemicals.
- ... The other *members of the Togni-group*: For sharing their synthetic knowledge (*Nico Santschi, Esteban Mejía*), supply with chemicals (*Nico Santschi, Amata Schira, Martino Rimoldi*), all the evening-beer- and chicken-loving members for the nice chats and everyone else for the pleasant time I had in this group.
- ... *Johannes Windisch* also for his support concerning trifluoromethylated phosphines, supply with reagents, and also for being a good friend and cohabitant throughout the past years. Thanks also to my other cohabitants for patiently listening to my lamentations.
- ... *Meinen Eltern und meiner Schwester* für all ihre Unterstützung und das Verständnis, das sie mir in all den Jahren entgegen gebracht haben. Es ist schön zu wissen, dass sie hinter mir stehen, obwohl sie keinen grossen Zugang zu meiner Arbeit haben.

## Abstract

In a series of variable temperature NMR experiments the influence of the metal-fluorine-interaction on the dynamics of several diene complexes was studied. Doing so, it was found that rhodium(cyclooctadiene)diphenyl(5-fluoronaphtalen-1-yl)phosphine chloride and rhodium(cyclooctadiene)diphenyl(5,6,7,8-tetrafluoronaphtalen-1-yl)phosphine chloride show three different conformers which were identified by NMR experiments and their respective structures were derived from the crystal structures combined with DFT calculations. From the DFT calculations also relative energy differences between the complexes could be derived which support the assumptions made for the structures of the conformers. Furthermore, the similar complexes Chloro(1,5-cyclooctadiene)(diisopropyl(8-fluoronaphtalen-1-yl)phosphine)rhodium(I), Chloro(1,5-cyclooctadiene)(diisopropyl(5,6,7,8-tetrafluoronaphtalen-1-yl)phosphine) rhodium(I) and Chloro(norbornadiene)(diphenyl(8-fluoronaphtalen-1-yl)phosphine)rhodium(I) have been prepared to obtain more information on the mechanisms of the exchange. The metal center was changed to iridium to study its influence, which was observed to be only marginal. Contrary, the temperature series on the nonfluorinated analogon of the studied complexes showed that the fluorine substituent has a crucial influence on the exchange. From these informations, a pseudopentacoordinate intermediate for the exchange of the diene has been proposed and the kinetic and thermodynamical properties of the exchange for three complexes have been derived by simulation of the phosphorus low temperature spectra.

Furthermore, the more electron withdrawing bis(trifluoromethyl)8-Fluoronaphtalen-1-ylphosphine and bis(trifluoromethyl)8-Fluoronaphtalen-1-ylphosphine were prepared but could be shown not to coordinate to the rhodium precursor. The latter ligand however was found to coordinate to the analogous iridium precursor.

In the second part, 1-fluoro-2-mesitylethane was prepared and further reacted to form the complex 2-Fluoroethyl-mesitylenetungsten(0)tricarbonyl. In a series of UV irradiation experiments it could be shown that the complex reacts, but dissociates to a black tungsten(0) species and the free ligand is regained. The ligand however dissociates with longer periods of irradiation. The complex was furthermore used for attempts of doing  $^{183}\text{W}$ ,  $^1\text{H}$ -correlation NMR experiments. To our knowledge, the first  $^{183}\text{W}$  chemical shift for  $\eta^6$ -arene tungsten(0) complexes was found to be -2695 ( $\text{CDCl}_3$ ).

# Table of Contents

<b>1</b>	<b>Introduction.....</b>	<b>1</b>
1.1	CF...Metal Interactions.....	1
1.1.1	Overview.....	1
1.1.2	Tetrafluoronaphthalenyl phosphine Containing Complexes.....	3
1.2	Dynamics of Dienes.....	3
1.2.1	Overview.....	3
1.2.2	Detection and Quantification of Exchange.....	3
1.3	Tungsten Chemistry.....	5
1.3.1	Overview.....	5
1.3.2	Tungsten Compounds from Tungsten(0) hexacarbonyl.....	5
1.3.2	<sup>183</sup> W – NMR Experiments.....	6
<b>2</b>	<b>Project Idea and Synthetic Approach.....</b>	<b>7</b>
2.1	The Influence of the Remote Fluorine-Metal Bond on Diene Dynamics.....	7
2.2	$\eta^6$ -Arene Tungsten(0) Complexes for <sup>183</sup> W, <sup>1</sup> H-Correlation NMR Experiments.....	8
<b>3</b>	<b>Results and Discussion.....</b>	<b>9</b>
3.1	Phosphines.....	9
3.1.1	Synthesis.....	9
3.1.2	Comparison of the Phosphines.....	11
3.2	Complexes.....	12
3.2.1	Synthesis.....	12
3.2.2	Structures of the Conformers by NMR.....	14
3.2.3	Structures of the Conformers from NMR Combined with X-ray Crystallography.....	17
3.2.4	Supporting Information from DFT Calculations.....	20
3.2.5	Conclusions for the Exchange Mechanism.....	20
3.2.6	Thermodynamical and Kinetic Properties for the Chemical Exchange.....	21
3.3	$\eta^6$ -Arene Tungsten(0) Complexes.....	23
3.3.1	Synthesis of the Ligand & Complex.....	23
3.3.2	Irradiation of the complex.....	24
3.3.3	<sup>183</sup> W-NMR Experiments.....	25
<b>4</b>	<b>Conclusion and Outlook.....</b>	<b>26</b>
4.1	Phosphines.....	26
4.2	Structures of the Rh-Complex Conformers.....	27

4.3	Tungsten complexes and NMR studies .....	27
<b>5</b>	<b>Experimental</b> .....	<b>29</b>
5.1	General Remarks.....	29
5.1.1	Chemicals .....	29
5.1.2	Techniques .....	29
5.1.3	Analytical techniques and instruments .....	29
5.2	Chloro diisopropylphosphine.....	31
5.2.1	Synthesis.....	31
5.2.2	Characterization.....	31
5.3	Chloro bis(pentafluorophenyl)phosphine .....	31
5.3.1	Synthesis.....	31
5.3.2	Characterization.....	32
5.4	Diisopropyl(5,6,7,8-tetrafluoronaphtalen-1-yl)phosphine (3).....	32
5.4.1	Synthesis.....	32
5.4.2	Characterization.....	32
5.5	Diisopropyl(5,6,7,8-tetrafluoronaphtalen-1-yl)phosphine (4).....	33
5.5.1	Synthesis.....	33
5.5.2	Characterization.....	33
5.6	(8-Fluoronaphtalen-1-yl)phosphine (5) .....	34
5.6.1	Synthesis.....	34
5.6.2	Characterization.....	34
5.7	Bis(trifluoromethyl)-(8-Fluoronaphtalen-1-yl)phosphine (6).....	34
5.7.1	Synthesis.....	34
5.7.1	Characterization.....	35
5.8	Bis(pentafluorophenyl)-(8-Fluoronaphtalen-1-yl)phosphine (7) .....	35
5.8.1	Synthesis.....	35
5.8.2	Characterization.....	35
5.9	Rh-Complexes: General Procedure.....	36
5.9.1	Synthesis.....	36
5.9.2	VT NMR Analysis.....	36
5.10	Chloro(1,5-cyclooctadiene)(diphenyl(8-fluoronaphtalen-1-yl)phosphine)rhodium(I) (Rh-1) .....	36
5.10.1	VT-NMR Analysis (203 K).....	36
5.11	Chloro(1,5-cyclooctadiene)(diphenyl(5,6,7,8-tetrafluoronaphtalen-1-yl)phosphine)rhodium(I) (Rh-2).....	37

5.11.1	VT-NMR Analysis (193 K).....	37
5.12	Chloro(norbornadiene)(diphenyl(8-fluoronaphtalen-1-yl)phosphine)rhodium(I) (nbd-Rh-1) ....	38
5.12.1	Room Temperature Characterization .....	39
5.12.2	VT-NMR Analysis (213 K).....	39
5.13	Chloro(1,5-cyclooctadiene)(diisopropyl(8-fluoronaphtalen-1-yl)phosphine)rhodium(I) (Rh-3)..	40
5.13.1	VT-NMR Analysis (193 K).....	40
5.14	Chloro(1,5-cyclooctadiene)(diisopropyl(5,6,7,8-tetrafluoronaphtalen-1-yl)phosphine)rhodium(I) (Rh-4) .....	41
5.14.1	VT-NMR Analysis (193 K).....	41
5.15	Chlor(1,5-cyclooctadiene)(diphenyl(8-tetrafluoronaphtalen-1-yl)phosphine)iridium(I) (Ir-1) ....	42
5.15.1	VT NMR Analysis (193 K).....	42
5.16	1-Fluoro-2-mesitylethane (A) .....	43
5.16.1	Synthesis.....	43
5.16.2	Characterization.....	43
5.17	1-(2-Fluoroethyl)mesitylene tungsten(0)tricarbonyl (B) .....	43
5.17.1	Synthesis.....	43
5.17.2	Characterization.....	44
<b>6</b>	<b>Literature</b> .....	<b>45</b>
<b>7</b>	<b>Appendix</b> .....	<b>48</b>
7.1	Abbreviations.....	48
7.2	NMR Spectra .....	50
7.2.1	Rh-1 .....	50
7.2.2	Rh-2 .....	54
7.2.3	nbd-Rh-1 .....	57
7.2.4	Rh-3 .....	60
7.2.5	Rh-4 .....	63
7.2.6	Rh-8 .....	66
7.2.7	Ir-1 .....	68
7.3	Crystallographic Data .....	71
7.3.1	Chloro(1,5-cyclooctadiene)(diphenyl(8-fluoronaphtalen-1-yl)phosphine)rhodium(I) (Rh-1)	71
7.3.2	Chloro(1,5-cyclooctadiene)(diphenyl(5,6,7,8-tetrafluoronaphtalen-1-yl)phosphine)rhodium(I) (Rh-2) .....	73
7.3.3	Chloro(norbornadiene)(diphenyl(8-fluoronaphtalen-1-yl)phosphine)rhodium(I) (nbd-Rh-1).....	75



7.3.4	Chloro(cyclooctadiene)(diisopropyl(5,6,7,8-tetrafluoronaphtalen-1-yl)phosphine)rhodium(I) (Rh-4) .....	77
7.4	Data for the Simulation .....	<b>79</b>
7.4.1	Program Code.....	79
7.4.2	Example Input File .....	80
7.4.3	Results for Rh-1 .....	81
7.4.4	Results for Rh-2 .....	82
7.4.5	Results for Ir-1 .....	82

# 1 Introduction

## 1.1 CF...Metal Interactions

### 1.1.1 Overview

Classically the interactions between the fluorine atom and a metal center are of ionic type, examples are  $\text{MoF}_6$  or  $\text{CaF}_2$ , where the fluorine acts as an anion for the cationic metal. In this case, the fluorine is called fluoride to account for the anionic character. However, also interactions between (uncharged) fluorine and metals are well-known, for example as an interaction of the counterions  $\text{BF}_4^-$  or  $\text{CF}_3\text{SO}_4^-$ , whereas the interaction between the metal and the fluorine is normally very weak due to the bad coordination properties of those counterions. There are reports though where the interaction has a big influence on catalytic properties.<sup>[1]</sup>

The interaction which is discussed here is the one between fluorine covalently bound to carbon and metal, further referred to as CF...M interaction. The observation of such interactions has long time been restricted to the use of X-ray crystallography. Whereas the group of *Glusker* were the first to predict a rather strong interaction based on X-ray structures<sup>[2]</sup>, *Plenio* and coworkers were able to describe the CF...M interaction in solution using NMR techniques<sup>[3]</sup>. *Plenio* used  $^1J_{\text{CF}}$  – values to make a statement about the strength of the CF...M interaction: The smaller the coupling constant, the stronger the interaction, as *vice versa* a large  $^1J_{\text{CF}}$  in the ligand in comparison to the one in the complex represents a weak C-F bond.

In a review one year later, *Plenio* has set some basic rules to determine the properties needed for a CF...M interaction<sup>[4]</sup>:

- 1) For intramolecular metal-fluorine interactions to be accepted as such, there must be a minimum of four bonds separating the two atoms. This eliminates metal complexes of fluorinated ligands such as  $\eta^1\text{-C}_6\text{F}_5$ ,  $\eta^6\text{-C}_6\text{F}_6$ ,  $\text{-CF}_3$ ,  $=\text{CF}_2$ ,  $\text{F}_2\text{C}=\text{CF}_2$  and related fluorocarbons as well as carbenoids. Although the presence of fluorine in these complexes can be stabilizing, it should be considered that such contacts are the unavoidable result of the existence of such metal complexes.
- 2) The comparison of the sum van der Waals radii of the fluorine atom and the metal with the distance between those two showed that this criterion would be too loose. Therefore the sum of ionic van der Waals radii was chosen to act as threshold for the interaction of fluorine and the alkali- and alkaline earth metals.

For first row transition metals, a reasonable (although arbitrary) overall threshold of  $\leq 2.7 \text{ \AA}$  was set, which is always shorter than the combined van der Waals radii. Applying the same principle for second and third row transition metals gives a threshold of  $\leq 3.0 \text{ \AA}$ . Even though arbitrary, this threshold has been chosen as the other thresholds given in the literature are rather contradictory and are therefore no better option.

To induce a CF...M interaction, it can be helpful to account for some motifs<sup>[4]</sup>:

- 1) A strongly binding ligand with a fluorine atom attached to it, which is forced close to the metal center due to its conformation.
- 2) A highly fluorinated ligand that lacks good donor atoms paired with an electron deficient metal center. This will force the metal to undergo a CF...M interaction.
- 3) Introducing a fluorine atom as a part of a strong, chelating ligand. Again, the conformational properties of the ligand can help reinforcing the CF...M interaction.

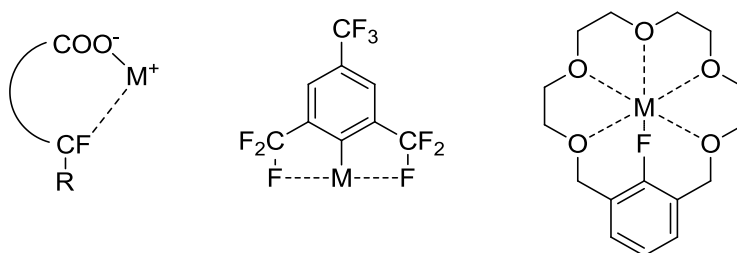


Figure 1. Representation of the three motifs for CF...M interactions.

Unsurprisingly the scope of possible metal centers for CF...M interactions involves mainly group I and II metals. Considering the hard-soft-acid-base (HSAB) concept,<sup>[5]</sup> these hard atoms fit best to the highly electron-dense and small fluorine atoms.

CF...M interactions with transition metals have been investigated only marginally and mostly concentrated on zirconium. Zirconium has been studied extensively in turns of the investigations concerning Ziegler-Natta polymerization. It was found that tetrakis(pentafluoro)borate stabilizes the zirconocene cation. The stabilizing effect was discovered by *Horton* and *Orpen* using <sup>19</sup>F-NMR. When they observed two signals in a 3:1 ratio where one was shifted by more than 50 ppm to high field, they suggested that there is a stabilizing effect due to a CF...M interaction.<sup>[6]</sup> This was later confirmed by studies from other groups based also on X-ray analysis<sup>[7]</sup>. A related structure with a very short fluorine – zirconium distance of 2.267(5) Å was presented by *Piers* and his coworkers (figure 2)<sup>[8]</sup>.

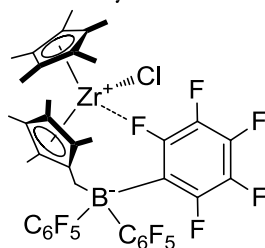


Figure 2. Zirconocene complex with a very short Zr-F distance of 2.267(10) Å.

Other investigations concerning CF...M interaction were carried out with silver, where mostly platinum-silver clusters with a perfluorinated phenyl group were investigated. This work was done predominantly by the group of *Usón* and *Forniés*<sup>[9]</sup>. Also, ruthenium have been studied by different groups in the past, most interesting in this context might be the work of the group of *Grubbs* which involves the influence of a 2,6-fluorophenyl substituent on the Grubbs II catalyst<sup>[10]</sup>. Even though the CF...Ru distance they found is 3.2311(10) Å and thus exceeds the 3 Å-threshold stated by *Plenio*, there must be an interaction of the fluorine with the metal that improves the catalyst, as the nonfluorinated analogue works slower. This is not the case for another ruthenium based complex from *Cruz-Garriz*, where the distance is 2.489(6) Å<sup>[11]</sup>, which is rather short. Further on, there are complexes using iridium<sup>[12]</sup> and platinum<sup>[13]</sup> as central metals.

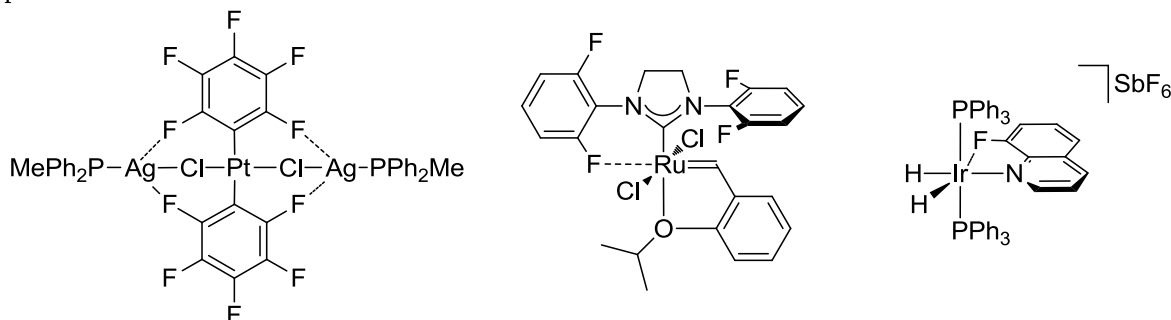


Figure 3. Examples of complexes for CF...M interactions with different central metals.

### 1.1.2 Tetrafluoronaphthalenyl phosphine Containing Complexes

In 2010, *Stanek et al.* presented 5,6,7,8-tetrafluoronaphthalene based ligands which show an unusually strong, lone-pair mediated through-space coupling between fluorine and phosphorus.<sup>[14]</sup>

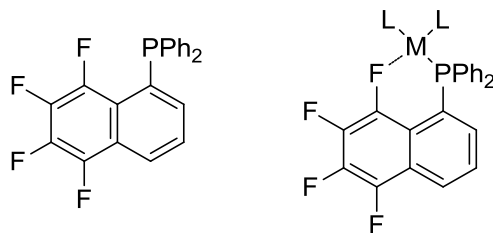


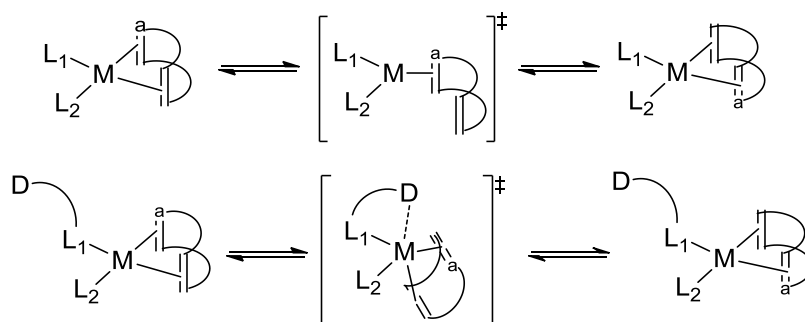
Figure 4. One of the ligands and the interaction investigated by *Stanek et al.*

By attaching the ligand to different central metals, namely Ir<sup>I</sup>, Ir<sup>III</sup>, Rh<sup>I</sup>, Pt<sup>II</sup>, Pd<sup>II</sup> and Au<sup>I</sup>, it could be shown that all the metal centers show CF...M interactions. For this, the crystal structures of the complexes were analyzed for the length of fluorine-metal interaction. Although the CF...M interactions were only visible through direct coupling with Pt<sup>II</sup> in the <sup>19</sup>F-NMR spectra, the existence could also be proven for the other spin ½ nucleus, rhodium, by <sup>103</sup>Rh,<sup>19</sup>F-correlation experiments.

## 1.2 Dynamics of Dienes

### 1.2.1 Overview

In several cases, fluxional behavior of dienes, typically norbornadiene<sup>[15]</sup> or cyclooctadiene<sup>[16]</sup>, has been observed on the NMR time scale. It can be observed as broad signals at room temperature, which can be resolved by cooling the sample to low temperature and thus “freezing out” the dynamics. The mechanism of the rotation of the diene has been proposed to proceed intramolecular over a pseudo-pentacoordinated species<sup>[17]</sup>, as well as an intermediary three-coordinated compound<sup>[18]</sup>. Another proposed mechanism is the change of complex geometry from square planar to tetrahedral.<sup>[19]</sup> The mechanism of the fluxional behavior is still not clear and investigations are ongoing. It is a common proposition that donor substituents on ligands play an important role as intermediary coordinating ligands, replacing either one olefin or leading to the pseudo-pentacoordinated species mentioned.<sup>[20]</sup>



Scheme 1. Examples for the three-coordinate and the pseudo-pentacoordinate transition state in diene dynamics. L<sub>1</sub> and L<sub>2</sub> denote arbitrary ligands, D is a covalently bound donor atom.

### 1.2.2 Detection and Quantification of Exchange

Chemical exchange is categorized into slow and fast exchange, depending on the size of the rate constant  $k$  in comparison with  $1/T_1$ : Very slow exchange takes place when  $k \ll 1/T_1$ , meaning the spectrum shows clearly separated peaks for the individual nuclei, with  $T_1$  being the longitudinal or spin-lattice relaxation time. When  $k > 1/T_1$ , the exchange can be identified in the NMR from the appearance of

saturation transfer (1D) or exchange peaks (2D). When the exchange gets faster, for example by heating, the signals fuse to one average peak.

When the exchange is fast ( $k \gg 1/T_1$ ), no subspectra of the different species can be identified, but only spectra with broadened lines. In this case, one cannot analyze the dynamics by magnetization transfer experiments. The method of choice is then the line shape analysis, meaning simulation of the spectra using software such as MEXICO<sup>[21]</sup> to fit the spectra obtained in the NMR experiments by changing the rate constants of the exchange processes and comparing the observed lines with the recorded spectra. The final rate constants then should correspond in a good approximation to those of the real molecule. Given the temperature at which the spectrum was recorded, one can use the information gathered from the line-shape analysis to obtain the activation energy of the exchange applying the Arrhenius equation:

$$\Delta G^\ddagger = -R \cdot T \cdot \ln(k)$$

This can also be applied using a series of variable temperature NMR spectra, where every spectrum is fitted *via* line-shape analysis. The slope of the regression line of the plot  $\ln(k)$  vs.  $1/T$  then gives the activation energy.

As mentioned, the exchanging dienes are already visible in the 1D NMR spectra, they show broad signals. Upon cooling down, the dynamics can be slowed down and thus the spectra can be recorded faster than the chemical exchange takes place. Next to temperature, the detection of dynamics visible in the NMR spectra is also dependent of the frequency of the spectrometer. High frequency spectrometers require a lower temperature for the recording of the spectra with the same line-broadening as on low frequency spectrometers.

To detect the exchanging sites, phase-sensitive NOESY (respectively EXSY) experiments can be applied.<sup>[22]</sup> For that, the system has to be brought into slow exchange, *ergo* the sample has to be cooled. The phase-sensitivity allows to distinguish between contact and exchange signals. Contact signals are in phase, meaning positive compared to the diagonal peaks and show the spatially close nuclei, whereas exchange signals negative phase and show the nuclei which are part of the exchange mechanism (EXSY). NOESY experiments however are limited to rather light molecules up to the mass of about 1000 g/mol, as the NOE vanishes when the tumbling of the molecules is too slow and gets negative when the tumbling gets much slower, meaning for very high molecular masses (figure 5).

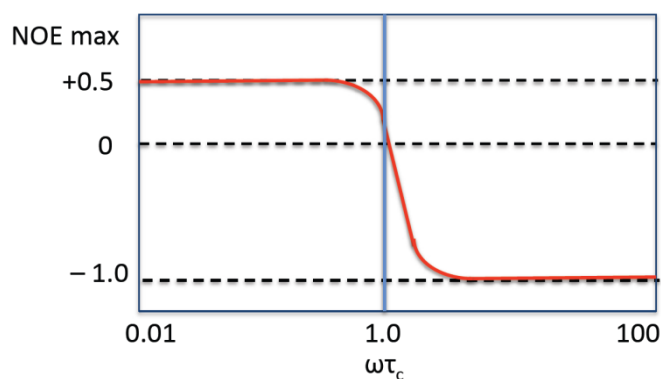


**Figure 5.** Behaviour of the NOE with the tumbling frequency  $\tau_c$  and the spectrometer frequency  $\omega$ . At  $\omega\tau_c = 1.0$ , the NOE vanishes.

The experiment can, still be carried out though in the rotating frame, as the so called ROESY experiment.<sup>[23]</sup> In any case, the “molar mass threshold” of ca. 1000 g/mol is only valid at room temperature and also depends on the spectrometer frequency. For lower temperatures, also lighter molecules tumble slower and thus the NOE may vanish also for lighter molecules.

### 1.3 Tungsten Chemistry

#### 1.3.1 Overview

Tungsten is a special chemical element: It has the highest melting point (3422 °C<sup>[24]</sup>) and the second highest boiling point (5555 °C<sup>[24]</sup>) of all the elements. Being also very resistant to *aqua regia* and hydrofluoric acid, it is a very stable element and thus a very interesting material. Its most prominent application is surely as a resistive wire in the incandescent light bulb.

But tungsten is not only interesting as an element but also in compounds. Staying in the field of material science, one important application are polytungstates, where the first structure, the one of 12-phosphotungstic acid has been published by *Keggin*<sup>[25]</sup> in 1933. The interest in heteropolytungstate has risen since the 1970s, as newer analytical techniques, mainly NMR, allowed to analyze the solution structure additionally to the solid structure<sup>[26]</sup>. They can be applied for example as very dense liquids for separation of minerals, capacitors or sensors. For further information the review on polyoxometallates by *Katsoulis* is recommended.<sup>[27]</sup>

Interesting from an organometallic point of view are the compounds that can be prepared from bis(cyclopentadienyl) tungsten(IV) dihydride. They have been shown to form dinuclear species with iridium<sup>[28]</sup> and platinum<sup>[29]</sup>.

#### 1.2.2 Tungsten Compounds from Tungsten(0) hexacarbonyl

Whereas polytungstates normally are prepared from sodium tungstate, the most used precursor for organometallic tungsten(0) compounds is tungsten hexacarbonyl. Unlike many of the other metal carbonyl compounds, the tungsten hexacarbonyl is very air- and moisture-stable. The most problematic step in the synthesis is therefore mostly the ligand exchange from the precursor. The methods often require high temperature and long reaction times. One popular method is for instance the replacement of three carbonyls by three propionitriles reported by the group of *Kubas*, which requires 6 days of refluxing in the nitrile (97 °C).<sup>[30]</sup> The reaction runs completely selective and replaces the ligands in facial manner. Having the ligands replaced, the newly formed compound opens the field for a whole range of new reactions. The precursor is especially helpful to prepare half-sandwich complexes, which can then be further used to introduce phosphines or weakly coordinating  $\eta^2$ -coordinating hydrogen.<sup>[30-31]</sup> Furthermore, some more sophisticated, multidecker tungsten carboranes have been prepared.<sup>[32]</sup>

In 1991, the group of *Angelici* published a new method for the preparation of a precursor for  $\eta^6$ -arene tungsten complexes.<sup>[33]</sup> It exploits the chelate effect to introduce a tridentate amino-ligand (PMTA), which helps to reduce the reaction time to 3-4 h, refluxing in *n*-decane. To remove the ligand in order

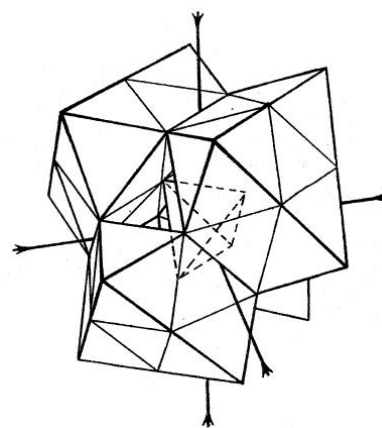
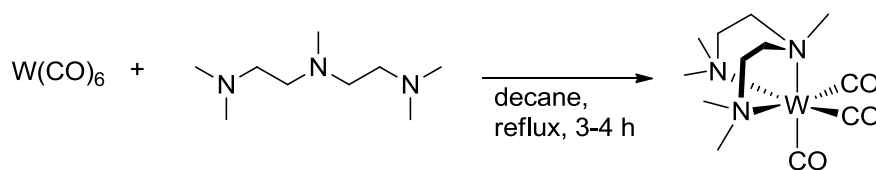


**Figure 6.** The structure of 12-Phosphotungstic acid as published by *Keggin*.

to react it further with arenes or phosphines,  $\text{BF}_3$  is added.  $\text{BF}_3$  is assumed to bind to the amines and thus lowers the reaction time again. In that way, half-sandwich and phosphine complexes of tungsten can be prepared in about 2 h reaction time.



**Scheme 2.** Synthesis of the precursor published by *Angelici*.

Coming from tungsten hexacarbonyl, there have also been syntheses of Fischer carbenes. In fact it was *Fischer* himself who reported the first tungsten based carbene in 1964<sup>[34]</sup>. Several applications for these carbenes were reported later, for example in 3+2 cycloadditions<sup>[35]</sup>. Compared to the other group 6 elements, chromium and molybdenum, though, the carbenes of tungsten have a rather small reaction scope and normally a worse reactivity, for example in alkyne-alkene cyclization.<sup>[36]</sup>

Another very important feature of tungsten complexes with carbonyl ligands is also photochemistry, where UV irradiation is used to selectively remove one carbonyl, which can then be replaced by other functionalities<sup>[37]</sup> or induces polymerization<sup>[38]</sup>.

### 1.3.2 $^{183}\text{W}$ – NMR Experiments

With the rising interest in tungsten chemistry, NMR experiments on the only NMR active spin  $\frac{1}{2}$  nucleus, namely  $^{183}\text{W}$  became more popular. However, the low sensitivity (frequency ratio  $\mathcal{E} = 4.166387$  vs. 100 of  $^1\text{H}$ <sup>[39]</sup>) of the nucleus and its rather low abundance of 14.31(4)%<sup>[24]</sup> make the direct detection of tungsten difficult. Thus, there have been many publications on indirect detection of  $^{183}\text{W}$  *via* HMQC pulse sequences. The nuclei used to transfer the magnetization are rather classical examples like  $^1\text{H}$ <sup>[40]</sup>,  $^{19}\text{F}$ <sup>[41]</sup> and  $^{31}\text{P}$ <sup>[42]</sup>, but there are also reports where  $^{119}\text{Sn}$  is used<sup>[43]</sup>. A good general review about X/Y-Correlation spectroscopy in organometallic chemistry was published recently by *Gudat*<sup>[44]</sup>, an elder collection of chemical shifts for several W(IV), W(II) and W(0) species was reported by *Minelli et al*<sup>[45]</sup>.

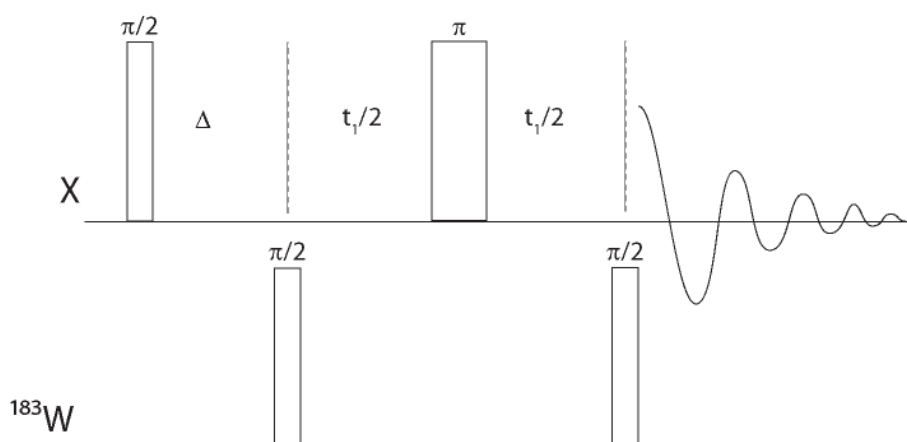


**Figure 7.** The HMQC pulse sequence commonly used to detect  $^{183}\text{W}$ . X denotes the various nuclei given in the text.  $\Delta$  denotes the delay which can be chosen individually based on the  $J_{\text{WX}}$ -value:  $1/(2J_{\text{WX}})$ .

Given the various possibilities to detect tungsten in NMR experiments, an extensive literature research<sup>[46]</sup> suggests that there have been no publications with applications of the  $^1\text{H}$ ,  $^{183}\text{W}$ -HMQC sequence on  $\eta^6$ -arene tungsten compounds so far, even though the same was done for example for molybdenum complexes in a study where also tungsten complexes were investigated<sup>[46a]</sup>.

## 2 Project Idea and Synthetic Approach

### 2.1 The Influence of the Remote Fluorine-Metal Bond on Diene Dynamics

In 2009, *Brück* and *Rubland* published a paper where the dynamic solution behavior of chloro(diene)rhodium(I) phosphine complexes was studied on the basis of a pyridylphosphine (figure 8).<sup>[20]</sup>

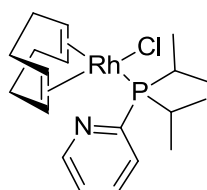


**Figure 8.** The compound used as benchmark complex by *Brück et al.*

Using cyclooctadiene (COD) as the diene, they found broadened lines in the low temperature  $^1\text{H}$ -NMR as well as in the  $^{13}\text{C}$ -NMR spectra for the COD signals, which account for magnetic exchange in the NMR time scale. Taking the given complex as the benchmark, they could determine the main influences on the dynamics. They identified the substituents on the phosphine and the diene to be crucial for the dynamics. Changing the central metal to iridium and a change of the halide had almost no consequences. Kinetic isotope effect (KIE) measurements by substituting the olefinic protons of COD to deuterium resulted in an inverse KIE and thus supported the interpretation of the authors, that the dynamic process of the diene runs over a change of hybridization of the olefinic carbons. Additionally, they used a  $^{15}\text{N}$ -enriched ligand without detecting a KIE and they observed no  $^1J_{\text{RhN}}$ . Nevertheless they could observe an interaction of the pyridyl and the complex by  $T_1$  relaxation measurements. In conclusion, supported by DFT calculations, *Brück* and *Rubland* proved that the mechanism runs over a temporarily coordination of the nitrogen to the metal center to yield a pseudo pentacoordinate species in the transition state.

When the Chloro(1,5-cyclooctadiene)(diphenyl(5,6,7,8-tetrafluoronaphtalen-1-yl)rhodium(I) complex **Rh-2** was analyzed at room temperature, it was seen that it shows a similar behavior. Upon cooling, three different species were found in the  $^{31}\text{P}$ -NMR spectrum, as well as in the  $^{19}\text{F}$ -NMR spectrum (figure 9).



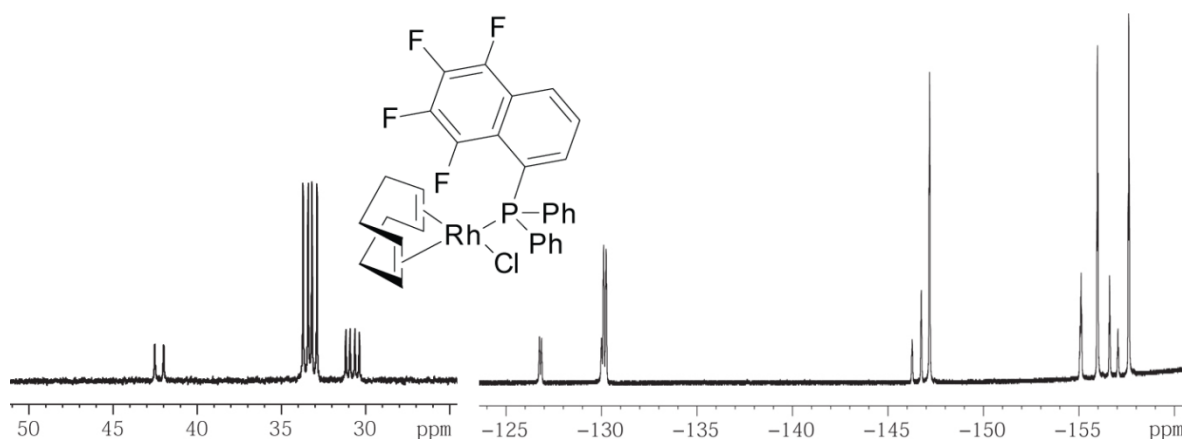


Figure 9.  $^{31}\text{P}$  and  $^{19}\text{F}$  NMR spectra of Rh-2 at 193 K.

Given those observations, the goal of this work was to determine the structure of these conformers at low temperature and find out, if and how they are influenced by the fluorine-metal interaction. To further define the mechanism of the dynamics of COD, the whole temperature series should be measured and the thermodynamical and kinetic properties of the complexes be determined. Given the availability of the almost analogous monofluorinated compound Rh-1, the same procedures could be applied in this case. The comparison would then allow to conclude whether or not the larger dipole of the tetrafluorinated species does play a role for the dynamics. Analogous, the non-fluorinated but else identical complex could be analyzed to investigate further the influence of the  $\text{CF}\cdots\text{M}$  interaction on the dynamics.

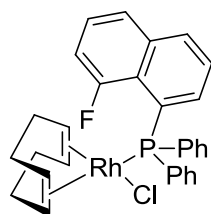
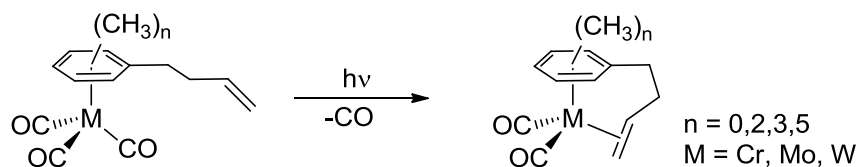


Figure 10. The complex Rh-1.

## 2.2 $\eta^6$ -Arene Tungsten(0) Complexes for $^{183}\text{W}, ^1\text{H}$ -Correlation NMR Experiments

As to the best of our knowledge, there have never been any reports on  $^{183}\text{W}, ^1\text{H}$ -correlation NMR experiments for  $\eta^6$ -arene tungsten complexes, the idea was to prepare such complexes and try to measure such spectra analogously to the well-working  $^{103}\text{Rh}, ^1\text{H}$ -correlation NMR measurements. A system, where the proton is relatively close to the metal center is the half-sandwich complex, as there are approximately 2 bonds between tungsten and the proton. In 1991, *Zanotti et al.*<sup>[33]</sup> reported that they could form chelate alkenylarene dicarbonyl complexes with chromium, molybdenum and tungsten upon irradiation of the corresponding half-sandwich complex (scheme 3).



**Scheme 3.** Irradiation of  $\eta^6$ -arenetricarbonyl complexes to form chelate alkenylarenedicarbonyl complexes.

These complexes have brought up the idea to exchange the olefin for a fluorine atom in such a way that UV irradiation would lead to a fluorine-tungsten interaction. This interaction would then give another opportunity to record  $^{183}\text{W}$ ,  $^{19}\text{F}$ -correlation NMR spectra, as in this case, the fluorine should be relatively close to the metal and thus a  $J_{\text{WF}}$  visible.

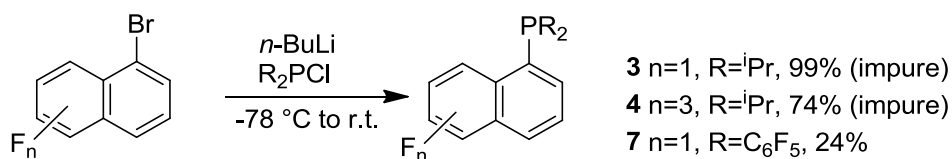
If the synthesis and NMR experiments would be successful, more analogous complexes could be synthesized and characterized using the correlation experiments, as  $\eta^6$ -arene tungsten complexes never have been characterized using  $^{183}\text{W}$  chemical shifts.

## 3 Results and Discussion

### 3.1 Phosphines

#### 3.1.1 Synthesis

Several phosphines have been prepared, mainly based on Bromo(8-Fluoronaphtalen-1-yl) (scheme 4). The synthesis of the phosphines could be done rather straight-forward after the standard procedure, namely lithiation of the naphthylbromide and further addition of the bis(alkyl/aryl)phosphine to yield a tertiary phosphine overnight. The lithiation of the naphthalene, however, was found to be a crucial step in the synthesis, it is very important to slowly add the butyl lithium solution, else there is formation of a lot of byproducts. The color of the solution after the lithiation varied in the experiment. For the Lithio (8-Fluoronaphtalen-1-yl), yellow clearly dominated, for the Lithio(5,6,7,8-Tetrafluoronaphtalen-1-yl), however, the color can be blue to green, sometimes rather pale, sometimes rather intense.

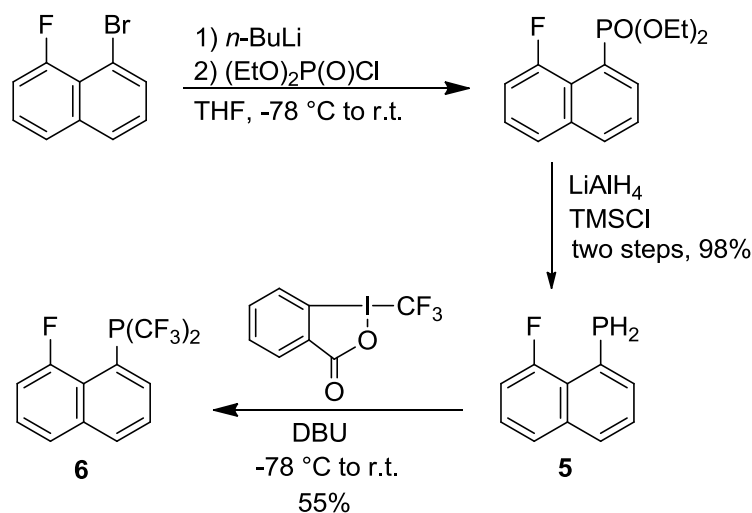


**Scheme 4.** Standard synthetic procedure for the phosphines 3, 4 and 7.

The isolation of the isopropyl phosphines 3 and 4 in pure form was not as easily achievable as in the other cases. The difficulty was mainly to prohibit the formation of the oxide, which made the separation of the byproducts feasible. Recrystallization did not help, such that the phosphines had to be protected with borane to allow the purification by flash chromatography. Even though the product could then be separated purely, after the deprotection by refluxing in diethylamine there were again impurities.

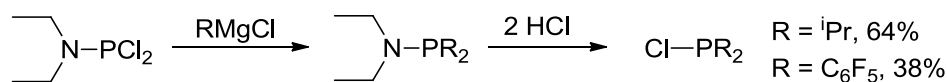
The synthesis of the bis(trifluoromethyl)phosphine was done according to a completely different procedure than the other phosphines. The procedure ran over the formation of a diethyl phosphonate

which was then further reduced to the primary (8-Fluoro-naphtalen-1-yl)phosphine, similar to a procedure reported by *Hiney et al.*<sup>[47]</sup>. This phosphine could then be trifluoromethylated using the 1-trifluoromethyl-1,2-benziodoxol-3(1*H*)-one in the presence of DBU, as published by *Armanino et al.* in 2010<sup>[48]</sup>.



**Scheme 5.** Synthesis of **6** over the primary phosphine **5**.

The synthesis of the chloro bis(isopropyl)phosphine as well as the synthesis of chloro bis(pentafluorophenyl)phosphine were carried out slightly different from the literature procedures (scheme 6).<sup>[49]</sup>



**Scheme 6.** Pathway for the preparation of the chlorophosphines.

For both syntheses, the starting material was chosen to be an amino-protected phosphine instead of using phosphorus trichloride. This was done to prohibit formation of byproducts, such as mono- or trisubstituted phosphines. The protected phosphine was prepared after the standard synthesis by *Perich and Johns*<sup>[50]</sup>, the introduction of the alkyl/aryl substituent was done with the respective Grignard reagent. The deprotection was then performed with hydrochloric acid solution. These syntheses went quite well, unfortunately though, in the synthesis of the chloro bis(pentafluorophenyl)phosphine, the vessel broke thus the yield was drastically lowered and it remains unclear which additional impurities were introduced. The product then could not be purified by distillation, as there were two species that coevaporated. Interestingly, there are two publications which report the synthesis of this chloro phosphine and both state another chemical shift in the <sup>31</sup>P-NMR spectra for the product<sup>[49b, 51]</sup>, each corresponds to one of the two species that were found in this synthesis. The synthesis of the tertiary phosphine was then carried out with the impure chloro phosphine, there were several products found, but the desired one could then be separated *via* flash chromatography.

Both the phosphines **6** and **7** were prepared with the idea to ease the assignment of the protons for the different conformers up by replacing some of the hydrogens by fluorine. Furthermore, it is interesting to see which influence the electron withdrawing properties of the two phosphines have on the dynamics. Thus, **6** and **7** can be looked at as the electron withdrawing analogue of **3** and **1**, respectively.

### 3.1.2 Comparison of the Phosphines

Given the different phosphines, that have been synthesized, it is interesting to analyze the properties of the phosphines by analyzing the “through-space-coupling” constant  $J_{PF}$  (table 1). One can see, that the primary phosphine **5** clearly stands out with a very low coupling constant compared to the others. In contrast the strongly electron poor, trifluoromethylated phosphine **6** shows a more than 100 Hz higher coupling constant. To predict a general trend is however difficult, though the electron donating rests like isopropyl show higher coupling constants than rather electron withdrawing pentatfluorophenyl phosphines.

**Table 1.** Comparison of the  $J_{PF}$  coupling constants of the prepared and used phosphines.  $R^1$  describes the type of Naphthyl-substituent,  $R^2$  the two other substituents of the  $R^1PR^2_2$  phosphine.

Compound	$R^1$	$R^2$	$J_{PF} / \text{Hz}$
<b>1</b>	NpF	Ph	194.0
<b>3</b>	NpF	<sup>i</sup> Pr	224.3
<b>5</b>	NpF	H	150.6
<b>6</b>	NpF	CF <sub>3</sub>	252.2
<b>7</b>	NpF	C <sub>6</sub> F <sub>5</sub>	204.6
<b>2</b>	NpF <sub>4</sub>	Ph	198.0
<b>4</b>	NpF <sub>4</sub>	<sup>i</sup> Pr	223.6

*Stanek* stated in his dissertation<sup>[52]</sup> (as well as in the aforementioned paper<sup>[14]</sup>), that the size of the coupling constant can be explained by change of hybridization, which interpreted according to *Bent's rule*<sup>[53]</sup>. Examining the values in table 1 though, it becomes obvious that this explanation does not hold true in this context. The comparison of the bis(pentafluorophenyl) phosphine **7** and the bis(isopropyl) phosphines **3** and **4** can be taken as an indicator in this case; even though **3** bears highly electron withdrawing substituents compared to the strong electron donating isopropyl groups of **4**, the value of  $J_{PF}$  is much higher for the latter. Furthermore, the compounds **7** and **1** differ only little, even though the electronic properties of the fully fluorinated and the non-fluorinated phenyls would suggest a stronger effect on the coupling constant.

Analogously, *Stanek's* comparison of the ligands in his dissertation also seems wrong. For example the coupling constant of (NpF<sub>4</sub>)PPh<sub>2</sub> (198 Hz) the one of (NpF<sub>4</sub>)PPh(NEt<sub>2</sub>) (200 Hz): The exchange of phenyl for diethylamine should change the electronics and thus the coupling constant much more than observed. If his reasoning that the coupling constants reflect the hybridization according to *Bent's rule*, the difference should be much higher.

It seems that *Stanek's* assertion lacks its basis, because it relies on the fact that the coupling mode is Fermi contact (FC) coupling. However, there are papers where exactly the coupling mode for the “through-space” coupling  $J_{FF}$  in 1,8-difluoronaphthalene is discussed. It was shown, that the  $\sigma$ -type orbitals dominate the FC coupling and that paramagnetic spin orbit (PSO) coupling cannot be neglected. It might be that the coupling mode in the somewhat analogous phosphine ligands is not only FC coupling too and thus all arguments should be reconsidered, even though  $J_{FF}$  is not comparable to  $J_{PP}$ . One other point to be respected would be the sterics, which was not at all considered.

To get an impression of the orbitals on the phosphorus and the fluorine atom in the two ligands **1** and **7**, these two were calculated using DFT methods (BP86<sup>[54]</sup> functional with SV(P) basis<sup>[55]</sup>), also mini-

mizing the energy of the other atoms, such that not only the electronic but also the steric effects can be compared. The resulting structures and orbital shapes can be seen in figure 11:

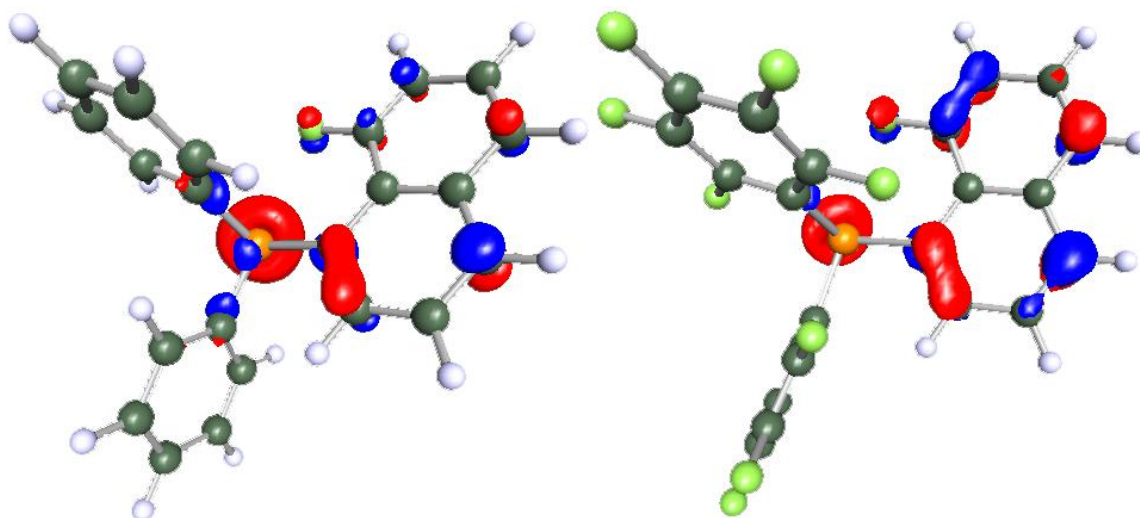


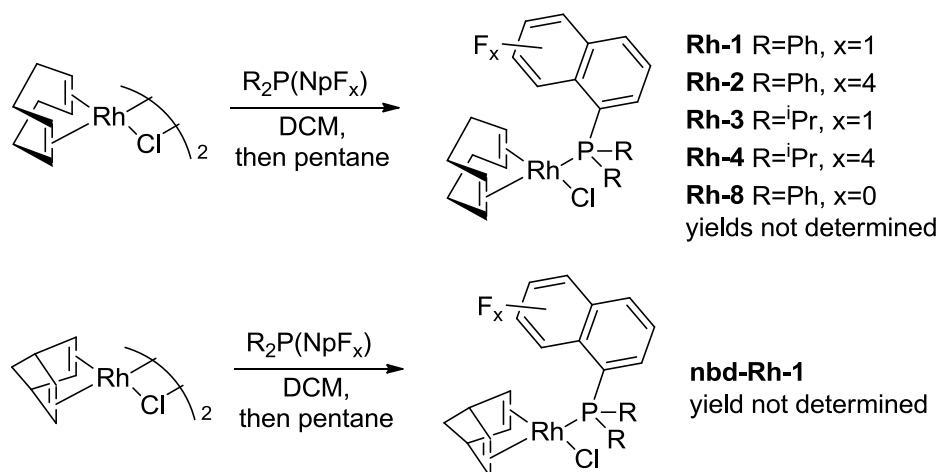
Figure 11. Structures and HOMOs of the Ligands 1 and 7.

Two major differences between the two ligands can be seen: First, one of the phenyl substituents in 7 is rotated such that it is almost perpendicular to the naphthalenyl. Second, it is obvious that the electron density in 7 is strongly localized on the naphthalenyl, whereas in 1, it can also be found in the phenyl. Drawing conclusions on the coupling mode is however not possible with the given results, it would require much more efforts.

## 3.2 Complexes

### 3.2.1 Synthesis

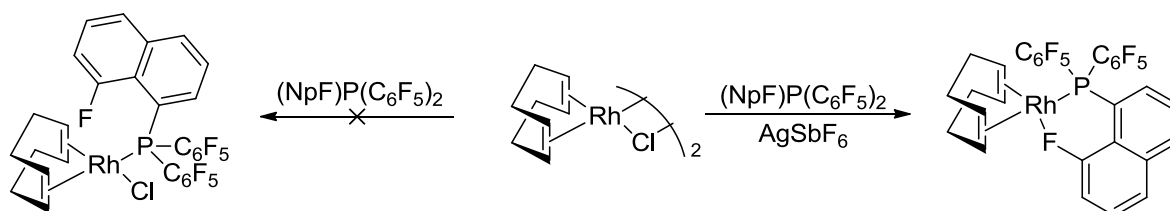
The synthesis of most of the complexes was more or less straight-forward. The ligand and the precursor were dissolved in dichloromethane and stirred for some time, then the mixture was concentrated and the product precipitated with pentane. This procedure was applied for the phenyl- and the isopropylphosphino complex, **Rh-1**, **Rh-2** and **Rh-4** respectively. Also the nbd complex **nbd-Rh-1** was obtained that way. The monofluorinated isopropyl complex **Rh-3** however did not yield the product that easily. Mixing the ligand and the complex in dichloromethane, there was first formation of a black precipitate forming from the solution that had to be filtered off. From the resulting solution, the product could be precipitated with pentane. As the product still showed impurities, it was washed again with pentane and then refluxed in diethyl ether for some time.



**Scheme 7.** Synthesis of the Rh-complexes.

No reaction could be observed for the more electron deficient phosphines **6** and **7**. A literature research after that finding then brought up a publication by the group of *Torrens* where the electronic and steric effects of triarylphosphines for rhodium(I)chlorides were studied<sup>[16]</sup>. In that paper, they show that maximally one pentafluorophenyl substituent can be introduced in a triarylphosphine to get coordination to the rhodium(cyclooctadiene)chloride dimer. Given the even bigger electron deficiency of the bis(trifluoromethyl)phosphine **6** it is reasonable that coordination in that case is also impossible.

Concerning the electron deficiency, one idea was also to scavenge a chloride from the precursor, such that in consequence the phosphine would coordinate more easily. In a second step, also the fluorine may then coordinate as the phosphine still draws a lot of electron density away from the central metal and thus it would more easily bind to the fluorine and accept its electrons. This way, the coordination of the fluorine would be enforced, also through the chelate effect (Scheme 6).



**Scheme 8.** Enforcement of a strong rhodium fluorine interaction by applying the energy deficient phosphine **7** and a halogen scavenger.

This experiment was done on NMR scale and it can be said, that there is a change in the spectra, however the concentration of the sample was rather low and thus it remains unclear if there are any by-products and whether isolation of the desired product is possible.

In another NMR tube experiment, the ligand **7** was also mixed with iridium(I)(cyclooctadiene)chloride dimer. Even though the precursor dissolved badly in the deuterated dichloromethane, a reaction could be observed. After short time, a new signal was found in the <sup>31</sup>P-NMR (figure 12).

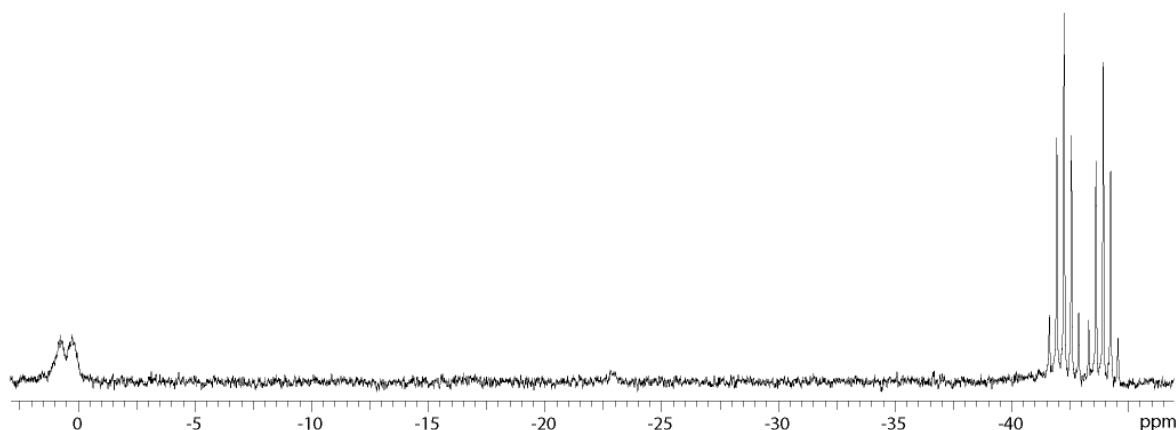


**Figure 12.** The phosphorus spectrum of the reaction of the iridium precursor with 7. The free ligand can be seen around -43 ppm, the newly formed signal is a doublet with  $J_{PF} = 62.4$  Hz around 1 ppm.

Furthermore, it could be seen that the  $^{19}\text{F}$ -NMR shows broadened peaks, which would suggest similar dynamic processes as for the other species discussed here. However, after two days of stirring in the tube, the reaction did not proceed further. Thus it seems advisable to repeat the experiment at a lower concentration, to see whether the reaction can be completed when the precursor dissolves better.

### 3.2.2 Structures of the Conformers by NMR

In VT-NMR experiments the different complexes it was found that there are three conformers for both the complexes **Rh-1** and **Rh-2**. The ratios between the conformers differed however greatly (table 2). For **Rh-1** the *major* and *minor* conformer have almost the same integral, in the  $\text{NpF}_4$ -complex **Rh-2** one sees a ratio of about 4:1 between the two. The third conformer is obviously different, as it does not show coupling of the fluorine and the metal. It was thus concluded that the naphthyl substituent in this case points away from the complex, called *exo* conformer. However the ratios could only be determined based on integration in either the  $^{19}\text{F}$ - or the  $^{31}\text{P}$ -NMR spectrum, as the  $^1\text{H}$ -NMR never showed isolated peaks.

**Table 2.** Ratios for the conformers of the different complexes prepared.

Compound	$R_1$	$R_2$	<i>Minor/Major</i> <sup>1</sup>	<i>Exo/Major</i> <sup>1</sup>
<b>Rh-1</b>	$\text{NpF}$	Ph	0.98	0.14
<b>Rh-2</b>	$\text{NpF}_4$	Ph	0.26	0.10
<b>Rh-3</b>	$\text{NpF}$	$i\text{Pr}$	0.13	- <sup>2</sup>
<b>Rh-4</b>	$\text{NpF}_4$	$i\text{Pr}$	-	-
<b>nbd-Rh-1</b>	$\text{NpF}$	Ph	-	0.25
<b>Rh-8</b>	$\text{Np}$	Ph	n.d. <sup>3</sup>	n.d. <sup>3</sup>
<b>Ir-1</b>	$\text{NpF}$	Ph	0.38	0.23

<sup>1</sup>Derived from integration of the  $^{19}\text{F}$ -NMR spectra at low temperature (193-213 K); <sup>2</sup>Coalescence between *minor* and *exo*, thus the ratio counts for both.; <sup>3</sup>Signals not separated enough, integration in the  $^{31}\text{P}$ -NMR spectra not possible.

Looking at the non-fluorinated complex **Rh-8**, one sees that it reaches coalescence of all peaks only at a temperature around 203 K, which is much lower than all fluorinated complexes where the signals in average begin to separate at temperatures lower than 253 K. One can thus state that the fluorinated naphthyl substituent has a crucial influence on the dynamics of the system.

It stands out that the complex **Rh-4** does not show any other conformer than the *major*. This could not be understood, looking at the other complexes and at the ideas that were drawn from the other observations. The explanation might be that the product was impure and the dynamics thus completely disturbed. This hypothesis is supported by the fact that there are some undefined peaks visible in the  $^1\text{H}$ -NMR spectra.

The low-temperature spectra of **nb-d-Rh-1** show only two conformers, *major* and *exo*, which can only be differed in the  $^{19}\text{F}$ -NMR spectra, as the shift is almost the same for both conformers in the  $^{31}\text{P}$ -NMR spectra, only a slight shoulder indicates the existence of the *exo* conformer there. Even though the  $^1\text{H}$  spectra shows well separated peaks, it is somewhat contradictory: From the HMBC spectrum, the proton that should be closest to the fluorine in the naphthalenyl substituent is not the same as the one that can be derived from HSQC and  $^1\text{H},^1\text{H}$ -COSY. Thus the spectra were only very incompletely solvable. The  $^{31}\text{P},^1\text{H}$ -correlation spectrum is not helpful in this case, as there is no separation of the peaks. An approach that would be applicable in this case would be using a spectrometer with lower frequency. Upon cooling down, this spectrometer would give less broadened peaks and less dynamical spectra. In contrast, the resolution of the spectra gets worse. *Vice versa*, a higher frequency would also not help to ease the assignment, as the linebroadening and dynamics would work against the gain in resolution.

Concerning assignment of the peaks to the respective conformers, the assignment of the proton and the carbon signals turned out to be very difficult. Most problematic was the assignment of the signal in the aromatic regime, as for example in **Rh-1** each of the three conformers contributes with 16 aromatic protons and 22 aromatic carbons, including some that couple to several other nuclei. In the case of **Rh-1** it was rather complicated due to the two conformers with almost the same abundance, whereas in most other cases, difficulties arose more from the fact, that the lower abundant protons were not recordable in the correlation spectra. Thus, none of the complexes could be characterized completely at low temperature. However, in most cases the *major* conformer could be assigned more or less completely. To this end and to further get an input of the exchange processes between the conformers,  $^{19}\text{F},^1\text{H}$ -HOESY and  $^1\text{H},^1\text{H}$ -NOESY spectra were recorded.  $^{19}\text{F},^1\text{H}$ -HOESY mostly served to get an impression of which protons of the COD are closer to the fluorinated naphthyl, and thus may interact in the exchange. It became visible, that only one COD-proton per conformer interacts with the fluorine, and in both cases it is the olefinic proton with the biggest shift to high field. The interactions of the *exo* conformer could not be seen in the  $^{19}\text{F},^1\text{H}$ -HOESY experiment.



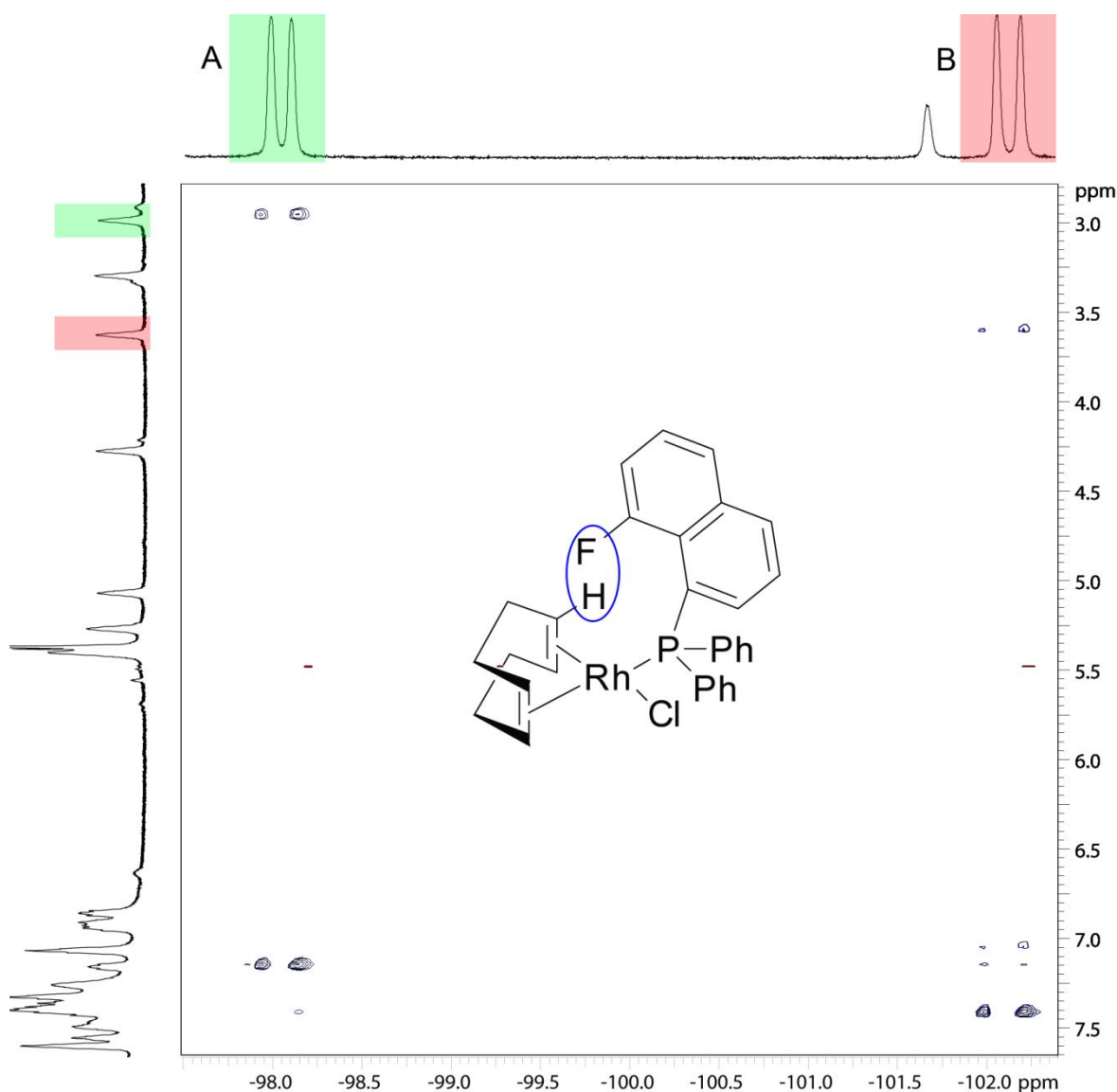


**Figure 13.** The  $^{19}\text{F},^1\text{H}$ -HOESY spectrum of **Rh-1** shows that the fluorine interacts (blue circle) with one proton of the COD per conformer ( $A=\text{major}$ ,  $B=\text{minor}$ ). Furthermore, interaction in the aromatic system is visible.

$^1\text{H},^1\text{H}$ -NOESY spectra unfortunately showed only crosspeaks with positive phase compared with the diagonal peaks, which would be interpreted as contacts in the same conformer. However, some of these crosspeaks were found between protons that could be assigned to different conformers, and thus have to be interpreted as exchange peaks, even though the phase is “incorrect”. As the spectra were recorded at 203 K, it was assumed that the correlation time is distinctively different from the one at room temperature and thus the phase change can be explained by negative NOE.  $^1\text{H},^1\text{H}$ -ROESY spectra basically showed the same signals but also with the “incorrect” phase. As ROESY is known to be probably the most artifact-ridden 2D-method (TOCSY- and COSY-artifacts, indirect NOEs, TOCSY-ROESY relay cross-peaks), the discussion of this spectrum is omitted here.

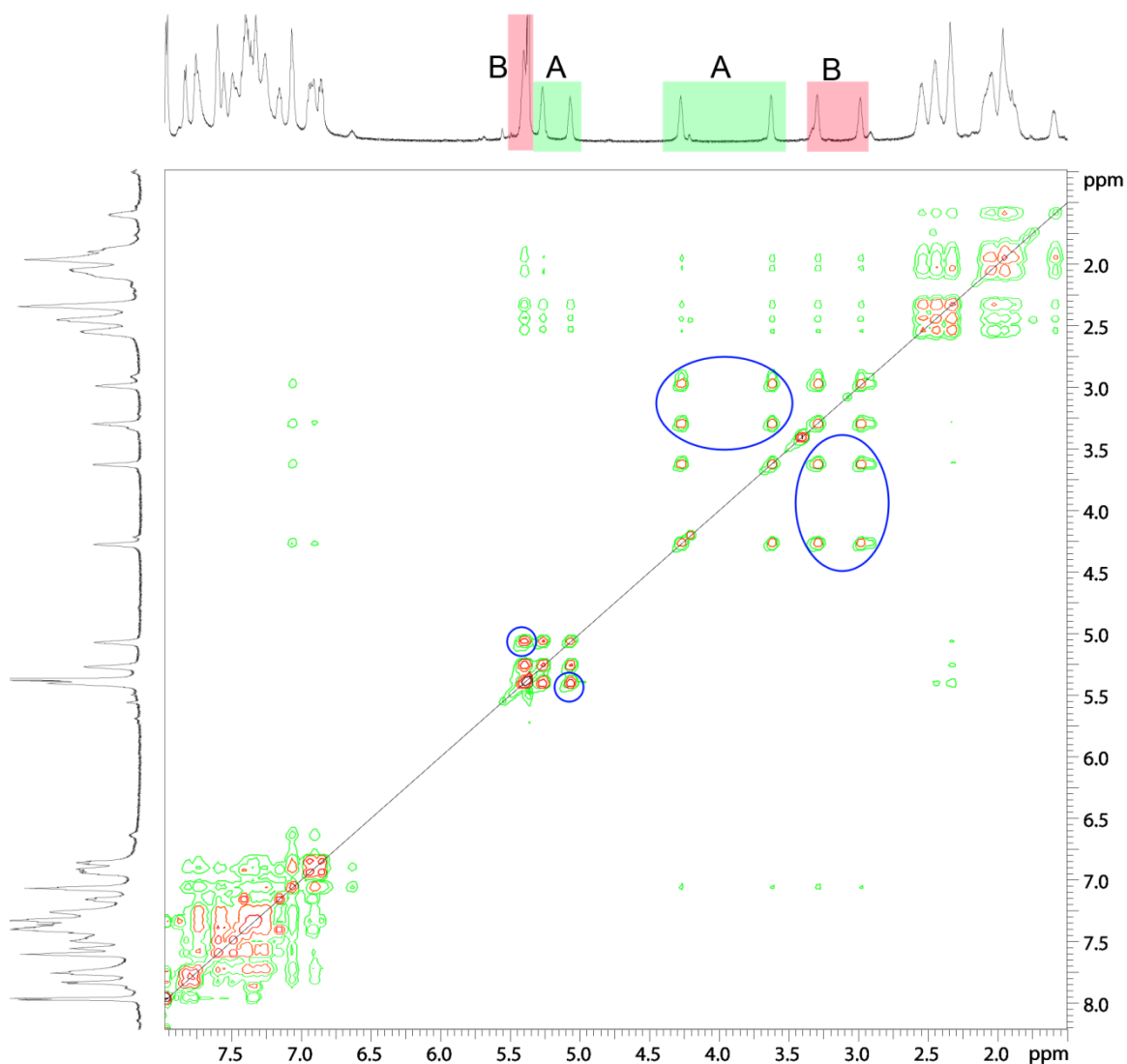
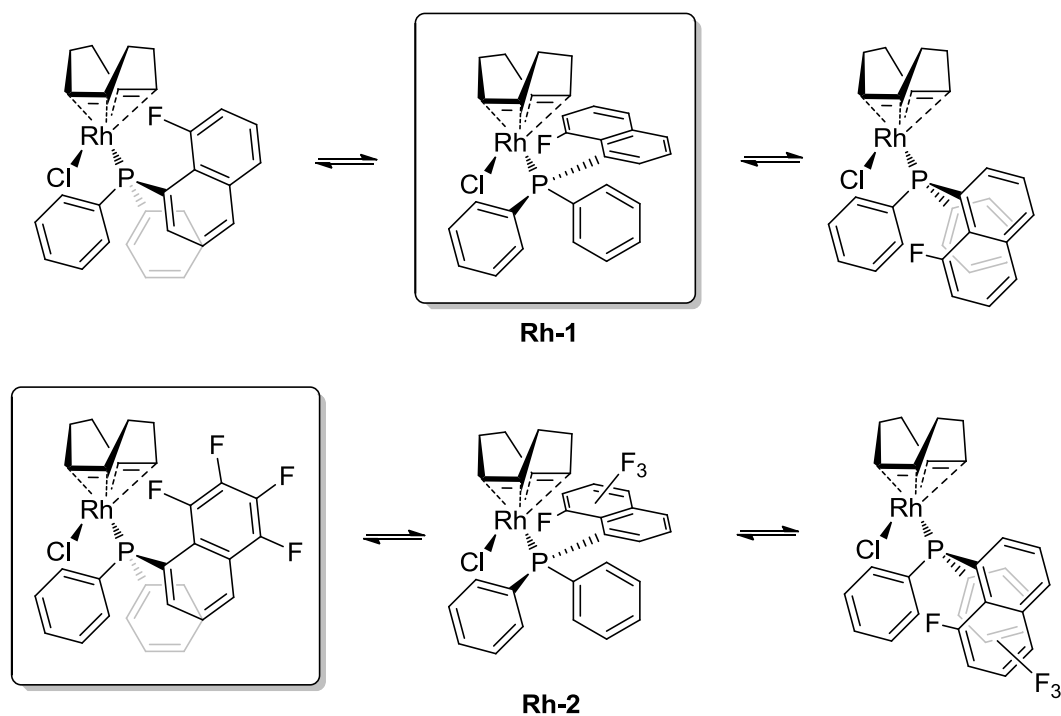


**Figure 14.**  $^1\text{H}, ^1\text{H}$ -NOESY spectrum of **Rh-1**. The "wrongly" phased exchange peaks for the olefinic protons of the *major* (A) and the *minor* (B) conformer are shown in blue circles. The area around 5 ppm for B includes also the solvent signal of  $\text{CDHCl}_2/\text{CH}_2\text{Cl}_2$ .

### 3.2.3 Structures of the Conformers from NMR Combined with X-ray Crystallography

The conclusions concerning structures of the complexes that were drawn from the spectra are to some extent also supported by the crystal structures: The structures of **Rh-1** and **Rh-2**<sup>1</sup> clearly show another conformation of the phosphine and therefore also of the diene. It was assumed that the other conformers of both complexes which are not found by crystallography are there in both cases but have the slightly or clearly disfavored structure. Together with the other conformer where the naphthyl-group on the phosphine points away from the metal, the three conformers were set. An illustration of those assumptions is given in scheme 9, the framed drawings correspond to the structure that could be found by x-ray crystallography.

<sup>1</sup> Details for these crystal structures can be found in the appendix.



**Scheme 9.** Proposed structures of the conformers for **Rh-1** and **Rh-2**. The structures obtained by x-ray crystallography are drawn in frames.

Additionally to the three conformers, the signal of the *exo* conformer is broadened at low temperatures in the NMR spectra. It seems that this conformer still shows dynamics of the COD, which cannot be frozen within the technically given temperature range. It seems that for the *major* and *minor* conformer, there is only one conformation of the diene possible, the two crystal structures show a slight torsion of the COD out of the plane for **Rh-2**, whereas the COD in **Rh-1** is perfectly in plane.

Looking at **nbd-Rh-1** which shows only two conformers at low temperature, namely a *major* and an *exo* conformer, it seems likely, that the difference between the *major* and *minor* structure is also predominantly influenced by the COD conformation. The conformation of the *major* conformer can presumably also be derived from the crystal structure, it seems to correspond more to the crystal structure of **Rh-1**. The mentioned torsion of the COD could not be observed in this case, the nbd takes over a perfect square-planar structure. With 3.4806(13) Å, the rhodium fluorine distance is, however well out of the range of 3 Å that has been set by *Plenio*<sup>[4]</sup>.

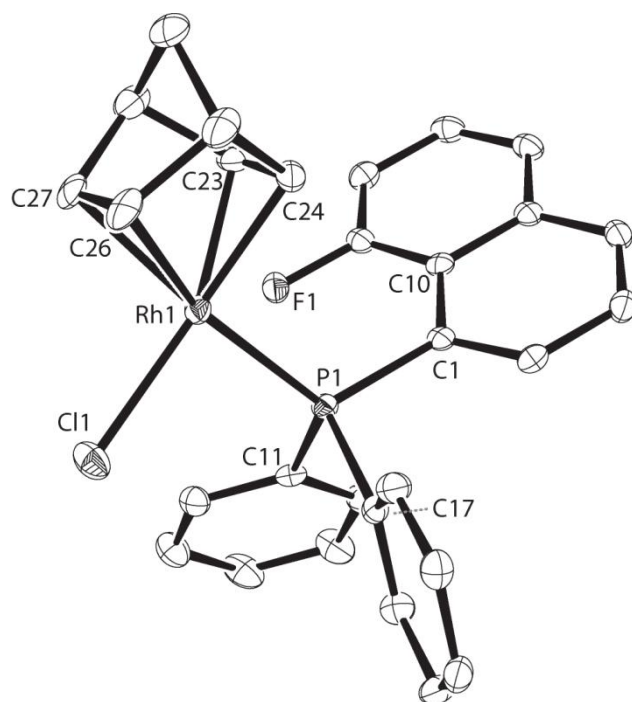


**Figure 15.** ORTEP drawing of **nbd-Rh-1**, hydrogen atoms and enclosed solvent molecules are omitted for clarity. Selected bond lengths and angles: Rh1-F1 3.4806(13) Å; Rh1-C23 2.097(2) Å; Rh1-C24 2.115(2) Å; Rh1-C26 2.203(2) Å; Rh1-C27 2.195(2) Å; Rh1-P1-C1 116.68(7)°; C1-P1-C11 102.44(10)°; C1-P1-C17 104.10(10)°; C11-P1-C17 102.59(10)°; Rh1-P1-C1-C10 68.84(18)°; Cl1-P1-centroid(C23/C24)-centroid(C26/C27) -1.54°.

The crystal structure of **Rh-4** shows a similar structure to the *major* of **Rh-2** and it can thus be concluded that the crystal structure and the *major* conformer are again similar. Interestingly, the crystal-structure shows again a rotation of the diene out of the square planar conformation.

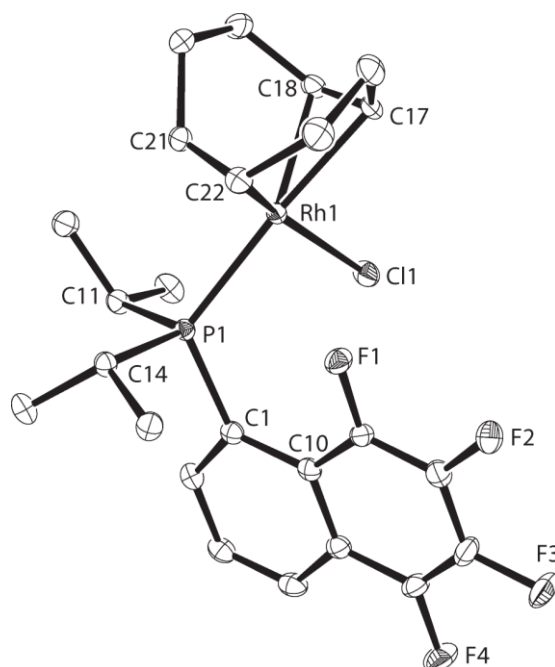


**Figure 16.** Ortep drawing of **Rh-4**, hydrogen atoms are omitted for clarity. Selected bond lengths, bond and torsion angles: Rh1-F1 2.8071(11) Å; Rh1-C17 2.2080(18) Å; Rh1-C18 2.1744(18) Å; Rh1-C21 2.1395(18) Å; Rh1-C22 2.1049(18) Å; Rh1-P1-C1 118.47(6)°; C1-P1-C11 104.12(8)°; C1-P1-C14 101.34(8)°; C11-P1-C14 104.77(8)°; Rh1-P1-C1-C10 41.03(17)°, P1-centroid(C21/C22)-centroid(C18/C17)-Cl1 -13.27°.

Furthermore, crystals were obtained for **Rh-3**, which were unfortunately not completely solvable. Nevertheless, the structure could be determined so far that it became visible that, like **Rh-1** and **nbd-Rh-1**, the COD is again nicely in plane with the chlorine and the phosphorus atom. Furthermore, the naphthyl substituent seems to align again analogous to the structure **Rh-1**, meaning more orthogonal to the plane.

### 3.2.4 Supporting Information from DFT Calculations

To further corroborate the assumptions for the dynamics in **Rh-1** and **Rh-2**, the two crystal structures were used for DFT calculations, which were performed using the program suite TURBOMOLE<sup>[56]</sup>. First the relative energy of the crystal structure was calculated and then the structures were adapted such that the second conformer **Rh-1** and **Rh-2** was assumed to overtake the first structure of **Rh-2** and **Rh-1**, respectively. For this, the H-atoms were replaced by fluorine atoms or *vice versa* at the respective positions. The bond lengths were adapted analogously to those found in the crystal structures. After the first results with the BP86<sup>[54]</sup> functional in the SV(P) basis and auxiliary basis set<sup>[55, 57]</sup> showed promising results, the method was kept the same but a bigger basis along with the corresponding auxiliary basis set was applied, namely TZVP<sup>[58]</sup>. All the values stayed in the same range but changed slightly. Lastly, the functional was exchanged to B3LYP<sup>[59]</sup> with the same basis set. The results of the different methods can be seen in table 3.

**Table 3.** The calculated relative energy difference between *major* and *minor* conformers of the respective compounds.

DFT method	Basis set	Rh-1 / kcal·mol <sup>-1</sup>	Rh-2 / kcal·mol <sup>-1</sup>
BP86	SV(P)	-2.56	4.75
BP86	TZVP	-1.80	+3.82
B3LYP	TZVP	-1.07	+3.37

It can be seen, that the energies that were calculated fit the experimental data very nicely, the energy difference between the conformers of **Rh-1** is only small, which corroborates the ratio 1:0.98 found by integration of the <sup>19</sup>F-NMR spectra. In the case of **Rh-2**, the energy difference is larger similar to the difference in the integrals (1:0.26). The structure of the *exo* conformer however was not calculated up to date.

### 3.2.5 Conclusions for the Exchange Mechanism

As a conclusion, one could thus state that the crystal structures of NpF-based complexes all attain the same (orthogonal) conformation of the naphthyl substituent to the plane and that they all show a complete planar conformation for the COD and the other substituents. In contrast, the two crystal structures NpF<sub>4</sub>-based complexes both show a parallel alignment of the naphthyl substituent and the COD is rotated slightly out of plane.

From these informations and given the rather small energy differences between the conformers that were calculated, it seems likely to assume that the exchange mechanism could go over a pseudo-pentacoordinate intermediate (figure 17), as this has also been stated by *Brück et al.* for their respective system<sup>[20]</sup>. The pentacoordinate species seems to be close to the structure that is found in the crystals of **Rh-2** and **Rh-4**.

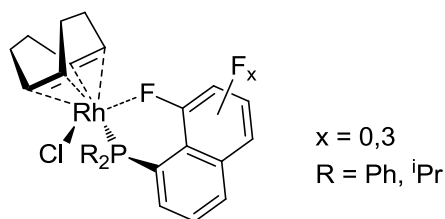
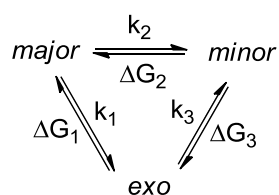


Figure 17. Proposition for the pseudo-pentacoordinate transition state of the COD exchange.

### 3.2.6 Thermodynamical and Kinetic Properties for the Chemical Exchange

Due to the bad resolution of the  $^1\text{H}$ -NMR spectra, the rate constant for the chemical exchange could not be measured *via* magnetization transfer experiments. It would have worked though with the  $^{19}\text{F}$ - or  $^{31}\text{P}$ -NMR spectra though, if the temperature range between the lowest measured temperature and the coalescence temperature would have been larger, because 5 or more  $(k, T)$ -values would be necessary for a regression. Instead, the spectra had to be simulated using the program GAMMA<sup>[60]</sup>. The program was chosen over MEXICO, as MEXICO is limited to two-site exchange, whereas in this case a three-site exchange had to be modeled. The input file for the program was thus adapted for a three-site exchange, where every conformers for which slow exchange was detected can go over into one of the other conformers (scheme 10).



Scheme 10. The exchange scheme applied for the simulations.

Furthermore, the coupling was implemented, such that the coupling pattern corresponds to the real spectra. The coupling pattern is after all also a bug help for the simulations, as it gives input about the correctness of the simulation, there are more linewidths and more peaks to compare and thus more information for the fitting, which are important as the method itself is not that precise. Problems arise therefore mostly at temperatures where the peaks merge and at higher temperatures, when the range of values for the rate constants gets wider. The deviance for the rate constants at high temperature is of course much higher there. This implies also that the simulations are easier for the  $^{31}\text{P}$ -NMR spectra, as there is one coupling more to judge the rate constants on. This was of course not possible for the iridium complex Ir-1, which made the simulations particularly difficult and therefore also a little less reliable.

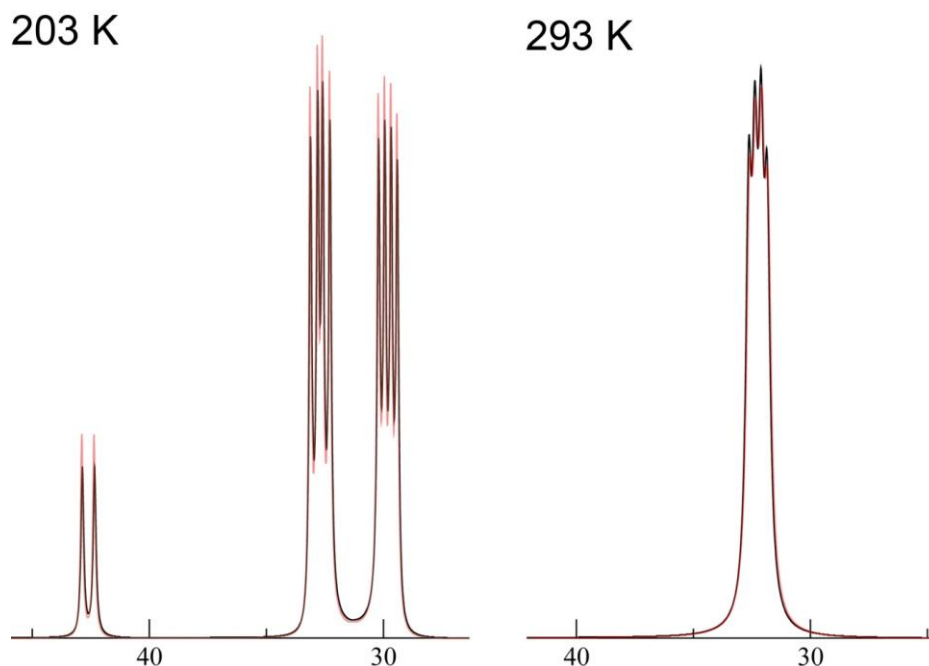


**Figure 18.** Illustration for the influence of the value of  $k$  on the lineshape: the red line corresponds to the original line, the black line is the line that corresponds to a change of +2 Hz and +1000 Hz for all three  $k$ -values at 203 K and 293 K respectively. The spectra are taken from the simulation for Rh-1 and the numbers are ppm values of the chemical shift.

The simulations could also only be performed when the dynamics were “frozen out”, as the simulation works only fine when the chemical shift for the signals is known and reliable. This condition limited the scope of application to three possible complexes: **Rh-1**, **Rh-2** and **Ir-1**. In particular the simulations yield interesting information about **Rh-1**, as on one hand, the difference in kinetics and thermodynamics for the introduction of three more fluorine atoms on the ligand (to form **Rh-2**) as well as on the other hand the change of central metal (to form **Ir-1**) can be studied and conclusions be drawn about this complex. Thus, **Rh-1** can be looked at as the “main complex” for these studies.

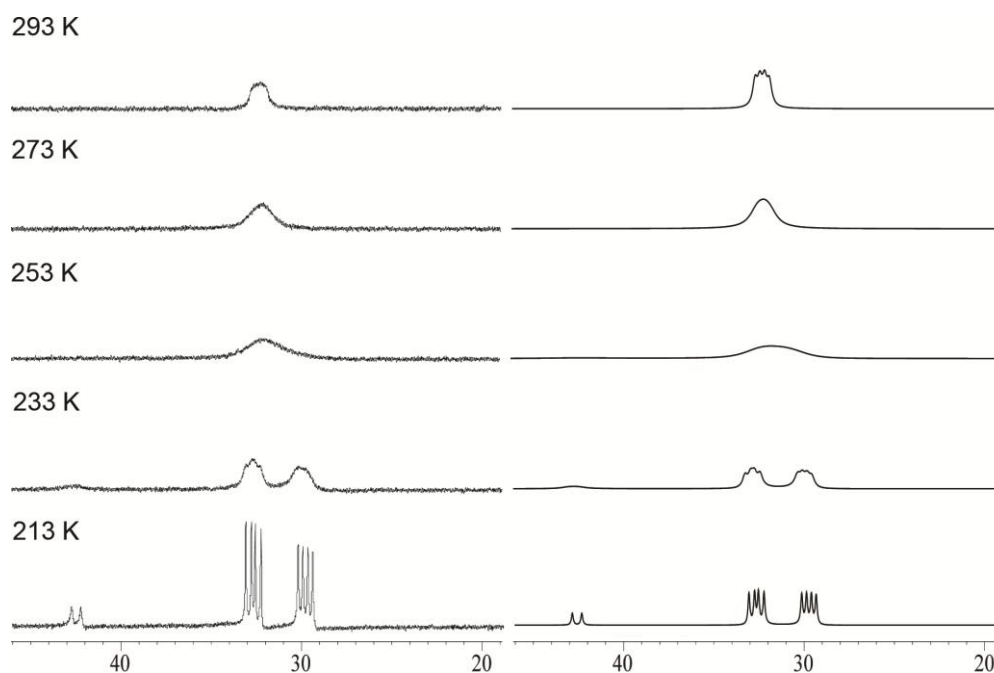


**Figure 19.** Comparison of the NMR spectra (left) with the simulation (right) for **Rh-1**. Due to limitations in datapoints (resolution) of the program GAMMA, the simulated peaks at 213 K are shortened.

From the simulations, the rate constants at the different temperatures were measured and the activation energy for the exchange determined *via* an Arrhenius plot and linear regression<sup>2</sup>. The values derived from the simulations for the three complexes are given in table 4.

**Table 4.** Results for activation energies obtained by simulation of the three exchange processes.

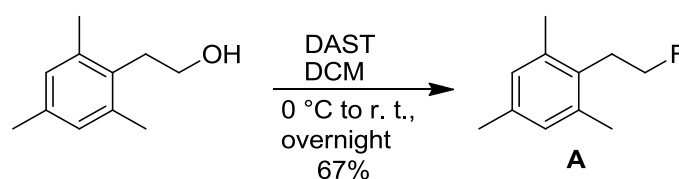
Complex	$\Delta G_1 / \text{kJ}\cdot\text{mol}^{-1}$	$\Delta G_2 / \text{kJ}\cdot\text{mol}^{-1}$	$\Delta G_3 / \text{kJ}\cdot\text{mol}^{-1}$
Rh-1	43	38	43
Rh-2	45	43	51
Ir-1	46	51	50

Looking at the activation energies one can see that the transitions in **Rh-1** all have lower energy barriers than for the other two complexes. This leads to the conclusion that more fluorine atoms respectively the exchange of the central metal have a similar effect; enhancement of the energy. The central metal seems to have a stronger energy enhancing effect, even though the  $\Delta G_3$  value is slightly higher for **Rh-2** than for **Ir-1**. Nevertheless it is difficult to see a trend: Whereas the activation energies to go from *exo* to *major* or *minor* are very close for **Rh-1**, there are much bigger differences in between for the two other complexes. As has been mentioned before, the **Ir-1** data have been difficult to obtain and thus all the values are just vaguely comparable.

### 3.3 $\eta^6$ -Arene Tungsten(0) Complexes

#### 3.3.1 Synthesis of the Ligand & Complex

The synthesis of  $\eta^6$ -arene tungsten(0) complexes generally proceeds in low yield<sup>[33, 61]</sup>. An analysis of the yields in the paper of the group of *Angelici*<sup>[33]</sup> that was taken as the basis for this project showed, that arenes with a larger number of electron-rich substituents increase the yields. The length of the alkyl chain between the arene and the fluorine atoms was set to be 2 or 3 atoms. With these two criteria in mind, the best commercially available substrate was found to be 2-mesitylethanol, as it has three methyl-groups and the alkyl chain of appropriate length. Moreover, the alcohol group could be substituted by fluorine in one step using DAST and following a known synthetic procedure<sup>[62]</sup>. The yield of 67% fits the expectations for this method.



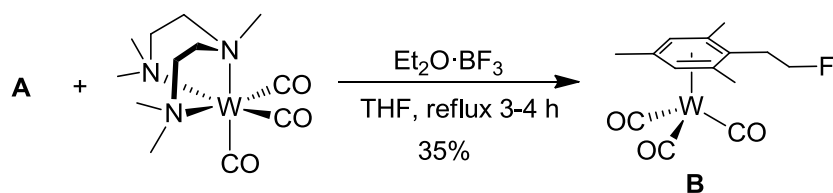
**Scheme 11.** Synthesis of the arene ligand **A**.

The synthesis of the complex **B** was done according to the publication by *Angelici*, but with 5 eq. of  $\text{BF}_3$  ether complex in comparison with the ligand. This was originally done by mistake, but later experiments with the “correct” 0.5 eq. were unsuccessful. A plausible explanation for this may be that there is an interaction between  $\text{BF}_3$  and the fluorine atom, such that it does not react with the ligand on the tungsten precursor. However this effect should vanish when more than 1 eq. of  $\text{BF}_3$  was added. Nevertheless, also with 2 eq. practically no product could be isolated. Later syntheses were then again carried

<sup>2</sup> The data and the plots are given in the appendix.



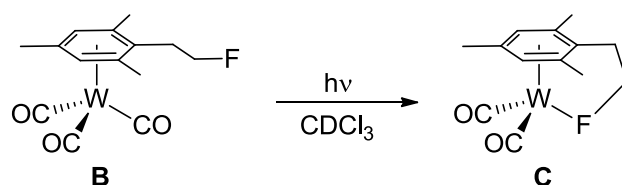
out with 5 eq. of  $\text{BF}_3$  and worked again well. The yield of 35% is well in the same range than for other complexes of this type.



Scheme 12. Preparation of the tungsten complex B.

### 3.3.2 Irradiation of the complex

The irradiation of the complex B could first only be done with a weak UV lamp, as the mercury arc lamp was not available due to a defect. The experiment was carried out in deuterated chloroform in a young NMR tube. After a short time of irradiation a very small signal could be observed in the  $^{19}\text{F}$ -NMR, furthermore the originally yellow solution started to turn green. The irradiation was continued over 12.5 h, with reaction control  $^1\text{H}$ - and  $^{19}\text{F}$ -NMR experiments in 2 h intervals, as the lamp could not be used for more than 2 h at once, out of technical reasons. A small kinetic study based on the ratio of integrals of a new and an old signal in the  $^1\text{H}$ -NMR then showed that the experiment would take about 45 h of irradiation until the reaction would be complete, assuming first order kinetics for the reaction, as this is normally the case for photochemical reactions. It was thus decided to continue the experiments when the coolable mercury arc lamp was available again.



Scheme 13. Proposed reactivity of B upon irradiation.

Another observation that could be made from the first experiment was that with more irradiation time, there is more formation of a black precipitate. Thinking of this precipitate as some decomposed tungsten species, the spectra were controlled again, finding that the newly formed peak in the  $^{19}\text{F}$ -NMR spectra was actually very similar to the signal observed for the free ligand, even though the coupling constants do not correspond perfectly to the ones of the free ligand. To better characterize the type of the new species, a  $^{13}\text{C}$ -NMR spectrum was recorded, as the carbonyl ligands have a rather characteristic shift, one would have to see 2 signals, one of the unreacted complex and one of the assumed product complex. Indeed, another signal in the range of the carbonyl  $^{13}\text{C}$  nuclei could be seen, however it is a very small signal (figure 20, A) and could as well be an artifact, given the fact, that many of the other signals correspond well to the ligand or to the complex (B).

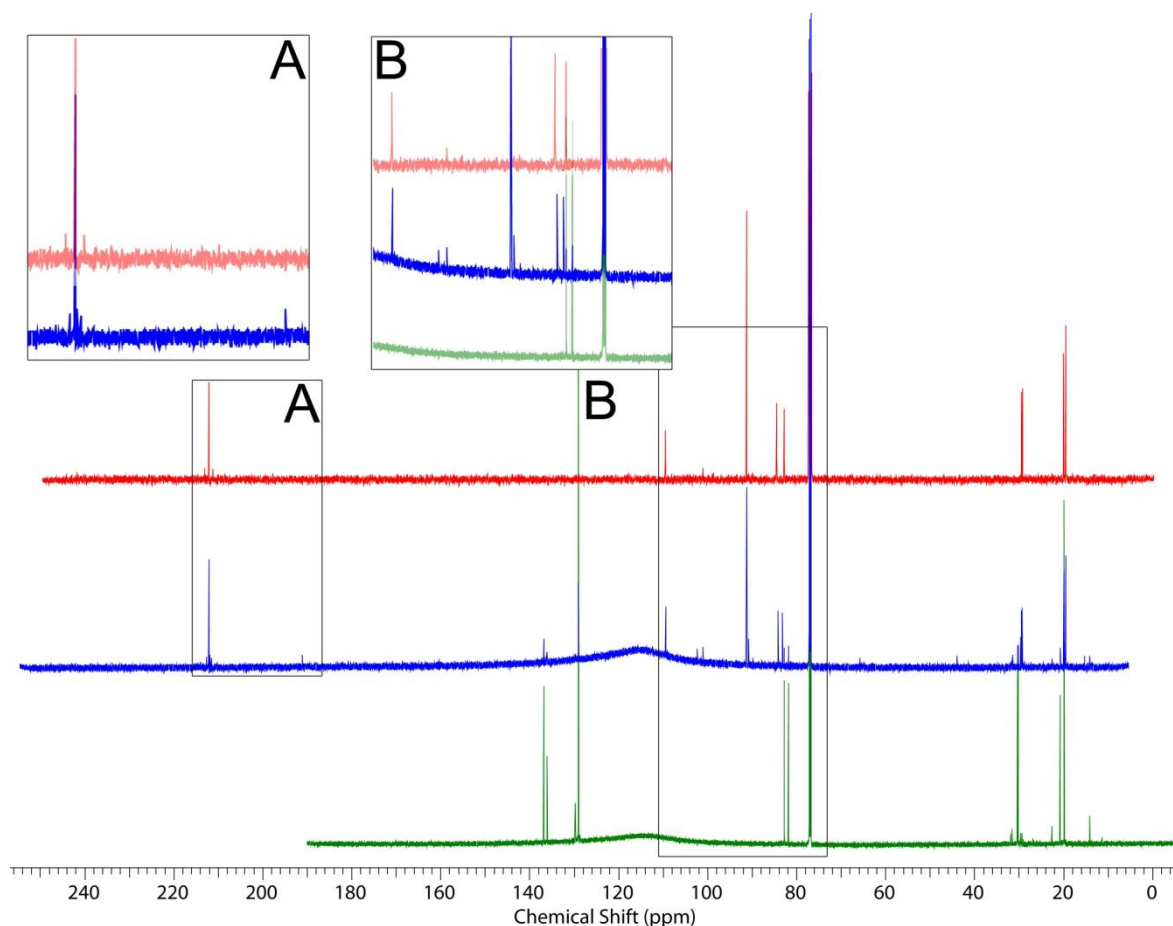


**Figure 20.** Comparison of the spectra of **B** (red) the irradiation product spectrum (blue) and spectrum of **A** (green).

Anyhow, the experiments were to be continued with the same complex but with the stronger lamp in order to get more of the new product. The first experiment with the mercury arc lamp was run for 5 h and lead to a brown solution, a lot of black precipitate and no signal could be observed in the  $^{19}\text{F}$ -NMR spectra anymore. Thus the experiment was redone with shorter irradiation durations and the product could be observed again after 20 min of irradiation, after 40 min of irradiation, there was already more than 50% of product in the mixture. After another 20 min of irradiation, there was again total decomposition as in the first experiment.

### 3.3.3 $^{183}\text{W}$ -NMR Experiments

Publications by the group of Pregosin pointed out, that it is possible to record  $^{183}\text{W},\text{X}$ -experiments on at least one available spectrometer (*Bruker AV 500*)<sup>[63]</sup>. Unfortunately, the parameters that have been used for these experiments were unavailable. Thus the first thing to do was to find the  $\pi/2$ -pulse for  $^{183}\text{W}$  nuclei but this already brought up the first problems: The 1D-NMR spectra of  $^{183}\text{W}$  could not be recorded, most probably due to the low frequency of the detection and therefore incompatibility with the hardware. This assumption was later confirmed when it was tried to measure the  $^{103}\text{Rh}$  standard as 1D NMR experiment, which did also not work.

It was then tried to find the signal for the complex **B** by just applying a  $^{183}\text{W},^1\text{H}$ -HMQC sequence that was adapted from the analogous  $^{103}\text{Rh},^1\text{H}$ -correlation experiment, using also the same  $\pi/2$ -pulse of 25  $\mu\text{sec}$ . This approach was unsuccessful at first, also given that that the chemical shift of this compound in the  $^{183}\text{W}$  NMR spectra was completely unknown and could only be assumed by deriving

from known shifts of scarcely similar compounds. To avoid this problem, a saturated sample of bis(cyclopentadienyl)tungstentricarbonyl dimer in  $\text{CDCl}_3$  was prepared, as here the chemical shift was known. Indeed, the signal could be found for the first time, using the 500 MHz spectrometer. Then new experiments were set up, screening the whole  $^{183}\text{W}$ -shift range to find the shift for complex **B**. Figure 21 shows the spectrum of complex **B** with  $\delta = -2695$  ppm (reference:  $\text{NaWO}_4$ ). Interestingly, only peaks for the methylgroups of the arene in complex **B** showed correlation peaks, not the aromatic protons. New spectra were recorded using a longer delay  $\Delta$  (delay before the  $\pi/2$ -pulse on the  $^{183}\text{W}$  channel, where the magnetization transfer takes place). The longer delay corresponds to a smaller coupling constant between  $^1\text{H}$  and  $^{183}\text{W}$ , but no correlation peaks with the aromatic protons could be observed with either 0.3 or 0.5 s delay.

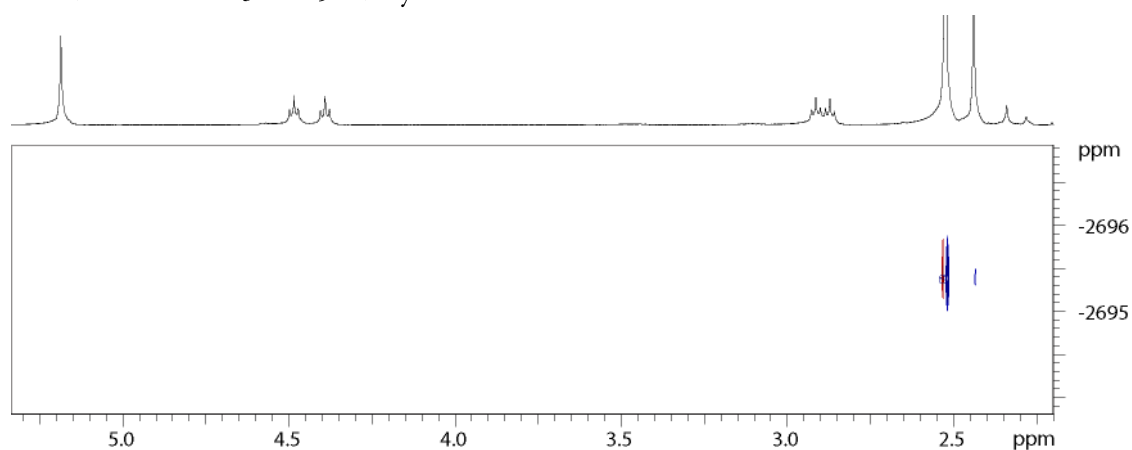


Figure 21.  $^1\text{H}, ^{183}\text{W}$ -HMQC spectrum of **B** with a delay  $\Delta$  of 0.1 s.

The final parameters used to record the spectra were chosen as follows:  $\pi/2$ -pulse on the  $^{183}\text{W}$  channel of 30  $\mu\text{sec}$  with a pulse output of 0.0 dB and a relaxation delay of 0.5 sec.

## 4 Conclusion and Outlook

### 4.1 Phosphines

The synthesis of the diisopropylphosphines was tedious and did never yield a perfectly pure product which would be the basis for pure complexes, even after borane protection and consequent column chromatography and deprotection, the product was still impure. Another approach that was found in the literature but never tried would be a palladium catalyzed synthesis of the phosphines, the procedure for that was published recently by the group of *Buchwald*<sup>[64]</sup>. This method was described as a very neat method to prepare dicyclohexylphosphines with a good yield, so it seems that the method would be worth a try. Nevertheless, one has to note that the synthesis was carried out not with the naphthylbromide but with the iodide, furthermore the fluorine atoms might influence the product formation. These differences might be crucial, as well as of course the change from cyclohexyl to isopropyl.

**4** has been seen to crystallize nicely when protected with borane, **7** can be crystallized unprotected. Thus it would be possible to get crystal structures of these two ligands, which could give a further information about these phosphines. Furthermore it would be possible to crystallize the borane adduct of **3** too when appropriate solvents are used.

Instead of fluorine, the NpF containing phosphines could also be prepared with bromine or iodine substituted naphthalenes at the position of the fluorine atom. In both cases the 1,8-bromo-/iodonaphthalene could be used as precursors. Complexes with these phosphines could then be studied in analogous manner to characterize the influence of the halide in that position.

## 4.2 Structures of the Rh-Complex Conformers

The only compound that was prepared in this thesis where the results of the VT-NMR experiments could not be explained was the complex **Rh-4**. Here it seems that minor impurities in the NMR sample had a large influence on the dynamics of the complex, such that only one conformer could be seen at low temperature. This could not be explained by the hypothesis stated in the discussion concerning the structures of the conformers. Thus it is obvious that these results must be confirmed using a complex which is as clean as possible. The sample that was used for the NMR study already was taken from the crystals that were obtained, so it should already have been rather pure, even though it could also be that the minor impurities were crucial for the crystallization process to set in.

Concerning DFT calculations, of course the methods could be refined but foremost it would be really interesting to find the third structure, the one of the *exo* conformer. This would take some more work, the basic structure is not already known from a crystal structure. After identifying the soft parameters of the complex, mainly, vibrational and rotational modes, one could try to find a somewhat low energy conformer for the *exo* structure and then refine this state.

In the discussion of the simulations for the kinetics and activation energies of the complexes, it has been mentioned how difficult a reliable simulation is, especially at high temperatures. To ease this problem, it would be possible to fit the data not by hand but let the computer fit the data, based on the spectra. This however would take more than a week to implement and was therefore not done in this thesis. If there would be a deeper interest in the kinetics and thermodynamics of the studied complexes, it might be a valuable expansion of the reliability of the collected data, and one could for instance also fit the fluorine spectra more easily than this can be done by hand.

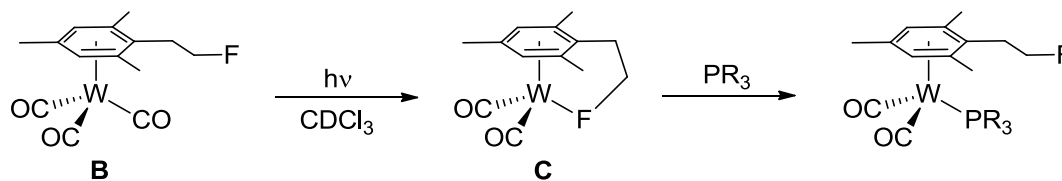
Otherwise it would be advisable to repeat the experiments with the ligand **7**: On one hand trying to get a complete reaction with the iridium precursor. On the other hand study the reaction with simultaneous chloride abstraction from the rhodium precursor. If both reactions would be carried out with appropriate concentrations, they could give interesting new input concerning the reaction with electron-poor ligands and induction of a stronger Rh-F interaction, respectively.

## 4.3 Tungsten complexes and NMR studies

The tungsten complexes have been treated rather marginally in the course of this project. This is mainly due to the long periods where it was unclear whether or not the irradiation works and yields the expected product. As it is clear that the irradiation was unsuccessful the idea is now to change the arene ligand slightly. This could be done in two ways: Either prolong the alkyl chain to the fluorine by one carbon unit or change the fluorine containing substituent to a CF<sub>2</sub> or CF<sub>3</sub> unit. Both approaches could help improving the coordination of fluorine to tungsten. It remains unclear, however, whether these slight changes would actually prohibit the irradiation from decomposing the complex.

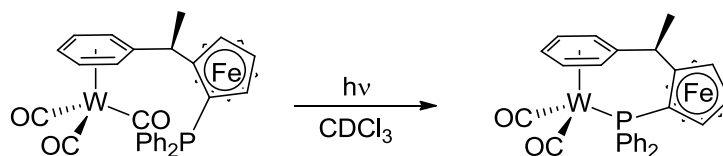
If the suggested coordination really would take place, it has further been shown that other ligands can be added to the solution such that the weakly coordinating ligand would give the coordination site

away again (scheme 14). With this method one could probably introduce a stereocenter at the central metal, as this has been shown to be possible with ruthenium.



**Scheme 14.** Use of the intermediary W-F bond to introduce a phosphine.

Another approach would be the introduction of a phosphine on the alkyl chain instead of fluorine. Even though this would somewhat contradict the idea of this project ( $\text{CF}\cdots\text{M}$  interaction), it would still be nice to see if a phosphine would be able to coordinate. A possible arene ligand would be the aryloxyferrocenephosphines (scheme 15) that have already been prepared in this group and have been shown to form half-sandwich complexes with other central metals<sup>[65]</sup>. These ligands would bring the advantage of already having a stereocenter, and the course of the reaction would be better observable in the NMR as the  $^{183}\text{W}$ ,  $^{31}\text{P}$  coupling is much larger than the one with fluorine ( $^1J_{\text{WP}} = 200\text{-}500$  Hz vs.  $^1J_{\text{WF}} = 12\text{-}71$  Hz<sup>[45]</sup>).



**Scheme 15.** Inducing a W-P bond by irradiation of an enantiomerically pure complex.

In any case it would be recommendable to screen some more of the  $\eta^6$ -arene tungsten(0) complexes, as these have been rather neglected in the course of publications on  $^{183}\text{W}$ -NMR. As it seems, complexes where the arene has methylsubstituents allow a better application of the  $^1\text{H}$ ,  $^{183}\text{W}$  – correlation experiments.

## 5 Experimental

### 5.1 General Remarks

#### 5.1.1 Chemicals

Bromo(8-Fluoronaphthalen-1-yl) and diphenyl(1-fluoronaphthalen-1-yl)phosphine **1** were provided by Barbara Czarniecki, as well as the corresponding rhodium **Rh-1** and iridium cyclooctadiene complex **Ir-1**. The nonfluorinated rhodium diphenylphosphino cyclooctadiene complex **Rh-8** was obtained from Nicolas Bennett. The acid trifluoromethylation agent, 1-trifluoromethyl-1,2-benziodoxol-3-(1H)-one, was prepared by Johannes Windisch.

DAST and 2-mesitylethanol were purchased from *ABCR*, tungsten hexacarbonyl from *ACROS*.

#### 5.1.2 Techniques

All reactions were carried out under argon-atmosphere using standard *Schlenk* techniques or in a glove box (*MBraun*, *MB 150B-G*) under nitrogen. Glassware were preheated in an oven at 140 °C, dried under HV and then put under argon.

The solvents for synthetic processes were of “purriss. P.a.” quality (*Fluka AG*, *Riedel-de-Häen*, *J. T. Baker* or *Merck*). Anhydrous solvents were distilled under argon from Na/benzophenon (THF, Et<sub>2</sub>O, pentane) or CaH<sub>2</sub> (CH<sub>2</sub>Cl<sub>2</sub>).

Deuterated solvents were purchased from *Cambridge Isotope Laboratories* (CD<sub>2</sub>Cl<sub>2</sub>) or *Armar Chemicals* (CDCl<sub>3</sub>), and distilled analogously, then degassed *via* 3 freeze-pump-thaw cycles and stored in a Young-schlenk under argon over activated 3 Å molecular sieves.

For flash chromatography and TLC, technical grade solvents were used.

Concentrations of purchased Grignard reagents were titrated according to the method of *Krasovskiy* and *Knoche*<sup>[66]</sup>.

#### 5.1.3 Analytical techniques and instruments

**Thin layer chromatography (TLC)** *Merck 60-F<sub>254</sub>* visualized by fluorescence quenching at 254 nm. R<sub>f</sub> is the retention factor for the ratio of given solvents

**Column chromatography** Chromatographic purification over *Fluka Silica Gel 60* (230-400 mesh) or neutral aluminum oxide (*Fluka, MP Biomedicals*) using the given solvent ratios. To increase the flow rate, a pressure of about 0.2 bar (nitrogen) was applied.

**Melting points (Mp)** were measured on a *Büchi Melting point B-540* melting point apparatus in open capillaries. The given temperatures (°C) are uncorrected.

**NMR spectra** were measured on *Bruker Avance 500*, 400, 250, 200 or *Bruker AV 700* spectrometers operating at the given spectrometer frequency. The samples were measured as solution in the given deuterated solvent at room temperature in non-spinning mode, if not stated otherwise. Chemical shifts ( $\delta$ ) are expressed in parts per million (ppm) with respect to TMS as an external standard for <sup>1</sup>H-NMR and <sup>13</sup>C-NMR spectra and are calibrated with the solvent residual peak<sup>[67]</sup>. For <sup>19</sup>F, <sup>31</sup>P, <sup>103</sup>Rh, <sup>183</sup>W-NMR spectra external standards according to IUPAC were used<sup>[39]</sup>: CCl<sub>3</sub>F, H<sub>3</sub>PO<sub>4</sub> (85%), Rh(acac)<sub>3</sub> (CDCl<sub>3</sub>, sat.) and NaWO<sub>4</sub> (1 M in D<sub>2</sub>O), respectively. Coupling constants *J* are given in Hertz (Hz) as

absolute values. The multiplicity is abbreviated as follows: s = singlet, d = doublet, t = triplet, q = quartet, quin = quintet, sept = septet, tt = triplet of triplet, br = broad, m = multiplet,  $\psi$  = appears as. Other abbreviations used: ar = aromatic, quat = quaternary, Me = methyl, Ph = phenyl, Np = naphthyl. The respective positions in the phenyl-rings are denoted with i = ipso, o = ortho, m = meta and p = para. The respective positions in Naphthyl, COD and nbd are denoted as follows:

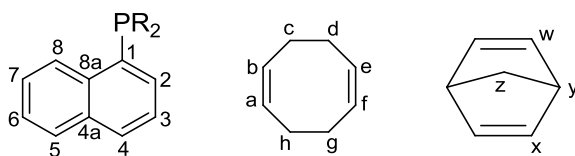
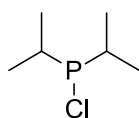


**Figure 22.** Denotation of the positions in Np, COD and nbd.

**High-resolution mass spectra (HiRes-MS)** were recorded by the *MS-Service* of the “*Laboratorium für organische Chemie der ETHZ*” on a *IonSpec (Varian) Ultima* (ESI-MS, MALDI-MS) or *Micromass (Waters) Autospec Ultima* (EI-MS) mass spectrometer. The signals are given as mass per charge number ( $m/z$ ) and the intensity in % of the basis peak.

**Crystallography** Intensity data of single crystals glued to a glass capillary were collected at 100 K on the *Bruker SMART APEX* platform with CCD detector and graphite monochromated Mo- $K_{\alpha}$ -radiation ( $\lambda = 0.71073 \text{ \AA}$ ). The program SMART served for data collection; integration was performed with the software SAINT<sup>[68]</sup>. The structure was solved by direct methods using the program SHELXS-97<sup>[69]</sup>. The refinement and all other calculation were carried out using SHELXL-97<sup>[70]</sup>. All non-hydrogen atoms were refined anisotropically using weighted full-matrix least-squares on  $F^2$ . The hydrogen atoms were included in calculated position and treated as riding atoms using SHELXL default parameters. In the end absorption correction was applied (SADABS)<sup>[71]</sup> and weights were optimized in the final refinement cycles. Associated crystallographic data and further experimental details are given in the Appendix.

## 5.2 Chloro diisopropylphosphine



$C_6H_{14}ClP$   
152.60 g/mol

### 5.2.1 Synthesis

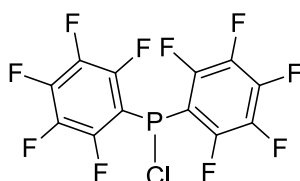
12.8 mL (88.2 mmol) of diethylphosphoramidous dichloride were dissolved in 100 mL diethyl ether, cooled with a NaCl/ice bath and a solution of isopropyl magnesiumchloride (90mL, 1.96 M in THF, 176.4 mmol, 2.0 eq.) was slowly added. The solution is filtered and the residues washed twice with 30 mL diethyl ether, then 92 mL of HCl solution in ether (2 M, 185.2 mmol, 2.1 eq.) were added dropwise at  $-20\text{ }^{\circ}\text{C}$ . The solution was then concentrated and the remaining oil is distilled (0.05 mbar,  $45\text{ }^{\circ}\text{C}$ ) to yield about 9 mL (56.6 mmol, 64%) of a colorless oil.

### 5.2.2 Characterization

$^1\text{H-NMR}$  (400.13 MHz,  $\text{CD}_2\text{Cl}_2$ ):  $\delta = 2.01$  (dsept,  $^3J_{\text{HH}} = 8.4\text{ Hz}$ ,  $^2J_{\text{PH}} = 7.0$ , 2 H,  $\text{CH}(\text{CH}_3)_2$ ), 1.18 (dd,  $^3J_{\text{PH}} = 13.8\text{ Hz}$ ,  $^3J_{\text{HH}} = 7.1$ , 12 H,  $\text{CH}(\text{CH}_3)_2$ ).

$^{31}\text{P-NMR}$  (162.0 MHz,  $\text{CD}_2\text{Cl}_2$ ):  $\delta = 136.7$  (s).

## 5.3 Chloro bis(pentafluorophenyl)phosphine



$C_{12}ClF_{10}P$   
400.54 g/mol

### 5.3.1 Synthesis

4.30 g (176.8 mmol, 1.26 eq.) of magnesium turnings were suspended in 30 mL diethyl ether and a crystal of iodine is added to activate the magnesium. Then, 17.5 mL (140.3 mmol) of 1-bromopentafluorobenzene in 50 mL diethyl ether were added dropwise, after the addition, the solution was heated to reflux for 45 min to form the Grignard reagent, a dark-brown mixture. This solution was then added dropwise to 10 mL (67.0 mmol, 0.5 eq.) diethylphosphoramidous dichloride in 60 mL diethyl ether, the reaction mixture then stirred for another hour. The solvent was then removed to store the product. Later, the dark-brown solid was dissolved in diethyl ether, when the flask broke. As much of the solid as possible was collected and dissolved in bottle diethyl ether and the solution then flushed with argon. 56 mL HCl solution in diethyl ether (2 M, 104 mmol) were added dropwise to the solution, then the solution was filtered, the residues washed with 40 mL diethyl ether and the solvent evaporated. The remaining oil was distilled twice, the second time using a vigreux column (0.014 mbar,  $94\text{ }^{\circ}\text{C}$ ), but the two species could not be separated.

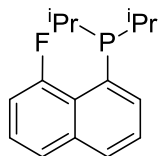


### 5.3.2 Characterization

$^{19}\text{F-NMR}$  (188.3 MHz,  $\text{CDCl}_3$ ):  $\delta = -127.8 - -128.3$  (m, 1F),  $-129.4 - -129.9$  (m, 2F),  $-146.3 - -146.7$  (m, 2F),  $-159.1 - -159.6$  (m, 5F).

$^{31}\text{P-NMR}$  (80.0 MHz,  $\text{CDCl}_3$ ):  $\delta = 36.1$  (quin,  $^3J_{\text{PF}} = 39.5$  Hz),  $11.6$  (quin,  $^3J_{\text{PF}} = 33.9$  Hz).

## 5.4 Diisopropyl(5,6,7,8-tetrafluoronaphthalen-1-yl)phosphine (3)



$\text{C}_{16}\text{H}_{20}\text{FP}$   
262.30 g/mol

### 5.4.1 Synthesis

198.4 mg (0.88 mmol) of Bromo(8-fluoronaphthalen-1-yl) were dissolved in 10 mL  $\text{Et}_2\text{O}$  and cooled to  $-78^\circ\text{C}$  by a dry ice/*i*-PrOH cooling bath. Then, 0.55 mL of *n*-Butyllithium (1.6 M in *n*-hexane, 1.07 mmol, 1 eq.) were added over 5 min. Upon the addition, the solution turned yellow. After 30 min of stirring, 0.14 mL (1.17 mmol, 1 eq.) of chloro diisopropylphosphine were added dropwise and the cooling bath was removed after 5 min, stirring was continued for about 18 h. The color of the solution changed from yellow to clear brown which got weaker over time.

For work-up, the reaction mixture was quenched with 5 mL brine/water (ratio about 4:1), the aqueous phase was separated off and the organic layer dried over magnesium sulfate. The liquid was then filtered through basic alumina, the filtrate washed two times with 2 mL  $\text{Et}_2\text{O}$ . The solvent was then evaporated to yield 229.0 mg of crude product (99% yield, about 10% impurities).

For a further purification, the phosphine was protected with borane by dissolving it in 2 mL  $\text{Et}_2\text{O}$  and adding 1 mL of  $\text{BH}_3\cdot\text{THF}$  (1M) and stirring over night. Then the phosphine was chromatographed over silica (hex/DCM 4:1 $\rightarrow$ 1:1) as an eluent, the ratio stepwise be changed to 1:1. Deprotection was done by refluxing the product in 5 mL of diethylamine over night followed by evaporation of the solvent. The product is a slightly yellow oil.

### 5.4.2 Characterization

$^1\text{H-NMR}$  (700.13 MHz,  $\text{CDCl}_3$ ):  $\delta = 7.85$  ( $\psi\text{d}$ ,  $J = 7.8$  Hz, 1H, H2),  $7.68$  ( $\psi\text{d}$ ,  $J = 6.4$  Hz, 1H, H4),  $7.67$  ( $\psi\text{d}$ ,  $J = 7.9$  Hz, 1H, H5),  $7.50$  ( $\psi\text{t}$ ,  $J = 7.7$  Hz, 1H, H2),  $7.40$  ( $\psi\text{dt}$ ,  $J = 8.1$  Hz, 4.8 Hz, 1H, H7),  $7.22$  ( $\psi\text{dd}$ ,  $J = 13.3$  Hz, 7.6 Hz, 1H, H9),  $2.26$  (m, 2H,  $\text{CH}(\text{CH}_3)_2$ ),  $1.16$  (dd,  $^3J_{\text{PH}} = 93.2$  Hz,  $^3J_{\text{HH}} = 7.1$  Hz, 6H,  $\text{CH}(\text{CH}_3)_2$ ),  $1.14$  (dd,  $^3J_{\text{PH}} = 92.1$  Hz,  $^3J_{\text{HH}} = 7.0$  Hz, 6H,  $\text{CH}(\text{CH}_3)_2$ ).

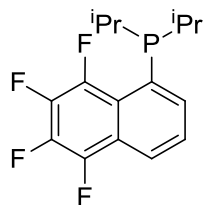
$^{13}\text{C-NMR}$  (176.0 MHz,  $\text{CDCl}_3$ ):  $\delta = 160.3$  (d,  $J = 257.0$ , 1C, C8),  $136.2$  (s, 1C,  $\text{C}_{\text{quat}}$ ),  $132.1$  (s, 1C, C4),  $128.9$  (s, 1C, C2),  $125.4$  (s, 1C, C7),  $125.4$  (s, 1C, C2),  $125.2$  (s, 1C,  $\text{C}_{\text{quat}}$ ),  $125.1$  (s, 1C, C5),  $111.7$  (s, 1C, C6),  $24.2$  (dd,  $^1J_{\text{PC}} = 15.7$  Hz,  $^2J_{\text{PC}} = 5.3$  Hz, 2C,  $\text{CH}(\text{CH}_3)_2$ ),  $19.8$  (d,  $^2J_{\text{PC}} = 12.8$  Hz, 2C,  $\text{CH}(\text{CH}_3)_2$ ),  $19.4$  (d,  $^2J_{\text{PC}} = 17.4$  Hz, 2C,  $\text{CH}(\text{CH}_3)_2$ ).

$^{19}\text{F-NMR}$  (376.5 MHz,  $\text{CDCl}_3$ ):  $\delta = -102.8$  (d,  $J_{\text{PF}} = 224.3$  Hz, F8).

$^{31}\text{P-NMR}$  (162.0 MHz,  $\text{CDCl}_3$ ):  $\delta = 11.6$  (br).

MS (ESI-MS): [M+H<sup>+</sup>], calc. 263.1359; found 263.1362 (100%).

## 5.5 Diisopropyl(5,6,7,8-tetrafluoronaphthalen-1-yl)phosphine (4)



C<sub>16</sub>H<sub>17</sub>F<sub>4</sub>P  
316.27 g/mol

### 5.5.1 Synthesis

271.8 mg (0.97 mmol) of Bromo(5,6,7,8-tetrafluoronaphthalen-1-yl) was dissolved in 10 mL Et<sub>2</sub>O and cooled to -78° C by a dry ice/*i*-PrOH cooling bath. Then, 0.67 mL of *n*-Butyllithium (1.6 M in *n*-hexane, 1.07 mmol, 1.1 eq.) were added over 5 min. Upon the addition, the solution turned green (color may differ to more yellow or blue). After 30 min of stirring, 0.19 mL (1.17 mmol, 1.2 eq.) of chloro diisopropylphosphine were added dropwise and the cooling bath was removed after 5 min, stirring is continued for about 18 h. The color of the solution first changed from yellow to colorless, then got suspensious dark grey to pale yellow, when the reaction was finished.

For work-up, the reaction mixture was quenched with 5 mL brine/water (ratio about 4:1), the aqueous phase was separated off and the organic layer was dried over magnesium sulfate. The liquid was then filtered through basic alumina, the filtrate washed two times with 2 mL Et<sub>2</sub>O. The solvent was then evaporated to yield 230.0 mg of crude product (74%, about 10% impurities).

For a further purification, the phosphine was protected with borane by dissolving it in 2 mL Et<sub>2</sub>O, adding 1 mL of BH<sub>3</sub>·THF (1M) and stirring over night. Then the phosphine was chromatographed over silica (hex/DCM 4:1). The clean phosphinoborane was then deprotected by refluxing in diethylamine over night and the solvent was evaporated to yield the clean product, a colorless solid.

### 5.5.2 Characterization

<sup>1</sup>H-NMR (500.23 MHz, CDCl<sub>3</sub>): δ = 8.05 (ψd, *J* = 8.4 Hz, 1H, H4), 7.75 (ψd, *J* = 6.6 Hz, 1H, H2), 7.58 (ψt, *J* = 7.7 Hz, 1H, H3), 2.22 (m, 2H, CH(CH<sub>3</sub>)<sub>2</sub>), 1.07 (dd, <sup>3</sup>*J*<sub>PH</sub> = 76.5 Hz, <sup>3</sup>*J*<sub>HH</sub> = 6.6 Hz, 6H, CH(CH<sub>3</sub>)<sub>2</sub>), 1.04 (dd, <sup>3</sup>*J*<sub>PH</sub> = 74.3 Hz, <sup>3</sup>*J*<sub>HH</sub> = 6.8 Hz, 6H, CH(CH<sub>3</sub>)<sub>2</sub>).

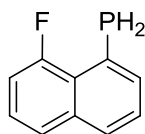
<sup>13</sup>C-NMR (125.8 MHz, CDCl<sub>3</sub>): δ = 145.1 (d, *J* = 259.9 Hz, 1C, C8), 142.4 (d, *J* = 250.8, 1C, C5), 139.5 (d, *J* = 248.3 Hz, 1C, C<sub>Np</sub>), 137.5 (d, *J* = 249.9, 1C, C<sub>Np</sub>), 134.0 (s, 1C, C2), 133.0 (s, 1C, C<sub>Np</sub>), 126.5 (s, 1C, C<sub>3</sub>), 123.9-123.6 (m, 1C, C1), 121.7 (s, 1C, C<sub>Np</sub>), 120.7 (s, 1C, C4), 24.6 (dd, <sup>1</sup>*J*<sub>PC</sub> = 17.2 Hz, <sup>2</sup>*J*<sub>CP</sub> = 5.4 Hz, 2C, CH(CH<sub>3</sub>)<sub>2</sub>), 19.7 (m, 4C, CH(CH<sub>3</sub>)<sub>2</sub>).

<sup>19</sup>F-NMR (470.7 MHz, CDCl<sub>3</sub>): δ = -133.2 (br d, *J*<sub>PF</sub> = 238.2 Hz, F8), -150.6 (ψt, *J* = 16.6 Hz, 1F, F5), -159.9 (ψt, *J* = 19.4 Hz, 1F, F7), -160.8 (ψt, *J* = 19.4 Hz, 1F, F6).

<sup>31</sup>P-NMR (202. MHz, CDCl<sub>3</sub>): δ = 11.0 (br).

MS (ESI-MS): [M+H<sup>+</sup>], calc. 317.1077; found 333.1037 ([M+OH<sup>+</sup>], 100%), 317.1078 (4.6%).

## 5.6 (8-Fluoronaphtalen-1-yl)phosphine (5)



$C_{10}H_8FP$   
178.14 g/mol

### 5.6.1 Synthesis

227.0 mg (1.01 mmol) of Bromo(8-Fluoronaphtalen-1-yl) were dissolved in 10 mL THF and cooled to  $-78\text{ }^{\circ}\text{C}$ . 0.69 mL *n*-Butyllithium (1.6 M in hexane, 1.04 mmol, 1.1 eq.) were slowly added, the solution turning yellow. The solution was stirred for 30 min, then 0.21 mL (1.71 mmol, 1.7 eq.) of diethyl chlorophosphate were added and the cooling bath was removed after 5 min, stirring was continued over night. The mixture was quenched with 5% HCl and the aqueous layer was extracted three times with diethyl ether. The combined organic layers were washed twice with brine and dried over magnesium sulfate, evaporation of the solvent yielded the diethyl(8-Fluoronaphtalen-1-yl)phosphonate.

130 mg (3.27 mmol, 3.3 eq.) LAH was suspended in diethyl ether and cooled to  $-78\text{ }^{\circ}\text{C}$ , 0.40 mL (3.12 mmol, 3.1 eq.) TMSCl were added dropwise, the cooling bath removed and the suspension was stirred for 30 min. Then the cooling bath was reapplied again, and the phosphonate was added as a solution in 1 mL ether and the cooling bath is immediately removed after the addition, the solution stirred over night. The workup was done analogous to the procedure of Fieser *et al.*<sup>[72]</sup> to yield 177.2 mg (0.99 mmol, 98%) of the slightly impure product.

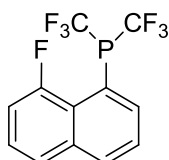
### 5.6.2 Characterization

$^1\text{H-NMR}$  (400,13 MHz,  $\text{CDCl}_3$ ): 7.76 ( $\psi\text{d}$ ,  $J = 8.4\text{ Hz}$ , 1H,  $\text{H}_{\text{Np}}$ ), 7.66 ( $\psi\text{t}$ ,  $J = 6.8\text{ Hz}$ , 1H,  $\text{H}_{\text{Np}}$ ), 7.62 ( $\psi\text{d}$ ,  $J = 8.4\text{ Hz}$ , 1H,  $\text{H}_{\text{Np}}$ ), 7.40 ( $\psi\text{q}$ ,  $J = 5.2\text{ Hz}$ , 1H,  $\text{H}_{\text{Np}}$ ), 7.37 ( $\psi\text{t}$ ,  $J = 10.0\text{ Hz}$ , 1H,  $\text{H}_{\text{Np}}$ ), 7.22-7.13 (m, 1H,  $\text{H}_{\text{Np}}$ ), 4.47 (dd  $^1J_{\text{PH}} = 206.5\text{ Hz}$ ,  $^2J_{\text{HH}} = 24,4\text{ Hz}$ , 2 H,  $\text{PH}_2$ ).

$^{19}\text{F-NMR}$  (376.5 MHz,  $\text{CDCl}_3$ ):  $\delta = -110.1$  (d,  $J = 150.6\text{ Hz}$ ).

$^{31}\text{P-NMR}$  (162.0 MHz,  $\text{CDCl}_3$ ):  $\delta = -104.3$  (d,  $J = 150.6\text{ Hz}$ ).

## 5.7 Bis(trifluoromethyl)-(8-Fluoronaphtalen-1-yl)phosphine (6)



$C_{12}H_6F_7P$   
314.14 g/mol

### 5.7.1 Synthesis

429.5 mg (1.36 mmol, 2.2 eq.) of 1-Trifluoromethyl-1,2-beziodoxol-3-(1*H*)-one were suspended in 9 mL DCM and cooled to  $-78\text{ }^{\circ}\text{C}$ , 110.0 mg (0.62 mmol) of the phosphonate was added as an emulsion in 1 mL DCM and the solution stirred for 30 min. Then, 0.37 mL (2.47 mmol, 4 eq.) DBU

were added and the cooling bath was removed. The solution slowly turned dark red while stirring over night. After that, the solvent was removed at the rotavap, with only slightly reduced pressure (about 750 mbar) at 40 °C. From the remaining red slurry, the product was extracted with pentane and the liquid filtered over silica. Removal of the solvent at the rotavap yielded the product as a colorless oil (104.8 mg, 333.61  $\mu\text{mol}$ , 55%).

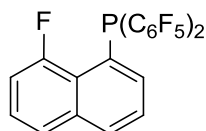
### 5.7.1 Characterization

$^1\text{H-NMR}$  (400.13 MHz,  $\text{CDCl}_3$ ):  $\delta = 8.14$  ( $\psi\text{dd}$ ,  $J = 6.6$  Hz, 3.6 Hz, 1H,  $\text{H}_{\text{Np}}$ ), 8.09 ( $\psi\text{d}$ ,  $J = 8.9$  Hz, 1H,  $\text{H}_{\text{Np}}$ ), 7.76 ( $\psi\text{d}$ ,  $J = 8.5$  Hz, 1H,  $\text{H}_{\text{Np}}$ ), 7.64 ( $\psi\text{t}$ ,  $J = 8.1$  Hz, 1H,  $\text{H}_{\text{Np}}$ ), 7.54 ( $\psi\text{td}$ ,  $J = 7.8$  Hz, 4.7 Hz, 1H,  $\text{H}_{\text{Np}}$ ), 7.36 ( $\psi\text{dd}$ ,  $J = 13.2$  Hz, 8.0 Hz, 1H,  $\text{H}_{\text{Np}}$ ).

$^{19}\text{F-NMR}$  (376.5 MHz,  $\text{CDCl}_3$ ):  $\delta = -53.32$  (dd,  $^2J_{\text{FF}} = 82.8$  Hz,  $^2J_{\text{FF}} = 7.5$  Hz, 6F,  $\text{CF}_3$ ),  $-104.3$  (dsept,  $^0J_{\text{PF}} = 250.1$  Hz,  $^2J_{\text{PF}} = 5.7$  Hz, 1F,  $\text{F}_{\text{Np}}$ ).

$^{31}\text{P-NMR}$  (162.0 MHz,  $\text{CDCl}_3$ ):  $\delta = 5.7$  (dsept,  $^0J_{\text{PF}} = 252.2$  Hz, 83.7).

## 5.8 Bis(pentafluorophenyl)-(8-Fluoronaphtalen-1-yl)phosphine (7)



$\text{C}_{22}\text{H}_6\text{F}_{11}\text{P}$   
510.24 g/mol

### 5.8.1 Synthesis

205.4 mg (0.91 mmol) of Bromo(8-Fluoronaphtalen-1-yl) were dissolved in 10 mL THF and cooled with a dry ice/isopropyl alcohol bath and 0.63 mL *n*-Butyllithium (1.6 M in hexane, 1.0 mmol, 1.1 eq.) were added slowly, the color of the solution changing to yellow. After 30 minutes of stirring, 0.25 mL (assumed 1.10 mmol, 1.2 eq.) of the (impure) chloro bis(pentafluorophenyl)phosphine were added dropwise. During the addition, the solutions color got pink before it changed back to yellow towards the end of the addition. The solution was stirred over night. For work-up, the reaction mixture was quenched with 5 mL of a degassed mixture of brine and deionized water, the aqueous phase removed and the organic phase filtered through alumina. The solvents were evaporated and the residues were chromatographed over silica (8:1 hex/DCM). The first fraction eluting the column was the product, 110.7 mg (0.22 mmol, 24%) of a slightly yellow solid were collected.

### 5.8.2 Characterization

$^1\text{H-NMR}$  (400.13, MHz,  $\text{CD}_2\text{Cl}_2$ ):  $\delta = 7.96$  ( $\psi\text{d}$ ,  $J = 8.1$  Hz, 1H,  $\text{H}_{\text{Np}}$ ), 7.76 ( $\psi\text{d}$ ,  $J = 8.1$  Hz, 1H,  $\text{H}_{\text{Np}}$ ), 7.51 ( $\psi\text{td}$ ,  $J = 7.8$  Hz, 5.5 Hz, 1H,  $\text{H}_{\text{Np}}$ ), 7.44 ( $\psi\text{t}$ ,  $J = 7.7$  Hz, 1H,  $\text{H}_{\text{Np}}$ ), 7.28 ( $\psi\text{t}$ ,  $J = 6.3$  Hz, 1H,  $\text{H}_{\text{Np}}$ ), 7.23 ( $\psi\text{dd}$ ,  $J = 13.2$  Hz, 7.7 Hz, 1H,  $\text{H}_{\text{Np}}$ ).

$^{19}\text{F-NMR}$  (376.5 MHz,  $\text{CD}_2\text{Cl}_2$ ):  $\delta = -108.7$  (dd,  $^0J_{\text{PF}} = 204.2$  Hz,  $^3J_{\text{HH}} = 13.2$  Hz, 1F,  $\text{F}_{\text{Np}}$ ),  $-129.9$  (m, 2F,  $\text{F}_{\text{o-Ph}}$ ),  $-150.3$  (m, 1F,  $\text{F}_{\text{p-Ph}}$ ),  $-161.0$  (m, 2 F,  $\text{F}_{\text{m-Ph}}$ ).

$^{31}\text{P-NMR}$  (162.0 MHz,  $\text{CDCl}_3$ ):  $\delta = -42.0$  (dqin,  $^0J_{\text{PF}} = 204.2$  Hz,  $^3J_{\text{PF}} = 37.7$  Hz).

## 5.9 Rh-Complexes: General Procedure

### 5.9.1 Synthesis

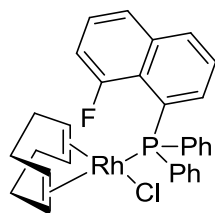
0.5 eq. of  $[\text{Rh}(\text{COD})\text{Cl}]_2$  were mixed with 1 eq. of the respective phosphine and dissolved in 1-2 mL DCM. After stirring for 2-3 h, the reaction mixture was concentrated to about 0.5 mL and the product precipitated with 10 mL pentane at low temperature (less than  $0^\circ$ ). Yields were not determined in most cases.

For further purification, the complex could be washed with pentane or recrystallized from diethyl ether with a small amount of DCM.

### 5.9.2 VT NMR Analysis

A full VT-NMR characterization was not possible due to the insufficient resolution of both 1D and 2D spectra. Therefore only the part of the signals is given which could be determined using the standard NMR techniques at low temperature: HMBC ( $^{13}\text{C}, ^1\text{H}$  and  $^{13}\text{C}, ^1\text{H}$  long-range),  $^{31}\text{P}, ^1\text{H}$ -HMQC,  $^1\text{H}, ^1\text{H}$ -COSY, and for some compounds also  $^1\text{H}, ^1\text{H}$ -NOESY,  $^1\text{H}, ^{19}\text{F}$ -HOESY,  $^{103}\text{Rh}, ^1\text{H}$  correlation.

## 5.10 Chloro(1,5-cyclooctadiene)(diphenyl(8-fluoronaphthalen-1-yl)phosphine)rhodium(I) (Rh-1)



$\text{C}_{30}\text{H}_{25}\text{ClFPRh}$   
576.87 g/mol

### 5.10.1 VT-NMR Analysis (203 K)

*Major*

$^1\text{H}$ -NMR (700.13 MHz,  $\text{CD}_2\text{Cl}_2$ ):  $\delta$  = 9.40-3.34 (m, 1H, H2), 7.76 ( $\psi\text{d}$ ,  $J$  = 6.2 Hz, 1H,  $\text{H}_{\text{p-Ph1}}$ ), 7.74 (underl. br, 1H, H3), 7.62-7.58 (m, 1H, H7), 7.57-7.53 (m, 1H,  $\text{H}_{\text{p-Ph2}}$ ), 7.46 (underl. br, 1H, H4), 7.44 (? , 2H,  $\text{H}_{\text{m-Ph1}}$ ), 7.36 ( $\psi\text{t}$ ,  $J$  = 7.1 Hz, 1H, H6), 7.33 ( $\psi\text{t}$ ,  $J$  = 7.1 Hz, 2H,  $\text{H}_{\text{m-Ph2}}$ ), 7.25 (br, 1H, H5), 7.05 ( $\psi\text{t}$ ,  $J$  = 7.2 Hz, 2H,  $\text{H}_{\text{o-Ph1}}$ ), 6.92-6.89 (m, 2H,  $\text{H}_{\text{o-Ph2}}$ ), 5.24 (br, 1H, Ha), 5.04 (br, 1H, Hb), 4.24 (br, 1H, Hf), 3.60 (br, 1H, He), 2.44 (br, 1H, 2H, Hd), 2.34 (br, 2H, Hg), 1.96 (br, 2H, Hc), 1.93-1.83 (m, 2H, Hh).

$^{13}\text{C}$ -NMR (176.0 MHz,  $\text{CD}_2\text{Cl}_2$ ):  $\delta$  = 158.1 (d,  $^1J_{\text{CF}}$  = 257.9 Hz, 1C, C8), 139.5 (s, 1C, C2), 133.5 (s, 2C,  $\text{C}_{\text{o-Ph2}}$ ), 132.8 (br, 2C,  $\text{C}_{\text{o-Ph2}}$ ), 130.8 (s, 1C, C7), 130.6 (s, 1C, C4), 129.4 (s, 1C, C6), 128.6 (s, 1C,  $\text{C}_{\text{p-Ph1}}$ ), 128.3 (s, 1C, C5), 126.6 (s, 2C,  $\text{C}_{\text{m-Ph1}}$ ), 125.2 (s, 3C,  $\text{C}_{\text{m/p-Ph2}}$ ), 125.2 (s, 1C, C3), 100.0 (br, 1C, Ca), 99.2 (br, 1C, Cb), 73.1 (br, 1C, Ce), 68.5 (br, 1C, Cf), 32.5 (s, 1C, Ch), 31.2 (s, 1C, Cc), 29.3 (s, 1C, Cd), 28.2 (s, 1C, Cg).

$^{19}\text{F}$ -NMR (658.8 MHz,  $\text{CD}_2\text{Cl}_2$ ):  $\delta$  = -97.9 (d,  $^2J_{\text{PF}}$  = 76.9 Hz).

$^{31}\text{P}$ -NMR (283.4 MHz,  $\text{CD}_2\text{Cl}_2$ ):  $\delta$  = 29.8 (d,  $^1J_{\text{RhP}}$  = 153.9 Hz,  $^2J_{\text{PF}}$  = 76.9 Hz).

$^{103}\text{Rh-NMR}$  (15.9 MHz,  $\text{CD}_2\text{Cl}_2$ ):  $\delta = -7625$ .

*Minor*

$^1\text{H-NMR}$  (700.13 MHz,  $\text{CD}_2\text{Cl}_2$ ):  $\delta = 6.86$  ( $\psi\text{dd}$ ,  $J = 11.4$  Hz, 7.4 Hz, 2H,  $\text{H}_{\text{o-Ph}_2}$ ), 5.40 (br, 1H,  $\text{H}_\text{a}$ ), 5.38 (br, 1H,  $\text{H}_\text{b}$ ), 3.30 (br, 1H,  $\text{H}_\text{f}$ ), 2.98 (br, 1H,  $\text{H}_\text{e}$ ) 2.55 (br, 2H,  $\text{H}_\text{g}$ ), 2.32 (br, 2H,  $\text{H}_\text{h}$ ), 1.96 (br, 2H,  $\text{H}_\text{d}$ ), 1.87 (br, 2H,  $\text{H}_\text{c}$ ).

$^{13}\text{C-NMR}$  (176.0 MHz,  $\text{CD}_2\text{Cl}_2$ ):  $\delta = 157.5$  (d,  $^1J_{\text{CF}} = 254.4$ , 1C, C8), 102.9 (s, 1C, Cb), 102.4 (s, 1C, Ca), 73.6 (s, 1C, Cf), 70.2 (s, 1C, Ce), 32.3 (s, 1C, Cd), 31.7 (s, 1C, Cg), 29.0 (s, 1C, Ch), 27.6 (s, 1C, Cc).

$^{19}\text{F-NMR}$  (658.8 MHz,  $\text{CD}_2\text{Cl}_2$ ):  $\delta = -101.9$  (d,  $^2J_{\text{PF}} = 87.3$  Hz).

$^{31}\text{P-NMR}$  (283.4 MHz,  $\text{CD}_2\text{Cl}_2$ ):  $\delta = 32.7$  (dd,  $^1J_{\text{RhP}} = 148.7$  Hz,  $^2J_{\text{PF}} = 87.3$  Hz).

$^{103}\text{Rh-NMR}$  (15.9 MHz,  $\text{CD}_2\text{Cl}_2$ ):  $\delta = -7667$ .

*Exo*

$^1\text{H-NMR}$  (700.13 MHz,  $\text{CD}_2\text{Cl}_2$ ):  $\delta = 9.85$  ( $\psi\text{d}$ ,  $J = 17.6$  Hz, 1H,  $\text{H}_2$ ), 8.23 (br, 1H,  $\text{H}_4$ ), 7.83 ( $\psi\text{d}$ ,  $J = 7.8$  Hz, 1H,  $\text{H}_{\text{p-Ph}_1}$ ),

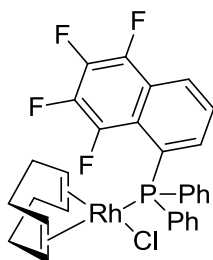
$^{13}\text{C-NMR}$  (176.0 MHz,  $\text{CD}_2\text{Cl}_2$ ):  $\delta =$

$^{19}\text{F-NMR}$  (658.8 MHz,  $\text{CD}_2\text{Cl}_2$ ):  $\delta = -101.5$  (br).

$^{31}\text{P-NMR}$  (283.4 MHz,  $\text{CD}_2\text{Cl}_2$ ):  $\delta = 42.5$  (d,  $^1J_{\text{RhP}} = 147.4$ ).

$^{103}\text{Rh-NMR}$  (15.9 MHz,  $\text{CD}_2\text{Cl}_2$ ):  $\delta = -7865$ .

## 5.11 Chloro(1,5-cyclooctadiene)(diphenyl(5,6,7,8-tetrafluoronaphthalen-1-yl)phosphine)rhodium(I) (Rh-2)



$\text{C}_{30}\text{H}_{25}\text{ClF}_4\text{PRh}$   
630.04 g/mol

### 5.11.1 VT-NMR Analysis (193 K)

*Major*

$^1\text{H-NMR}$  (700 MHz,  $\text{CD}_2\text{Cl}_2$ ):  $\delta = 8.14$  ( $\psi\text{d}$ ,  $J = 8.2$  Hz, 1H,  $\text{H}_4$ ), 7.44 ( $\psi\text{t}$ ,  $J = 7.4$  Hz, 1H,  $\text{H}_{\text{p-Ph}_1}$ ), 7.41 ( $\psi\text{t}$ ,  $J = 7.3$  Hz, 1H,  $\text{H}_3$ ), 7.29 (br, 2H,  $\text{H}_{\text{m-Ph}_1}$ ), 7.05-6.98 (m, 2H,  $\text{H}_{\text{o-Ph}_1}$ ), 6.92 ( $\psi\text{dd}$ ,  $J = 11.8$

Hz, 7.5 Hz, 1H, H2), 5.24 (br, 1H, Ha), 5,12 (br, 1H, Hb), 4.30 (br, 1H, He), 3.63 (br, 1H, Hf), 2.38 (m, 4H, Hd/h), 2.01 (br, 4H, Hc/g).

$^{13}\text{C-NMR}$  (176 MHz,  $\text{CD}_2\text{Cl}_2$ ):  $\delta = 143.3$  (d,  $^1J_{\text{CF}} = 255.8$  Hz, 1C, C8), 142.3 (d,  $^1J_{\text{CF}} = 250.6$  Hz, 1C, C5), 139.7 (d,  $^1J_{\text{CF}} = 249.5$  Hz, 1C,  $\text{C}_{\text{Np}}$ ), 137.7 (d,  $^1J_{\text{CF}} = 249.2$  Hz, 1C,  $\text{C}_{\text{Np}}$ ), 134.9-134.7 (underl. m, 1C, C4a), 134.8 (s, 1C, C2), 126.18 (s, 1C, C3), 122.1 (s, 1C, C4), 121.5-121.3 (m, 1C, C5a).

$^{19}\text{F-NMR}$  (658 MHz,  $\text{CD}_2\text{Cl}_2$ ):  $\delta = -130.7$  (dt,  $^0J_{\text{FP}} = 87.7$  Hz,  $^3J_{\text{FF}} = 16.8$ , 1F, F8),  $-147.7$  ( $\psi\tau$ ,  $J = 17.5$  Hz, 1F, F5),  $-156.5$  ( $\psi\tau$ ,  $J = 21.4$  Hz, 1F, F7),  $-158.2$  ( $\psi\tau$ ,  $J = 20.6$  Hz, 1F, F6).

$^{31}\text{P-NMR}$  (283.4 MHz,  $\text{CD}_2\text{Cl}_2$ ):  $\delta = 33.2$  (dd,  $^1J_{\text{RHP}} = 149.5$  Hz,  $^2J_{\text{PF}} = 87.7$  Hz).

$^{103}\text{Rh-NMR}$  (15.9 MHz,  $\text{CD}_2\text{Cl}_2$ ):  $\delta = -7626$ .

#### Minor

$^1\text{H-NMR}$  (700 MHz,  $\text{CD}_2\text{Cl}_2$ ):  $\delta = 9.32$  ( $\psi\text{dd}$ ,  $J = 12.0$  Hz, 8.1 Hz, 1H), 7.57 ( $\psi\tau$ ,  $J = 7.3$  Hz, 1H), 7.50 (br, 1H)

$^{19}\text{F-NMR}$  (658 MHz,  $\text{CD}_2\text{Cl}_2$ ):  $\delta = -127.4$  ( $\psi\text{dt}$ ,  $^0J_{\text{FP}} = 72.5$  Hz,  $^3J_{\text{FF}} = 16.3$ , 1F, F8),  $-147.3$  ( $\psi\tau$ ,  $J = 15.3$  Hz, 1F, F5),  $-155.7$  ( $\psi\tau$ ,  $J = 21.4$  Hz, 1F, F7),  $-157.2$  ( $\psi\tau$ ,  $J = 19.8$  Hz, 1F, F6).

$^{31}\text{P-NMR}$  (283.4 MHz,  $\text{CD}_2\text{Cl}_2$ ):  $\delta = 30.8$  (dd,  $^1J_{\text{RHP}} = 153.0$  Hz,  $^2J_{\text{PF}} = 72.5$  Hz).

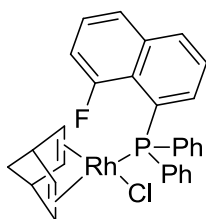
#### Exo

$^1\text{H-NMR}$  (700 MHz,  $\text{CD}_2\text{Cl}_2$ ):  $\delta = 9.91$  ( $\psi\text{dd}$ ,  $J = 11.8$  Hz, 7.0 Hz, 1H, H2), 8.42 ( $\psi\text{d}$ ,  $J = 8.3$  Hz, 1H, H4), 7.97 ( $\psi\tau$ ,  $J = 7.7$  Hz, 1H, H3), 7.81 ( $\psi\tau$ ,  $J = 7.9$  Hz, 1H, H3), 6.59 ( $\psi\tau$ ,  $J = 8.8$  Hz, 1H, H3),

$^{19}\text{F-NMR}$  (658 MHz,  $\text{CD}_2\text{Cl}_2$ ):  $\delta = -130.5$  -  $-130.6$  (m, 1F, F8),  $-147.8$  ( $\psi\tau$ ,  $J = 16.8$  Hz, 1F, F5),  $-155.6$  ( $\psi\tau$ ,  $J = 19.8$  Hz, 1F, F7),  $-157.6$  ( $\psi\tau$ ,  $J = 21.4$  Hz, 1F, F6).

$^{31}\text{P-NMR}$  (283.4 MHz,  $\text{CD}_2\text{Cl}_2$ ):  $\delta = 42.2$  (d,  $^1J_{\text{RHP}} = 150.4$  Hz).

## 5.12 Chloro(norbornadiene)(diphenyl(8-fluoronaphtalen-1-yl)phosphine)rhodium(I) (nbd-Rh-1)



$\text{C}_{29}\text{H}_{24}\text{ClFPRh}$   
560.03

### 5.12.1 Room Temperature Characterization

Mp 210 °C (decomp.).

<sup>1</sup>H-NMR (700.13 MHz, CD<sub>2</sub>Cl<sub>2</sub>):  $\delta$  = 7.97 ( $\psi$ d,  $J$  = 7.6 Hz, 1H, H4), 7.86 (br, 4H, H<sub>o-Ph</sub>), 7.80 ( $\psi$ d,  $J$  = 8.2 Hz, 1H, H6), 7.54 ( $\psi$ dd,  $J$  = 11.8 Hz, 7.7 Hz, 1H, H2), 7.50-7.46 (m, 2H, H<sub>p-Ph</sub>), 7.45-7.41 (m, 4H, H<sub>o-Ph</sub>), 7.40 (underl.  $\psi$ t,  $J$  = 7.3 Hz, 1H, H3), 7.24 ( $\psi$ dd,  $J$  = 12.4 Hz, 7.8 Hz, 1H, H5), 7.05 ( $\psi$ dd,  $J$  = 10.0 Hz, 7.4 Hz, 1H, H2), 5.13 (br, 2H, Hx), 3.78 (br, 2H, Hy), 3.19 (br, 2H, Hw), 1.35 (dd,  $J$  = 64.2 Hz, 8.8 Hz, 2H, Hz).

<sup>13</sup>C-NMR (176.0 MHz, CD<sub>2</sub>Cl<sub>2</sub>):  $\delta$  = 158.7 (d, <sup>1</sup> $J_{CF}$  = 255.5 Hz, 1C, C8), 135.7-135.6 (m, 1C, C1), 134.6 (s, 1C, C2), 134.4 (s, 2C, C<sub>p-Ph</sub>), 134.0 (d, <sup>1</sup> $J_{CP}$  = 39.2 Hz, 2C, C<sub>i-Ph</sub>), 130.6 (s, 1C, C4), 130.1 (s, 4C, C<sub>m-Ph</sub>), 128.4 (d, <sup>1</sup> $J_{CP}$  = 9.7 Hz, 4C, C<sub>o-Ph</sub>), 126.5 (d, <sup>1</sup> $J_{CF}$  = 8.3 Hz, 1C, C7), 125.6 (s, 1C, C3), 125.5 (s, 1C, C6), 125.4 (s, 1C, C4a), 124.6-124.4 (m, 1C, C8a), 112.3 (s, 1C, C5), 80.2 (s, 2C, Cx), 63.4 (s, 2C, Cz), 50.5 (s, 2C, Cy), 50.4 (d, <sup>2</sup> $J_{CP}$  = 11.5 Hz, 2C, Cw).

<sup>19</sup>F-NMR (658.8 MHz, CD<sub>2</sub>Cl<sub>2</sub>):  $\delta$  = -98.77(d, <sup>2</sup> $J_{PF}$  = 83.2 Hz).

<sup>31</sup>P-NMR (283.4 MHz, CD<sub>2</sub>Cl<sub>2</sub>):  $\delta$  = 33.1 (dd, <sup>1</sup> $J_{RHP}$  = 173.9 Hz, <sup>2</sup> $J_{PF}$  = 83.2 Hz).

MS (HiRes MALDI-MS): calc. [M<sup>+</sup>]: 560.0343; found

### 5.12.2 VT-NMR Analysis (213 K)

*Major*

<sup>1</sup>H-NMR (700.13 MHz, CD<sub>2</sub>Cl<sub>2</sub>):  $\delta$  = 7.96 ( $\psi$ d,  $J$  = 7.1 Hz, 1H, H7), 7.79 ( $\psi$ d,  $J$  = 8.2 Hz, 1H, H6), 7.56-7.51 (m, 1H, H5), 7.39-7.34 (m, 1H, H4), 5.30 (br, 1H, H<sub>nb</sub>d), 5.03 (br, 1H, H<sub>nb</sub>d), 3.81 (br, 1H, H<sub>nb</sub>d), 3.67 (br, 1H, H<sub>nb</sub>d), 2.92 (br, 1H, H<sub>nb</sub>d), 2.79 (br, 1H, H<sub>nb</sub>d), 1.32 (br, 1H, H<sub>nb</sub>d), 1.17 (br, 1H, H<sub>nb</sub>d).

<sup>13</sup>C-NMR (176.0 MHz, CD<sub>2</sub>Cl<sub>2</sub>):  $\delta$  = 158.2 (d, <sup>1</sup> $J_{CF}$  = 254.1 Hz, 1C, C8), 135.9 (s, 1C, C4a), 130.8 (s, 1C, C7), 127.0-126.8 (m, 1C, C7) 125.8 (s, 1C, C4), 125.7 (s, 1C, C5), 80.3 (s, 1C, C<sub>nb</sub>d), 63.5 (s, 1C, C<sub>nb</sub>d), 50.5 (s, 1C, C<sub>nb</sub>d), 15.1 (s, 1C, C<sub>nb</sub>d).

<sup>19</sup>F-NMR (658.8 MHz, CD<sub>2</sub>Cl<sub>2</sub>):  $\delta$  = -99.7 (dd,  $J$  = 65.6 Hz, 9.2 Hz).

<sup>31</sup>P-NMR (283.4 MHz, CD<sub>2</sub>Cl<sub>2</sub>):  $\delta$  = 32.4 (dd,  $J$  = 173.0 Hz, 78.7 Hz).

*Exo*

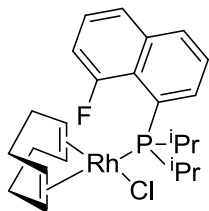
<sup>1</sup>H-NMR (700.13 MHz, CD<sub>2</sub>Cl<sub>2</sub>):  $\delta$  = 9.51 (dd,  $J$  = 19.1 Hz, 6.8 Hz, 1H, H)

<sup>19</sup>F-NMR (658.8 MHz, CD<sub>2</sub>Cl<sub>2</sub>):  $\delta$  = -101.0 (br).

<sup>31</sup>P-NMR (283.4 MHz, CD<sub>2</sub>Cl<sub>2</sub>):  $\delta$  = 33.0 (underl. br).



### 5.13 Chloro(1,5-cyclooctadiene)(diisopropyl(8-fluoronaphthalen-1-yl)phosphine)rhodium(I) (Rh-3)



$C_{24}H_{32}ClFPRh$   
508.84 g/mol

#### 5.13.1 VT-NMR Analysis (193 K)

##### Major

$^1H$ -NMR (700 MHz,  $CD_2Cl_2$ ):  $\delta$  = 7.98 ( $\psi d$ ,  $J$  = 8.1 Hz, 1H, H2), 7.72 ( $\psi d$ ,  $J$  = 8.0 Hz, 1H, H5), 7.67 ( $\psi t$ ,  $J$  = 7.8 Hz, 1H, H4), 7.54 ( $\psi t$ ,  $J$  = 7.6 Hz, 1H, H3), 7.50 ( $\psi td$ ,  $J$  = 7.6 Hz, 4.4 Hz, 1H, H6), 7.36 ( $\psi dd$ ,  $J$  = 12.7 Hz, 7.7 Hz, 1H, H7), 5.24 ( $\psi t$ ,  $J$  = 6.4 Hz, 1H, Ha), 4.61 ( $\psi$ quin,  $J$  = 7.2 Hz, 1H, Hb), 4.37 (br, 1H Hz, He), 3.70 (br, 1H, Hf), 2.88-2.80 (m, 1H, Hd), 2.59-2.51 (m, 1H, Hh), 2.19 ( $\psi q$ ,  $J$  = 17.6 Hz, 1H, Hc), 2.13 ( $\psi q$ ,  $J$  = 16.5 Hz, 1H, Hg), 2.70 (br, 1H,  $CH(CH_3)_2$ ), 2.70 (br, 1H,  $CH(CH_3)_2$ ), 2.02 (br, 1H,  $CH(CH_3)_2$ ), 1.64 (dd,  $^2J_{HH}$  = 15.7 Hz,  $^3J_{HH}$  = 6.6 Hz, 3H,  $CH(CH_3)_2$ ), 1.40 (dd,  $^2J_{HH}$  = 14.5 Hz,  $^3J_{HH}$  = 6.7 Hz, 3H,  $CH(CH_3)_2$ ), 0.92 ( $\psi dd$ ,  $^2J_{HH}$  = 9.3 Hz,  $^3J_{HH}$  = 7.5 Hz, 3H,  $CH(CH_3)_2$ ), 0.87-0.82 (m, 3H,  $CH(CH_3)_2$ ).

$^{13}C$ -NMR (176.0 MHz,  $CD_2Cl_2$ ):  $\delta$  = 159.6 (d,  $^1J_{CF}$  = 259.2 Hz, 1C, C8), 135.68 (s, 1C, C8a), 133.1 (s, 1C, C4), 130.9 (s, 1C, C2), 126.7 (br, 1C, C4a), 126.1 (d,  $^1J_{CP}$  = 7.8 Hz, below s, 2C, C1, C6), 125.5 (s, 1C, C5), 125.2 (br, 1C, C3), 112.6 (d,  $^2J_{CF}$  = 23.1 Hz, 1C, C7), 98.6 (br, 1C, Ca), 94.22 ( $\psi d$ ,  $J$  = 16.7 Hz, 1C, Cb), 73.2 (br, 1C, Ce), 68.1 (d,  $J$  = 12.6, 1C, Cf), 35.6 (br, 1C, Cd), 32.4 ((br, 1C, Ch), 30.4 (br 1C, Cc), 25.9 (br, 1C, Cg), 25.5 ( $\psi d$ ,  $^1J_{CP}$  = 18.0 Hz, 1C,  $CH(CH_3)_2$ ), 20.9 ( $\psi d$ ,  $^2J_{CP}$  = 2.5 Hz, 2C,  $CH(CH_3)_2$ ), 20.7 (d,  $^1J_{CP}$  = 15.6 Hz, 1C,  $CH(CH_3)_2$ ), 19.6 (d,  $^2J_{CP}$  = 5.6 Hz, 1C,  $CH(CH_3)_2$ ), 16.2 (d,  $^2J_{CP}$  = 6.4 Hz, 1C,  $CH(CH_3)_2$ ).

$^{19}F$ -NMR (658 MHz,  $CD_2Cl_2$ ):  $\delta$  = -98.9 (d,  $^2J_{PF}$  = 89.3 Hz).

$^{31}P$ -NMR (283.4 MHz,  $CD_2Cl_2$ ):  $\delta$  = 33.3 (dd,  $^1J_{RHP}$  = 144.7,  $^2J_{PF}$  = 90.0).

$^{103}Rh$ -NMR (15.9 MHz,  $CD_2Cl_2$ ):  $\delta$  = -7550.

##### Minor/Exo

$^1H$ -NMR (700.13 MHz,  $CD_2Cl_2$ ):  $\delta$  = 7.75 ( $\psi d$ ,  $J$  = 8.2 Hz, 1H,  $H_{Np}$ ), 7.65 ( $\psi t$ ,  $J$  = 8.2 Hz, 1H,  $H_{Np}$ ), 7.42 ( $\psi dd$ ,  $J$  = 12.8 Hz, 7.6 Hz, 1H,  $H_{Np}$ ),

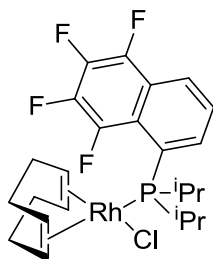
$^{13}C$ -NMR (176.0 MHz,  $CD_2Cl_2$ ):  $\delta$  = 158.3 (br d,  $^1J_{CF}$  = 257.4 Hz, 1C, C8), 136.0 (br, 1C, C8a), 126.7 (s, 1C,  $C_{Np}$ ), 126.6 (s, 1C,  $C_{Np}$ ), 125.9 (br, 1C,  $C_{Np}$ ), 125.7 (s, 1C,  $C_{Np}$ ), 122.1 (br, 1C,  $C_{Np}$ ), 122.0 (br, 1C,  $C_{Np}$ ), 112.8 (br, 1C,  $C_{Np}$ ), 126.5 (s, 1C,  $C_{Np}$ )

$^{19}F$ -NMR (658 MHz,  $CD_2Cl_2$ ):  $\delta$  = -96.8 (br).

$^{31}\text{P}$ -NMR (283.4 MHz,  $\text{CD}_2\text{Cl}_2$ ):  $\delta = 32.1$  (br dd,  $^1J_{\text{RhP}} = 142.6$ ,  $^2J_{\text{PF}} = 72.6$ ).

$^{103}\text{Rh}$ -NMR (15.9 MHz,  $\text{CD}_2\text{Cl}_2$ ):  $\delta = -7868$ .

#### 5.14 Chloro(1,5-cyclooctadiene)(diisopropyl(5,6,7,8-tetrafluoronaphthalen-1-yl)phosphine)rhodium(I) (Rh-4)



$\text{C}_{24}\text{H}_{29}\text{ClF}_4\text{PRh}$   
562.81 g/mol

##### 5.14.1 VT-NMR Analysis (193 K)

*Major*

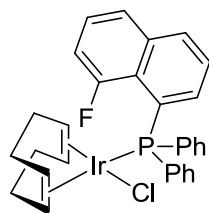
$^1\text{H}$ -NMR (700 MHz,  $\text{CD}_2\text{Cl}_2$ ):  $\delta = 8.18$  ( $\psi\text{d}$ ,  $J = 8.3$  Hz, 1H, H4), 7.74 ( $\psi\text{t}$ ,  $J = 7.7$  Hz, 1H, H2), 7.64 ( $\psi\text{t}$ ,  $J = 7.9$  Hz, 1H, H3), 5.24 ( $\psi\text{t}$ ,  $J = 6.8$  Hz, 1H, Ha), 4.69 ( $\psi\text{quin}$ ,  $J = 6.9$  Hz, 1H, Hb), 4.32 ( $\psi\text{t}$ ,  $J = 5.9$  Hz, 1H, He), 3.69 (b, 1H, Hf), 2.80-2.74 (m, 1H, Hg), 2.74-2.67 (m, 1H,  $\text{CH}(\text{CH}_3)_2$ ), 2.55-2.48 (m, 1H, Hd), 2.26-2.20 (m, 1H, Hc), 2.18-2.12 (m, 1H, Hh), 2.04-2.00 (m, 1H,  $\text{CH}(\text{CH}_3)_2$ ), 1.62 (dd,  $^3J_{\text{PH}} = 16.5$  Hz,  $^3J_{\text{HH}} = 6.1$  Hz, 2H,  $\text{CH}(\text{CH}_3)_2$ ), 1.34 (dd,  $^3J_{\text{PH}} = 14.8$  Hz,  $^3J_{\text{HH}} = 6.9$  Hz, 3H,  $\text{CH}(\text{CH}_3)_2$ ), 0.94 (dd,  $^3J_{\text{PH}} = 9.7$  Hz,  $^3J_{\text{HH}} = 7.3$  Hz, 3H,  $\text{CH}(\text{CH}_3)_2$ ), 0.86 (dd,  $^3J_{\text{PH}} = 13.3$  Hz,  $^3J_{\text{HH}} = 5.5$  Hz, 3H,  $\text{CH}(\text{CH}_3)_2$ ).

$^{13}\text{C}$ -NMR (176 MHz,  $\text{CD}_2\text{Cl}_2$ ):  $\delta = 142.9$  ( $\psi\text{d}$ ,  $^1J_{\text{CF}} = 261.1$  Hz, 1C, C8), 141.2 ( $\psi\text{d}$ ,  $^1J_{\text{CF}} = 247.4$  Hz, 1C, C5), 138.1 ( $\psi\text{d}$ ,  $^1J_{\text{CF}} = 249.6$  Hz, 1C,  $\text{C}_{\text{Np}}$ ), 136.6 ( $\psi\text{d}$ ,  $^1J_{\text{CF}} = 252.5$  Hz, 1C,  $\text{C}_{\text{Np}}$ ), 133.7 (s, 1C, C2), 125.9-125.7 (m, 1C, C8a), 125.2 (s, 1C, C3), 122.5-122.2 (m, 2C, C4, C8a), 120.0-119.8 (m, 1C, C4a), 99.0-98.9 (m, 1C, Ca), 95.5 (d,  $J = 17.2$  Hz, 1C, Cb), 72.5 (d,  $J = 10.8$  Hz, 1C, Ce), 67.7 (d,  $J = 12.9$  Hz, 1C, Cf), 34.9 (s, 1C, Cd), 31.4 (s, 1C, Ch), 30.11 (s, 1C, Cg), 25.6 (s, 1C, Cc), 25.2 (d,  $J_{\text{CP}} = 18.8$  Hz, 2C,  $\text{CH}(\text{CH}_3)_2$ ), 20.3-20.1 (m, 1C,  $\text{CH}(\text{CH}_3)_2$ ), 19.0 (s, 1C,  $\text{CH}(\text{CH}_3)_2$ ), 15.6 (d,  $J = 6.7$  Hz, 1C,  $\text{CH}(\text{CH}_3)_2$ ).

$^{19}\text{F}$ -NMR (658 MHz,  $\text{CD}_2\text{Cl}_2$ ):  $\delta = -128.2$  (br d,  $J = 86.2$  Hz, 1F, F8), -148.9 ( $\psi\text{t}$ ,  $J = 14.5$  Hz, 1F, F5), -157.2 ( $\psi\text{t}$ ,  $J = 23.7$  Hz, 1F, F7), -158.8 ( $\psi\text{t}$ ,  $J = 22.1$  Hz, 1F, F5).

$^{31}\text{P}$ -NMR (283.4 MHz,  $\text{CD}_2\text{Cl}_2$ ):  $\delta = 34.6$  (d,  $^1J_{\text{RhP}} = 144.8$  Hz,  $^2J_{\text{PF}} = 87.4$ ).

## 5.15 Chlor(1,5-cyclooctadiene)(diphenyl(8-tetrafluoronaphthalen-1-yl)phosphine)iridium(I) (Ir-1)



$C_{30}H_{28}ClIrP$   
666.19 g/mol

### 5.15.1 VT NMR Analysis (193 K)

#### Major

$^1H$ -NMR (700 MHz,  $CD_2Cl_2$ ):  $\delta$  = 9.08-9.02 (m, 1H,  $H_{o-Ph1}$ ), 7.98 ( $\psi d$ ,  $J$  = 8.5 Hz, 1H, H4), 7.77 ( $\psi d$ ,  $J$  = 8.4 Hz, 1H, H5), 7.70-7.65 (m, 1H,  $H_{m-Ph1}$ ), 7.54 ( $\psi t$ ,  $J$  = 6.8 Hz, 1H,  $H_{p-Ph1}$ ), 7.52-7.48 (m, 1H, H7), 7.38 (? , 1H, H3), 7.32 ( $\psi t$ ,  $J$  = 7.3 Hz, 1H,  $H_{m-Ph1}$ ), 7.13 ( $\psi dd$ ,  $J$  = 12.7 Hz, 7.5 Hz, 1H, H6), 7.00 ( $\psi dd$ ,  $J$  = 12.2 Hz, 7.3, 1H, H2), 6.88 ( $\psi t$ ,  $J$  = 8.9 Hz, 1H,  $H_{o-Ph1}$ ), 5.08 (br, 1H, Ha), 4.91 (br, 1H, Hb), 2.80 (br, 1H, Hf), 2.59 (br, 1H, He), 2.32-2.19 (m, 2H, Hc), 1.96-1.89 (m, 2H, Hh), 1.69-1.59 (m, 2H, Hd), 1.33-1.27 (m, 2H, Hg)

$^{13}C$ -NMR (176 MHz,  $CD_2Cl_2$ ):  $\delta$  = 157.9 (d,  $^1J_{CF}$  = 256.3 Hz, 1C, C8), 139.8 (s, 1C,  $C_{o-Ph1}$ ), 136.0, (br, 1C, C2), 133.7 (s, 1C,  $C_{o-Ph1}$ ), 131.9 (s, 1C, C4), 131.2 (s, 1C,  $C_{p-Ph1}$ ), 130.9 (s, 1C,  $C_{i-Ph1}$ ), 128.9 (s, 1C,  $C_{m-Ph1}$ ), 125.7 (s, 1C,  $C_{m-Ph1}$ ), 127.1 (s, 1C, C7), 125.6 (underl. s, 2C, C3, C5), 112.7 (br, 1C, C6), 91.8 (s, 1C, Cb), 91.7 (s, 1C, Ca), 56.5 (s, 1C, Cf), 54.1 (underl. s, 1C, Ce), 33.7 (s, 1C,  $C_{COD}$ ), 33.0 (s, 1C,  $C_{COD}$ ), 29.6 (s, 1C,  $C_{COD}$ ), 29.1 (s, 1C,  $C_{COD}$ ).

$^{19}F$ -NMR (658 MHz,  $CD_2Cl_2$ ):  $\delta$  = -97.7 (dd,  $^2J_{PF}$  = 66.4, 9.2).

$^{31}P$ -NMR (283.4 MHz,  $CD_2Cl_2$ ):  $\delta$  = 22.0 (d,  $^2J_{PF}$  = 66.4).

#### Minor

$^1H$ -NMR (700 MHz,  $CD_2Cl_2$ ):  $\delta$  = 4.90 (br, 1H, Ha), 4.60 (br, 1H, Hb), 3.90 (br, 1H, Hf), 3.42 (br, 1H, He), 2.31-2.24 (m, 2H, Hh), 2.16-2.06 (m, 2H, Hc), 1.56-1.50 (m, 2H, Hd), 1.87-1.80 (m, 1H, Hg).

$^{13}C$ -NMR (176 MHz,  $CD_2Cl_2$ ):  $\delta$  = 92.9 (br, 1C, Cb), 91.7 (underl. s, 1C, Ca), 57.2 (s, 1C, Ce), 51.7 (s, 1C, Cf), 33.9 (s, 1C,  $C_{COD}$ ), 32.6 (s, 1C,  $C_{COD}$ ), 30.4 (s, 1C,  $C_{COD}$ ), 28.6 (s, 1C,  $C_{COD}$ )

$^{19}F$ -NMR (658 MHz,  $CD_2Cl_2$ ):  $\delta$  = -100.5 (dd,  $^2J_{PF}$  = 75.5, 10.7).

$^{31}P$ -NMR (283.4 MHz,  $CD_2Cl_2$ ):  $\delta$  = 24.6 (d,  $^2J_{PF}$  = 74.4).

#### Exo

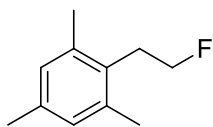
$^1H$ -NMR (700 MHz,  $CD_2Cl_2$ ):  $\delta$  = 9.51 (dd,  $J$  = 19.1, 6.8, 1H, H)

$^{13}C$ -NMR (176.0 MHz,  $CD_2Cl_2$ ):  $\delta$  =

$^{19}\text{F}$ -NMR (658 MHz,  $\text{CD}_2\text{Cl}_2$ ):  $\delta = -100.9$  (br).

$^{31}\text{P}$ -NMR (283.4 MHz,  $\text{CD}_2\text{Cl}_2$ ):  $\delta = 32.1$  (d,  $^2J_{\text{PH}} = 7.1$ ).

## 5.16 1-Fluoro-2-mesitylethane (A)



$\text{C}_{11}\text{H}_{15}\text{F}$   
166.24 g/mol

### 5.16.1 Synthesis

495.1 mg of 2-mesitylethanol (3.01 mmol) are dissolved in 20 mL DCM, the solution is cooled to  $0^\circ\text{C}$ . Then, 0.65 mL (5.32 mmol, 1.8 eq.) are dropwisely added. The solution is stirred and left the cooling bath to warm up slowly over night. The reaction mixture is then quenched with a saturated aqueous solution of  $\text{NaHCO}_3$  and the aqueous phase is extracted two times with 5 mL DCM; the combined organic layers are washed with 0.5 N HCl solution and dried over magnesium sulfate. After evaporation of the solvent, the product is purified by flash chromatography on silica (9:1 hex/DCM). The product is isolated as a colorless oil (337.8 mg, 2.03 mmol, 67%).

### 5.16.2 Characterization

$R_f$ -value: 0.28 (9:1 hex/DCM).

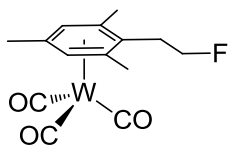
$^1\text{H}$ -NMR (700.13 MHz,  $\text{CDCl}_3$ ):  $\delta = 6.88$  (s, 2H,  $\text{H}_{\text{ar}}$ ), 4.51 (dt,  $^2J_{\text{FH}} = 47.0$  Hz,  $^3J_{\text{HH}} = 6.7$  Hz, 2H,  $\text{H}_1$ ), 3.09 (dt,  $^3J_{\text{FH}} = 18.1$  Hz,  $^3J_{\text{HH}} = 8.3$  Hz, 2H,  $\text{H}_2$ ), 2.33 (s, 6H,  $\text{CH}_{3,\text{o}}$ ), 2.27 (s, 3H,  $\text{CH}_{3,\text{p}}$ ).

$^{13}\text{C}$ -NMR (176 MHz,  $\text{CDCl}_3$ ):  $\delta = 136.9$  (s, 2 C,  $\text{C}_{\text{o}}$ ), 136.1 (s, 1 C,  $\text{C}_{\text{p}}$ ), 129.1 (s, 2 C,  $\text{C}_{\text{m}}$ ), 82.3 (d,  $^1J_{\text{CF}} = 171.7$  Hz, 1 C,  $\text{C}_1$ ) 30.3 (d,  $^2J_{\text{CF}} = 20.7$  Hz, 1 C,  $\text{C}_2$ ), 20.8 (s, 1 C,  $\text{CH}_{3,\text{p}}$ ), 19.9 (s, 2 C,  $\text{CH}_{3,\text{o}}$ ).

$^{19}\text{F}$ -NMR (658 MHz,  $\text{CDCl}_3$ ):  $\delta = -212.8$  (tt,  $^2J_{\text{FH1}} = 47.3$  Hz,  $^3J_{\text{FH2}} = 16.8$  Hz).

MS (EI-MS): calc. 166.115; found 166.1149 (29.08%), 133.1008 (100%).

## 5.17 1-(2-Fluoroethyl)mesitylene tungsten(0)tricarbonyl (B)



$\text{C}_{14}\text{H}_{15}\text{FO}_3\text{W}$   
434.11 g/mol

### 5.17.1 Synthesis

$\text{W}(\text{PMTA})(\text{CO})_3$  (173.0 mg, 0.39 mmol, 0.25 eq.) were suspended in 15 mL THF, then 0.97 mL of  $\text{BF}_3 \cdot \text{OEt}_2$  complex (0.97 mL, 7.80 mmol, 5 eq.) and 260 mg (1.56 mmol) of the Ligand A are added. The solution is heated to reflux for 2.5 h. After cooling down, the mixture is filtered and the the volatiles evaporated. The product is chromatographed over alumina using DCM. The yellow fraction is

collected and evaporation of the solvent leaves 58.8 mg of the product as a yellow solid (0.135 mmol, 35%).

### 5.17.2 Characterization

$^1\text{H-NMR}$  (400 MHz,  $\text{CDCl}_3$ ):  $\delta$  = 5.15 (s, 2H,  $\text{H}_m$ ), 4.41 (dt,  $^2J_{\text{FH}} = 47.00$  Hz,  $^3J_{\text{HH}} = 6.30$  Hz, 2H,  $\text{H}_1$ ), 2.86 (dt,  $^3J_{\text{FH}} = 21.2$  Hz,  $^3J_{\text{HH}} = 6.1$  Hz, 2H,  $\text{H}_2$ ), 2.49 (s, 6H,  $\text{CH}_{3,o}$ ), 2.41 (s, 3H,  $\text{CH}_{3,p}$ ).

$^{13}\text{C-NMR}$  (101 MHz,  $\text{CDCl}_3$ ):  $\delta$  = 212.1 (t,  $^1J_{\text{CW}} = 94.50$  Hz Hz, 3 C,  $\text{C}_{\text{CO}}$ ), 109.5 (s, 1 C,  $\text{C}_p$ ), 109.5 (s, 2 C,  $\text{C}_o$ ), 91.3 (s, 2C,  $\text{C}_m$ ), 83.7 (d,  $^1J_{\text{CF}} = 172.91$  Hz, 1 C,  $\text{C}_2$ ), 29.4 (d,  $^2J_{\text{CF}} = 20.9$  Hz, 1 C,  $\text{C}_1$ ), 20.0 (s, 1 C,  $\text{CH}_{3,p}$ ), 19.6 (d,  $^5J_{\text{CF}} = 1.3$  Hz, 2C,  $\text{CH}_{3,o}$ ).

$^{19}\text{F-NMR}$  (376 MHz,  $\text{CDCl}_3$ ):  $\delta$  = -213.59 (tt,  $^2J_{\text{FH}} = 47.00$  Hz,  $^3J_{\text{FH}} = 21.20$  Hz).

$^{183}\text{W-NMR}$  (20.8 MHz,  $\text{CDCl}_3$ ):  $\delta$  = -2695.

## 6 Literature

- [1] a) D. Drago, P. S. Pregosin, A. Pfaltz, *Chem. Commun.* **2002**, 286-287; b) A. Lightfoot, P. Schnider, A. Pfaltz, *Angew. Chem. Int. Ed.* **1998**, *37*, 2897-2899.
- [2] P. Murray-Rust, W. C. Stallings, C. T. Monti, R. K. Preston, J. P. Glusker, *J. Am. Chem. Soc.* **1983**, *105*, 3206-3214.
- [3] H. Plenio, R. Diodone, *J. Am. Chem. Soc.* **1996**, *118*, 356-367.
- [4] H. Plenio, *Chem. Rev.* **1997**, *97*, 3363-3384.
- [5] R. G. Pearson, *J. Am. Chem. Soc.* **1963**, *85*, 3533-3539.
- [6] A. D. Horton, A. G. Orpen, *Organometallics* **1991**, *10*, 3910-3918.
- [7] a) X. Yang, C. L. Stern, T. J. Marks, *Angew. Chem. Int. Ed.* **1992**, *31*, 1375-1377; b) J. Karl, G. Erker, R. Fröhlich, *J. Am. Chem. Soc.* **1997**, *119*, 11165-11173.
- [8] Y. Sun, R. E. v. H. Spence, W. E. Piers, M. Parvez, G. P. A. Yap, *J. Am. Chem. Soc.* **1997**, *119*, 5132-5143.
- [9] R. Usón, J. Forniés, *Inorg. Chim. Acta*, *198-200*, 165-177.
- [10] T. Ritter, M. W. Day, R. H. Grubbs, *J. Am. Chem. Soc.* **2006**, *128*, 11768-11769.
- [11] R. M. Catala, D. Cruz-Garriz, A. Hills, D. L. Hughes, R. L. Richards, P. Sosa, H. Torrens, *J. Chem. Soc., Chem. Commun.* **1987**, 261-262.
- [12] R. J. Kulawiec, E. M. Holt, M. Lavin, R. H. Crabtree, *Inorg. Chem.* **1987**, *26*, 2559-2561.
- [13] A. Castellanos, J. J. Garcia, H. Torrens, N. Bailey, C. O. R. de Barbarin, A. Gutierrez, F. del Rio, *J. Chem. Soc., Dalton Trans.* **1994**, 2861-2866.
- [14] K. Stanek, B. Czarniecki, R. Aardoom, H. Rüegger, A. Togni, *Organometallics* **2010**, *29*, 2540-2546.
- [15] a) H. F. Haarman, F. R. Bregman, J.-M. Ernsting, N. Veldman, A. L. Spek, K. Vrieze, *Organometallics* **1997**, *16*, 54-67; b) V. César, S. Bellemin-Laponnaz, H. Wadepohl, L. H. Gade, *Chem. Eur. J.* **2005**, *11*, 2862-2873.
- [16] J. Tiburcio, S. Bernès, H. Torrens, *Polyhedron* **2006**, *25*, 1549-1554.
- [17] V. César, S. Bellemin-Laponnaz, Lutz H. Gade, *Eur. J. Inorg. Chem.* **2004**, *2004*, 3436-3444.
- [18] a) A. S. Weller, M. F. Mahon, J. W. Steed, *J. Org. Chem.* **2000**, *614-615*, 113-119; b) M. Valentini, K. Selvakumar, M. Wörle, P. S. Pregosin, *J. Org. Chem.* **1999**, *587*, 244-251.
- [19] S. Filipuzzi, E. Maennel, P. S. Pregosin, A. Albinati, S. Rizzato, L. F. Veiros, *Organometallics* **2008**, *27*, 4580-4588.
- [20] A. Brück, K. Ruhland, *Organometallics* **2009**, *28*, 6383-6401.
- [21] S. Berger, S. Braun, *200 and More NMR Experiments*, Wiley-VCH, Weinheim, **2004**.
- [22] J. Jeener, B. H. Meier, P. Bachmann, R. R. Ernst, *J. Chem. Phys.* **1979**, *71*, 4546-4553.
- [23] a) A. A. Bothner-By, R. L. Stephens, J. Lee, C. D. Warren, R. W. Jeanloz, *J. Am. Chem. Soc.* **1984**, *106*, 811-813; b) T. L. Hwang, A. J. Shaka, *J. Am. Chem. Soc.* **1992**, *114*, 3157-3159.
- [24] W. M. Haynes, ed., *CRC Handbook of Chemistry and Physics*, 91<sup>st</sup> Edition (Internet Version 2011).
- [25] a) J. F. Keggin, *Nature* **1933**, *131*, 2; b) J. F. Keggin, *Proc. R. Soc. A* **1934**, *144*, 75-100.
- [26] L. Pettersson, I. Andersson, L. O. Oehman, *Inorg. Chem.* **1986**, *25*, 4726-4733.
- [27] D. E. Katsoulis, *Chem. Rev.* **1998**, *98*, 359-388.
- [28] P. S. Pregosin, A. Togni, L. M. Venanzi, *Angew. Chem. Int. Ed.* **1981**, *20*, 668-669.
- [29] A. Albinati, R. Naegeli, A. Togni, L. M. Venanzi, *J. Organomet. Chem.* **1987**, *330*, 85-100.
- [30] G. J. Kubas, *Inorg. Chem.* **1983**, *22*, 692-694.
- [31] G. J. Kubas, C. J. Unkefer, B. I. Swanson, E. Fukushima, *J. Am. Chem. Soc.* **1986**, *108*, 7000-7009.
- [32] M. A. Curtis, E. J. Houser, M. Sabat, R. N. Grimes, *Inorg. Chem.* **1998**, *37*, 102-111.
- [33] V. Zanotti, V. Rutar, R. J. Anelici, *J. Organomet. Chem.* **1991**, *414*, 177-191.
- [34] E. O. Fischer, A. Maasböl, *Angew. Chem. Int. Ed.* **1964**, *3*, 580-581.

- [35] K. S. Chan, M. L. Yeung, W.-k. Chan, R.-J. Wang, T. C. W. Mak, *J. Org. Chem.* **1995**, *60*, 1741-1747.
- [36] D. F. Harvey, D. M. Sigano, *Chem. Rev.* **1996**, *96*, 271-288.
- [37] R. J. Kazlauskas, M. S. Wrighton, *J. Am. Chem. Soc.* **1982**, *104*, 6005-6015.
- [38] T. Masuda, K. Yamamoto, T. Higashimura, *Polymer* **1982**, *23*, 1663-1666.
- [39] R. K. Harris, E. D. Becker, S. M. Cabral de Menezes, R. Goodfellow, P. Granger, *Solid State Nucl. Magn. Reson.* **2002**, *22*, 458-483.
- [40] J. L. Templeton, C. C. Philipp, P. S. Pregosin, H. Rügger, *Magn. Reson. Chem.* **1993**, *31*, 58-62.
- [41] R. Benn, A. Rufinska, M. A. King, C. E. Osterberg, T. G. Richmond, *J. Organomet. Chem.* **1989**, *376*, 359-366.
- [42] a) C. Brevard, R. Schimpf, *J. Magn. Reson.* **1982**, *47*, 528-534; b) R. Benn, H. Brenneke, J. Heck, A. Rufinska, *Inorg. Chem.* **1987**, *26*, 2826-2829; c) L. Carlton, A. Emdin, A. Lemmerrer, M. A. Fernandes, *Magn. Reson. Chem.* **2008**, *46*, S56-S62.
- [43] T. A. Mobley, E. G. Tennyson, G. S. Hisao, *Magn. Reson. Chem.* **2010**, *48*, 787-792.
- [44] D. Gudat, *Annual Reports on NMR Spectroscopy, Vol. Volume 51*, Academic Press, **2003**, pp. 59-103.
- [45] M. Minelli, J. H. Enemark, R. T. C. Brownlee, M. J. O'Connor, A. G. Wedd, *Coord. Chem. Rev.* **1985**, *68*, 169-278.
- [46] a) M. J. Aroney, R. M. Clarkson, R. J. Klepetko, A. F. Masters, R. K. Pierens, *J. Organomet. Chem.* **1990**, *393*, 371-378; b) J. T. Price, T. S. Sorensen, *Can. J. Chem.* **1968**, *46*, 515-522.
- [47] R. M. Hiney, L. J. Higham, H. Müller-Bunz, D. G. Gilheany, *Angew. Chem. Int. Ed.* **2006**, *45*, 7248-7251.
- [48] N. Armanino, R. Koller, A. Togni, *Organometallics* **2010**, *29*, 1771-1777.
- [49] a) A. Hinke, W. Kuchen, *Phosphorous Sulfur Rel. El.* **1983**, *15*, 93 - 98; b) G. Mancino, A. J. Ferguson, A. Beeby, N. J. Long, T. S. Jones, *J. Am. Chem. Soc.* **2004**, *127*, 524-525.
- [50] J. W. Perich, R. B. Johns, *Synthesis* **1988**, *1988*, 142,144.
- [51] T. V. RajanBabu, B. Radetich, K. K. You, T. A. Ayers, A. L. Casalnuovo, J. C. Calabrese, *J. Org. Chem.* **1999**, *64*, 3429-3447.
- [52] K. Stanek, Diss. ETH No. 18493, ETH Zürich (Zürich), **2009**.
- [53] H. A. Bent, *Chem. Rev.* **1961**, *61*, 275-311.
- [54] A. D. Becke, *Phys. Rev. A* **1988**, *38*, 3098.
- [55] A. Schafer, H. Horn, R. Ahlrichs, *J. Chem. Phys.* **1992**, *97*, 2571-2577.
- [56] R. Ahlrichs, M. Bär, M. Häser, H. Horn, C. Kölmel, *Chem. Phys. Lett.* **1989**, *162*, 165-169.
- [57] K. Eichkorn, F. Weigend, O. Treutler, R. Ahlrichs, *Theor. Chem. Acc.* **1997**, *97*, 119-124.
- [58] a) A. Schafer, C. Huber, R. Ahlrichs, *J. Chem. Phys.* **1994**, *100*, 5829-5835; b) F. Weigend, R. Ahlrichs, *Phys. Chem. Chem. Phys.* **2005**, *7*, 3297-3305.
- [59] A. D. Becke, *The Journal of Chemical Physics* **1993**, *98*, 5648-5652.
- [60] S. A. Smith, T. O. Levante, B. H. Meier, R. R. Ernst, *J. Magn. Reson. A* **1994**, *106*, 75-105.
- [61] A. N. Nesmeyanov, V. V. Krivykh, V. S. Kaganovich, M. I. Rybinskaya, *J. Organomet. Chem.* **1975**, *102*, 185-193.
- [62] K.-Y. Kim, B. C. Kim, H. B. Lee, H. Shin, *J. Org. Chem.* **2008**, *73*, 8106-8108.
- [63] a) A. Macchioni, P. S. Pregosin, H. Rügger, G. van Koten, P. A. van der Schaaf, R. A. T. M. Abbenhuis, *Magn. Reson. Chem.* **1994**, *32*, 235-241; b) P. S. Pregosin, *Personal Communication*, **2011**.
- [64] D. Gelman, L. Jiang, S. L. Buchwald, *Org. Lett.* **2003**, *5*, 2315-2318.
- [65] R. Aardoom, *Unpublished Results*, ETH Zürich, Zürich, **2011**.
- [66] A. Krasovskiy, P. Knochel, *Synthesis* **2006**, *2006*, 0890,0891.

- [67] a) H. E. Gottlieb, V. Kotlyar, A. Nudelman, *J. Org. Chem.* **1997**, *62*, 7512-7515; b) G. R. Fulmer, A. J. M. Miller, N. H. Sherden, H. E. Gottlieb, A. Nudelman, B. M. Stoltz, J. E. Bercaw, K. I. Goldberg, *Organometallics* **2010**, *29*, 2176-2179.
- [68] a) Bruker AXS, 6.02 ed., Madison, WI, **2001**, Software for CCD Diffractometers; b) Bruker AXS, 6.01 ed., Madison, WI, **2001**, Software for CCD Diffractometers.
- [69] G. M. Sheldrick, *Acta Cryst. A* **1990**, *46*, 7.
- [70] G. M. Sheldrick, Universität Göttingen, Göttingen, Germany, **1999**, Program for Crystal Structure Refinement.
- [71] R. Blessing, *Acta Cryst. A* **1995**, *51*, 33.
- [72] L. F. Fieser, M. Fieser, *Reagents for Organic Synthesis*, Wiley & Sons: New York **1967**, *1*, 584.



## 7 Appendix

### 7.1 Abbreviations

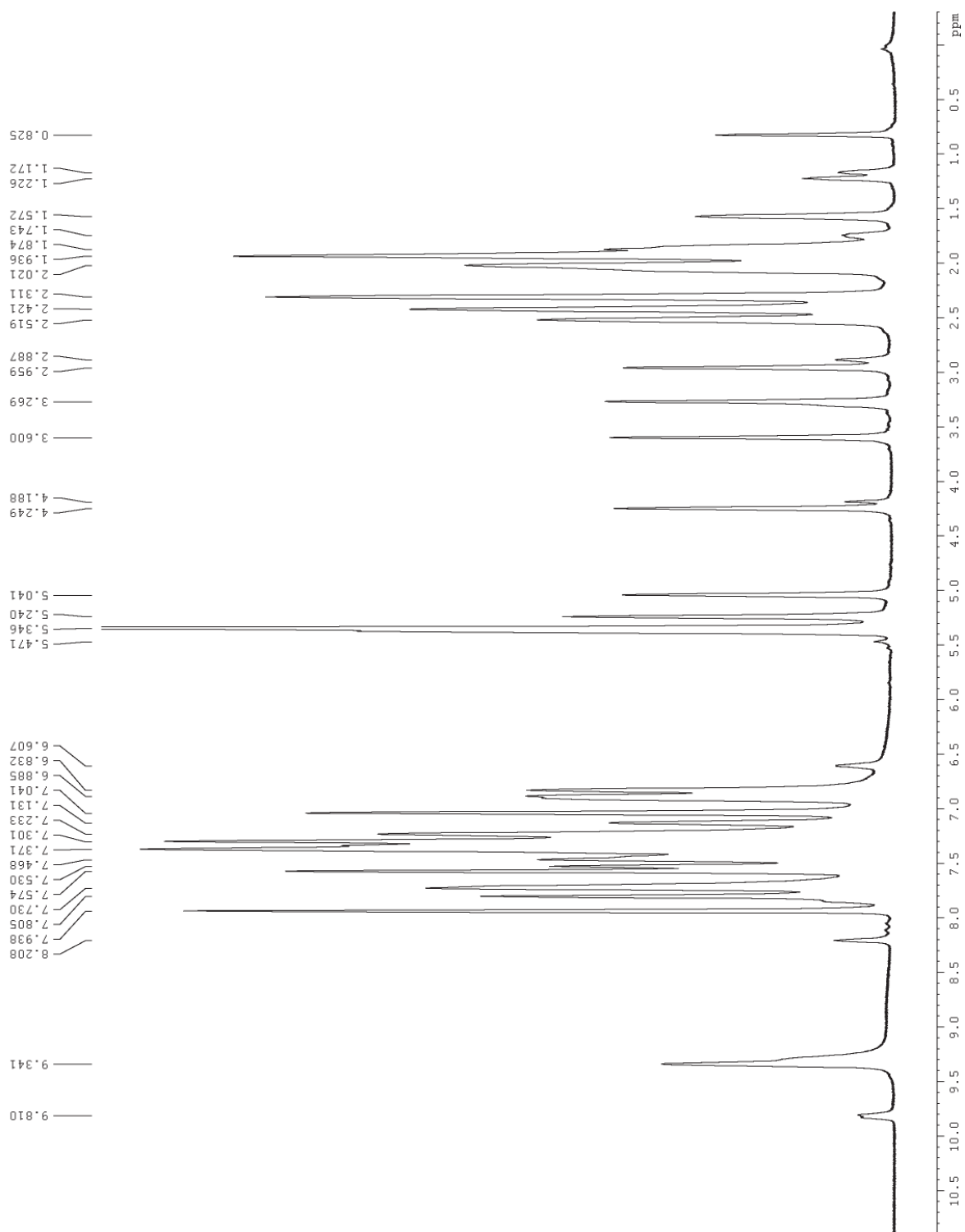
ar	aromatic (NMR)
br	broad (NMR)
B3LYP	Becke-2-Parameter-Lee-Yang-Parr
BP86	Becke-Perdew 1986
calc.	calculated
COD	<i>cis-cis</i> -cycloocta-1,5-diene
COSY	Correlation Spectroscopy
Cy	Cyclohexyl
$\delta$	Chemical shift [ppm] (NMR)
d	doublet (NMR)
DCM	Dichloromethane
dd	doublet of doublet (NMR)
DFT	Density Functional Theory
EI	Electron ionization
EtOAc	Ethylacetate
eq.	equivalent
hex	<i>n</i> -hexane
HMBC	Heteronuclear Multiple Bond Correlation
HOESY	Heteronuclear Overhauser Effect Spectroscopy
HSAB	Hard Soft Acid Base
HSQC	Heteronuclear Multiple Quantum Coherence
HV	high vacuum
INEPT	Insensitive Nuclei Enhanced by Polarization Transfer
<sup>i</sup> Pr	isopropyl
<i>J</i>	coupling constant [Hz] (NMR)
KIE	Kinetic Isotope Effect
MALDI	Matrix assisted laser desorption / ionization
Mes	mesityl
MS	Mass Spectrometry
nbd	Norbornadiene
NMR	Nuclear Magnetic Resonance
NOESY	Nuclear Overhauser Effect Spectroscopy
NpF	5-Fluoronaphthalen-1-yl
NpF <sub>4</sub>	5,6,7,8-Tetrafluoronaphthalen-1-yl
ORTEP	Oak Ridge Thernal Ellipsoid Plot
$\psi$	pseudo / appears as (NMR)
Ph	Phenyl
PMTA/PMDTA	N,N,N',N',N''-pentamethyldiethylenetriamine
ppm	parts per million
q	quartet (NMR)
quin	quintet (NMR)
<i>R<sub>f</sub></i>	Retention factor
RT	room temperature
s	singlet (NMR)
sept	septet (NMR)
SV(P)	Split Valence (Polarization)
t	triplet (NMR)

THF	Tetrahydrofuran
TLC	Thin Layer Chromatography
TMS	Tetramethylsilane
TZVP	Triple Zeta Valence Polarization
UV	Ultraviolet
underl.	underlying (NMR)
vdW	van der Waals
VT	Variable Temperature (NMR)

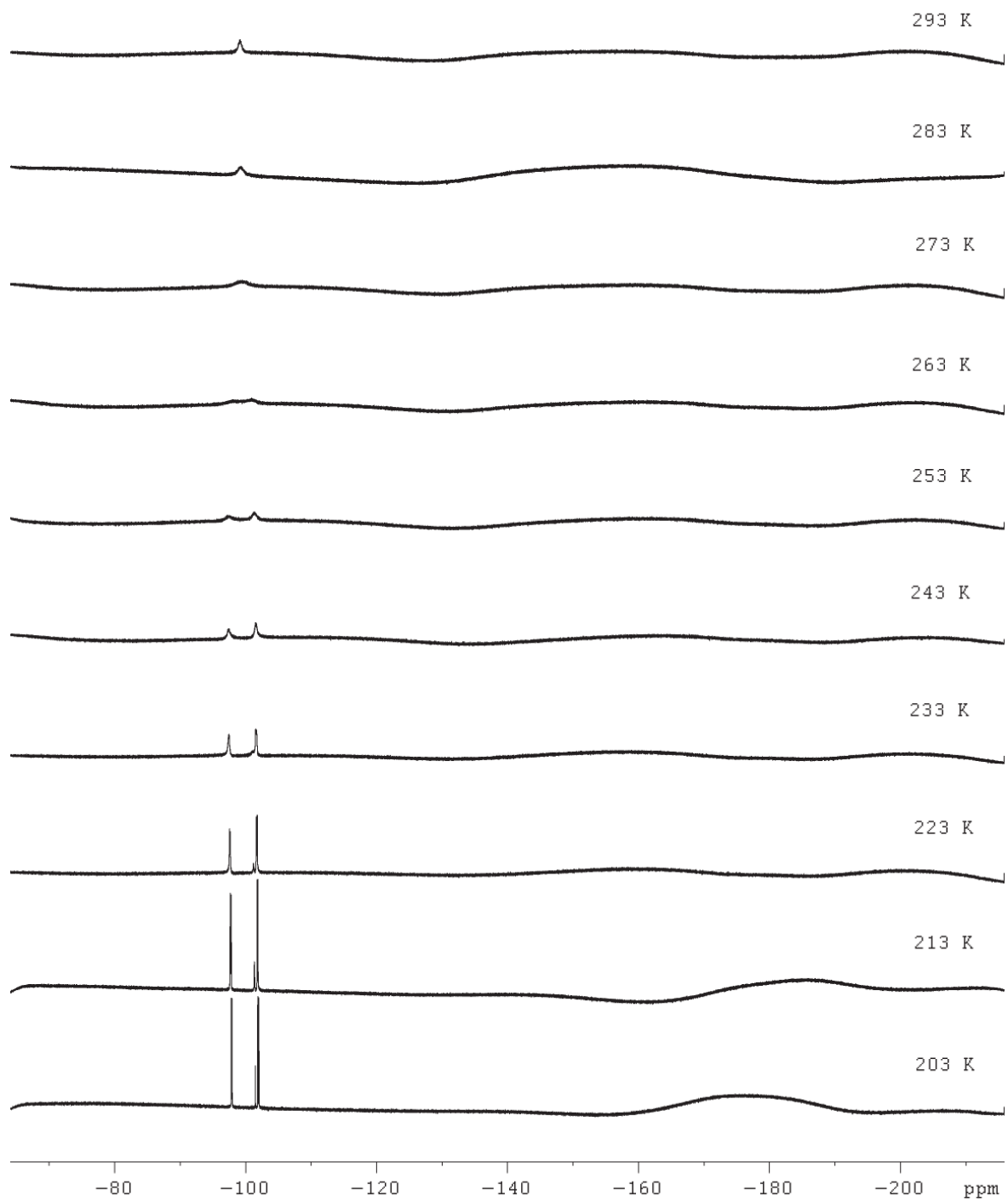
## 7.2. NMR Spectra

### 7.2.1 Rh-1

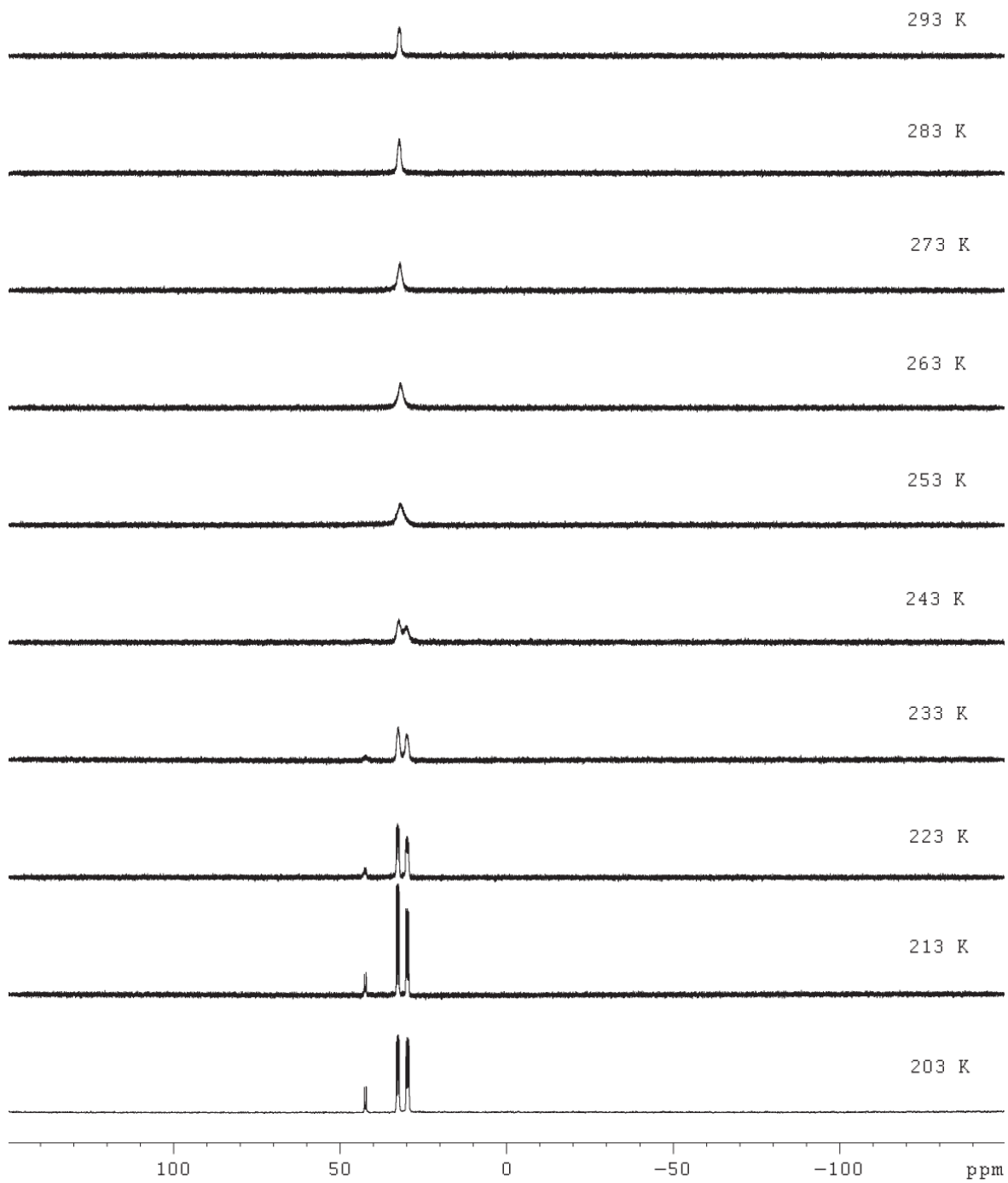
$^1\text{H-NMR}$  Spectrum at 203 K



*<sup>19</sup>F-NMR SpectraVT Series*

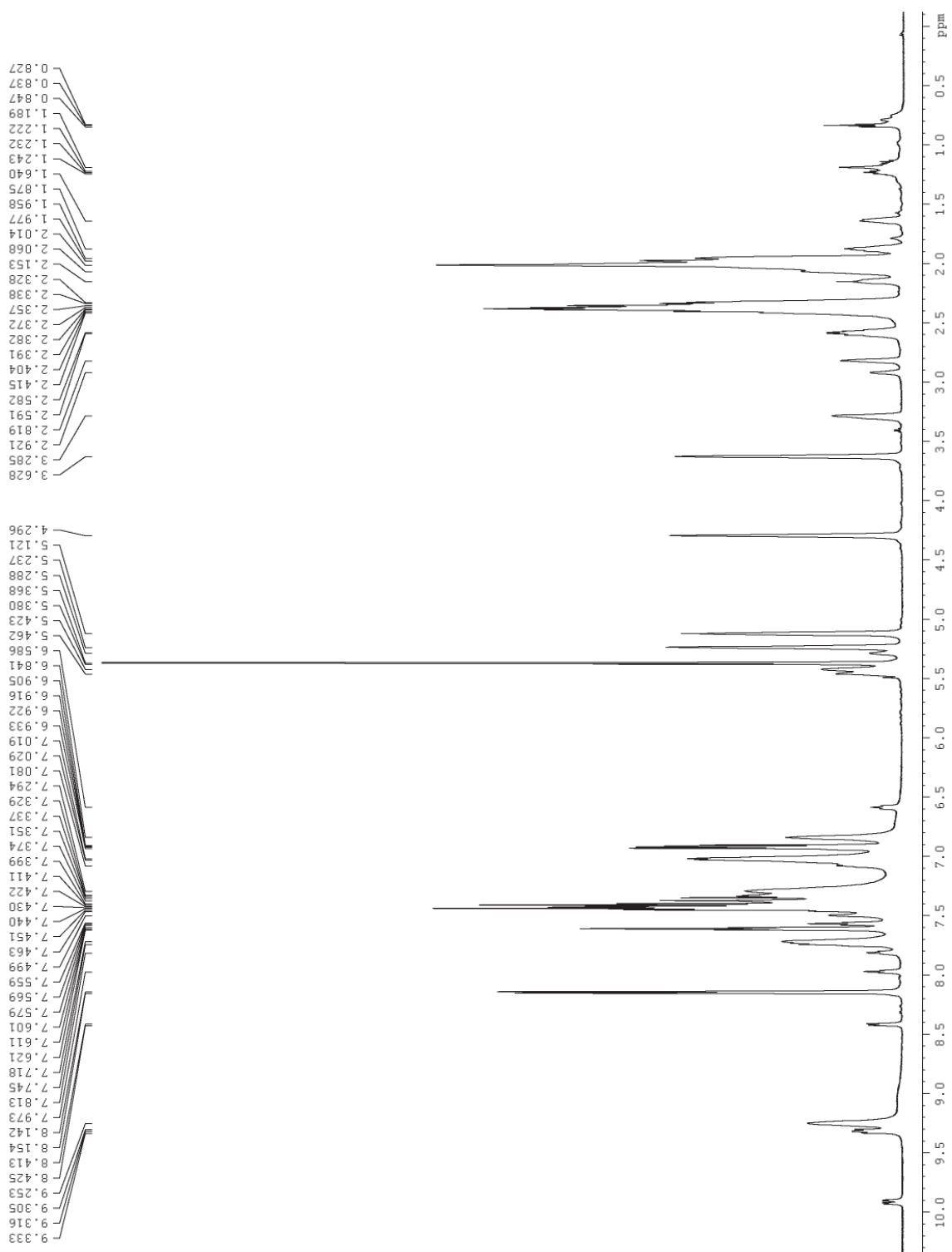




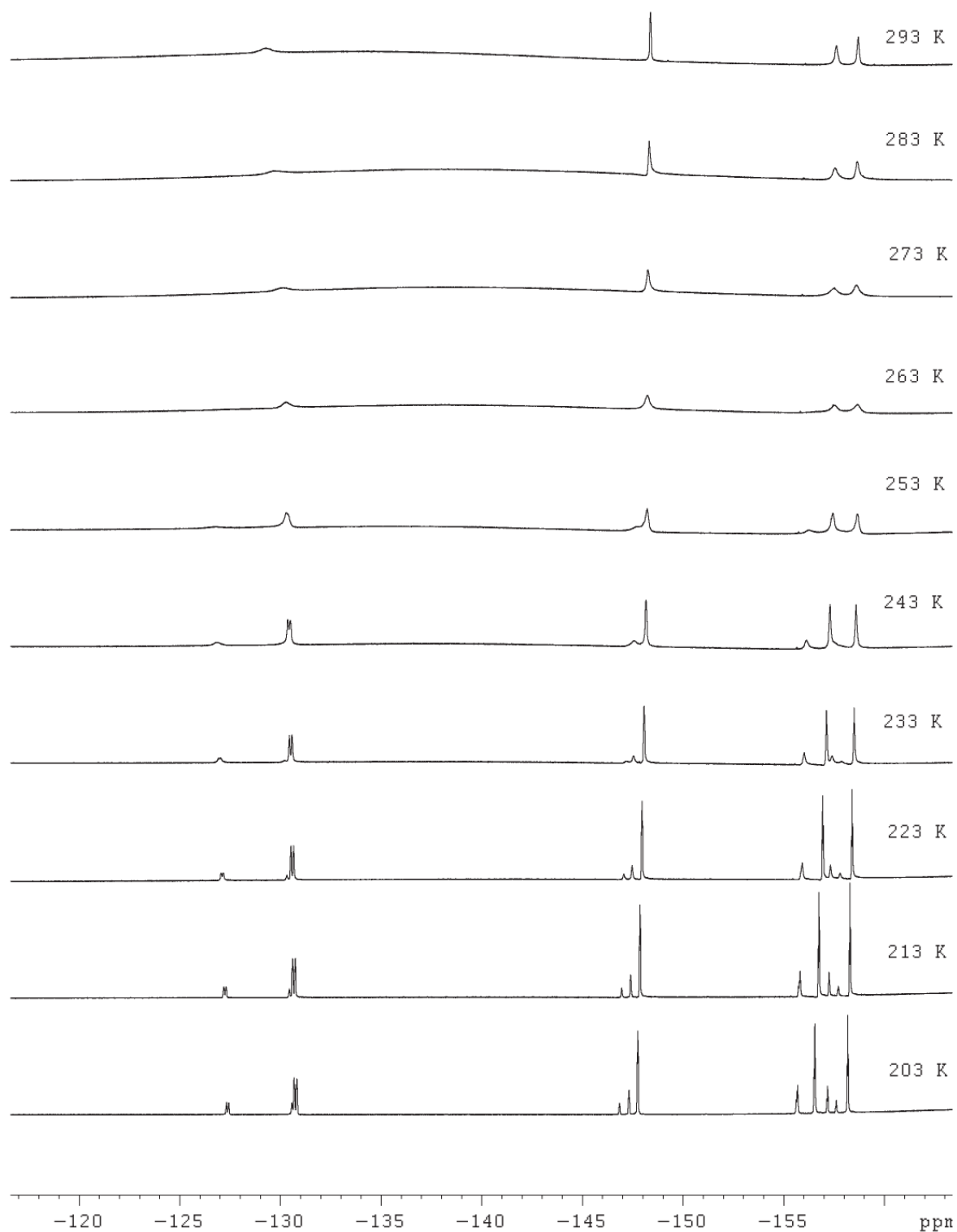


### 7.2.2. Rh-2

<sup>1</sup>H-NMR Spectrum at 193 K

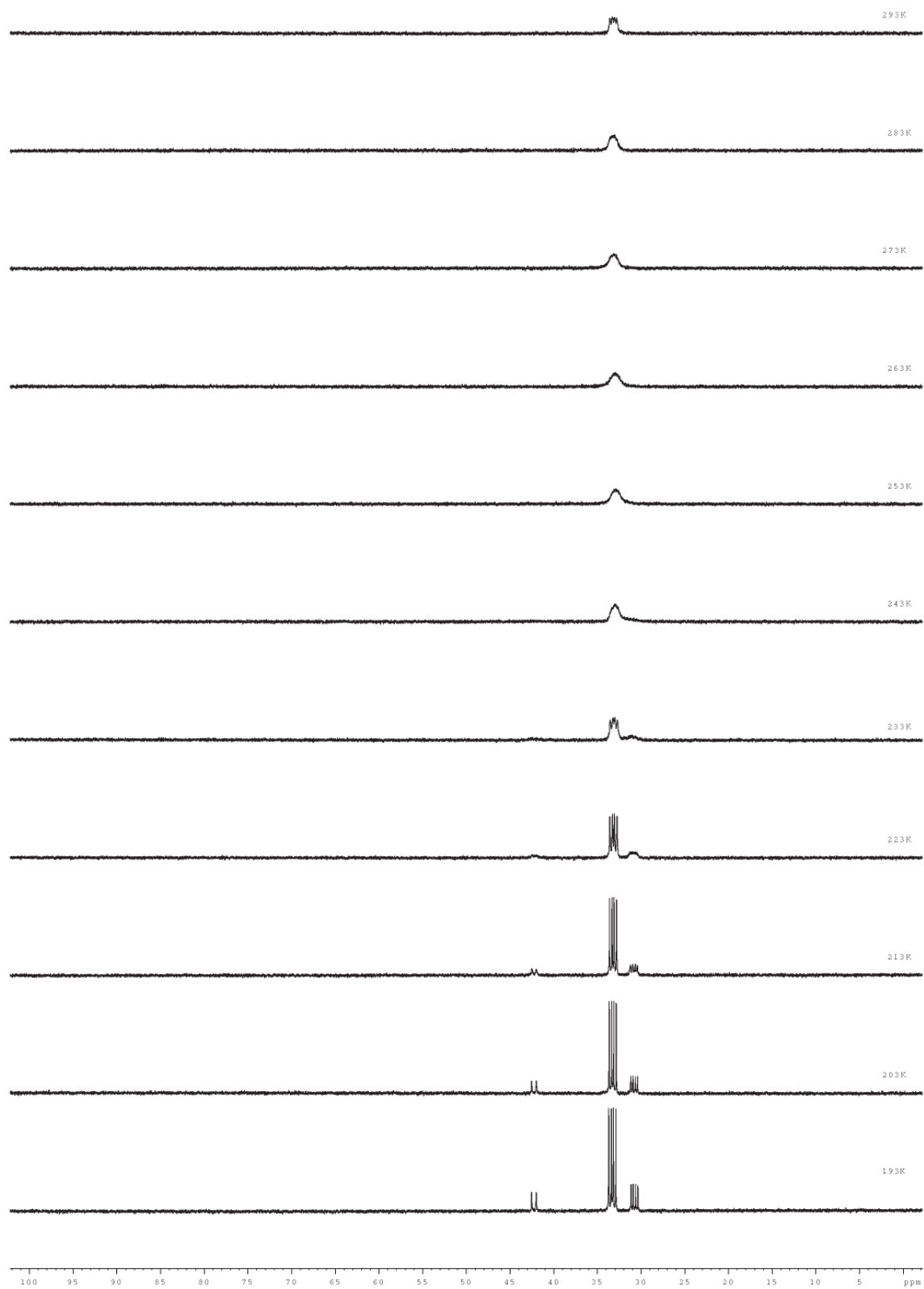


*<sup>19</sup>F-NMR SpectraVT Series*



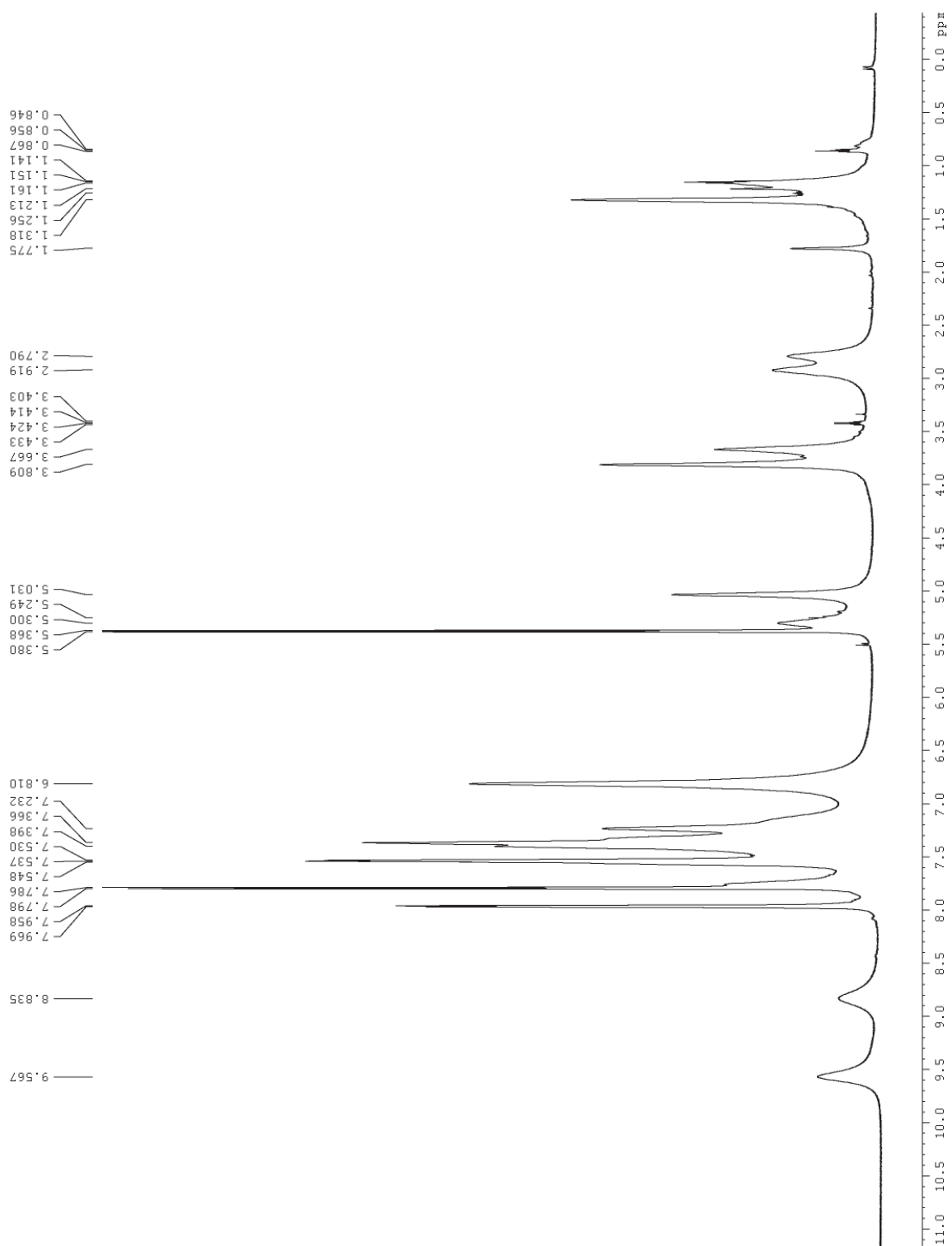


*<sup>31</sup>P-NMR Spectra VT Series*

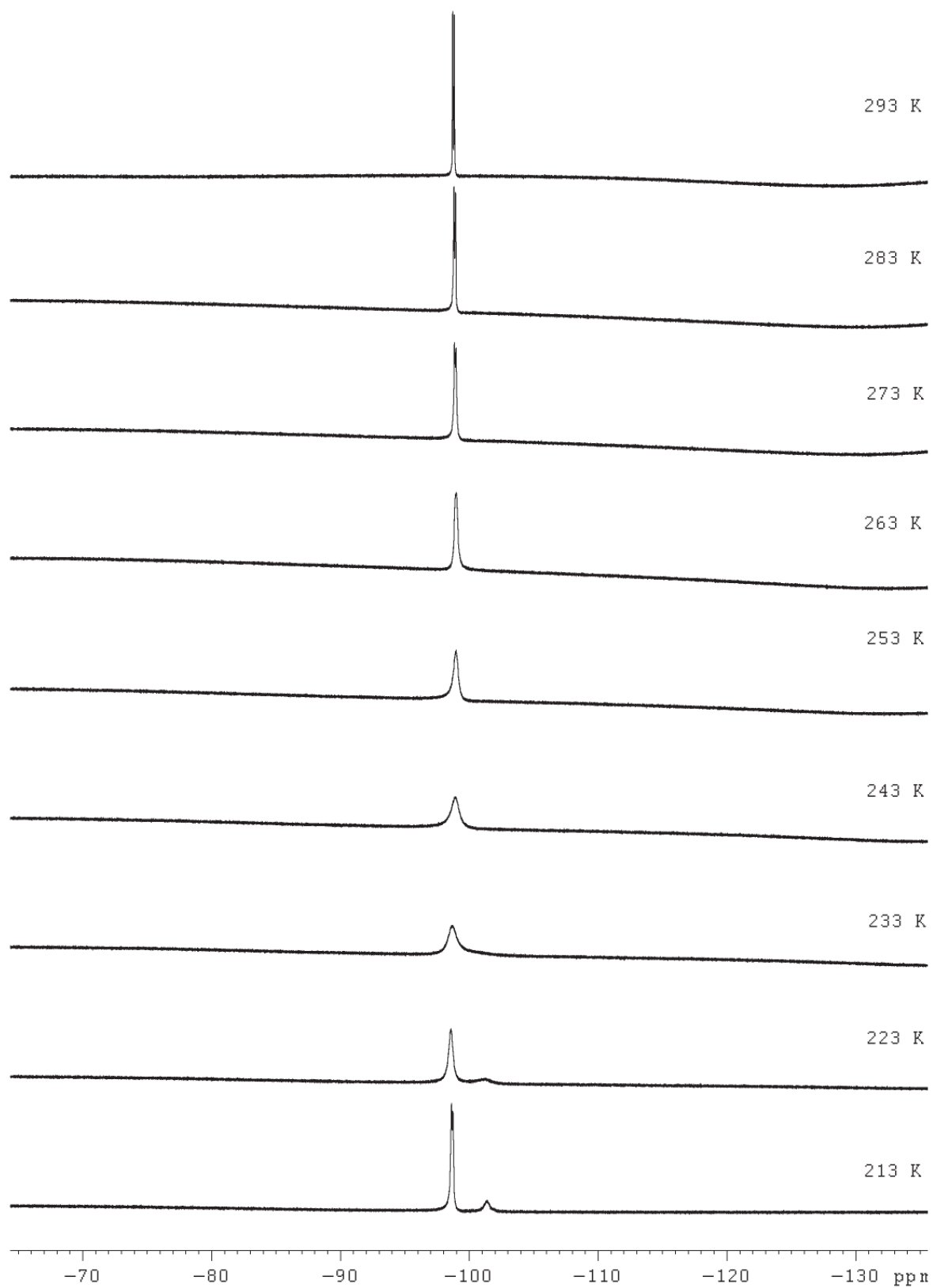


### 7.2.3 nbd-Rh-1

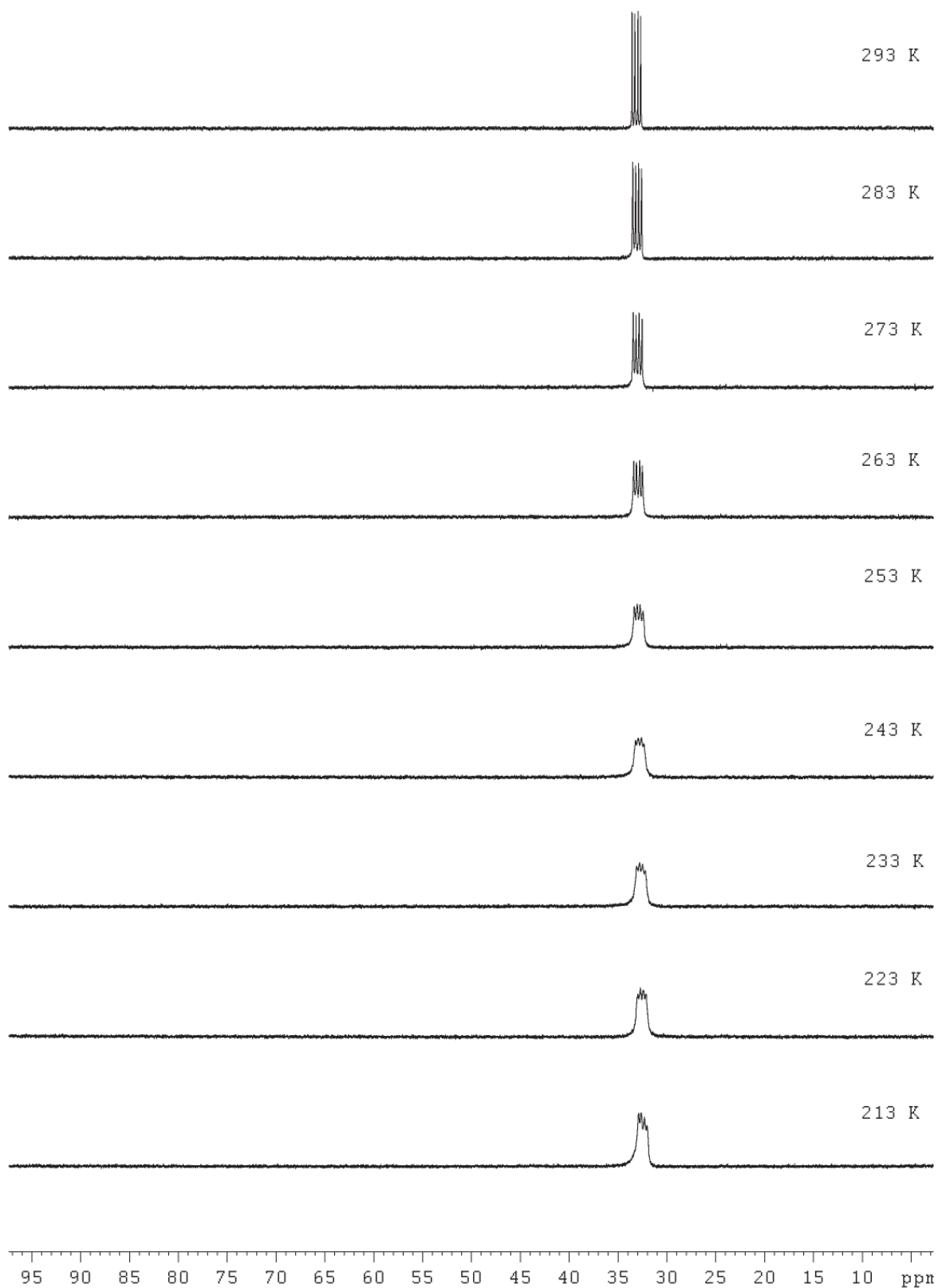
<sup>1</sup>H-NMR Spectrum at 193 K



*<sup>19</sup>F-NMR Spectra VT Series*

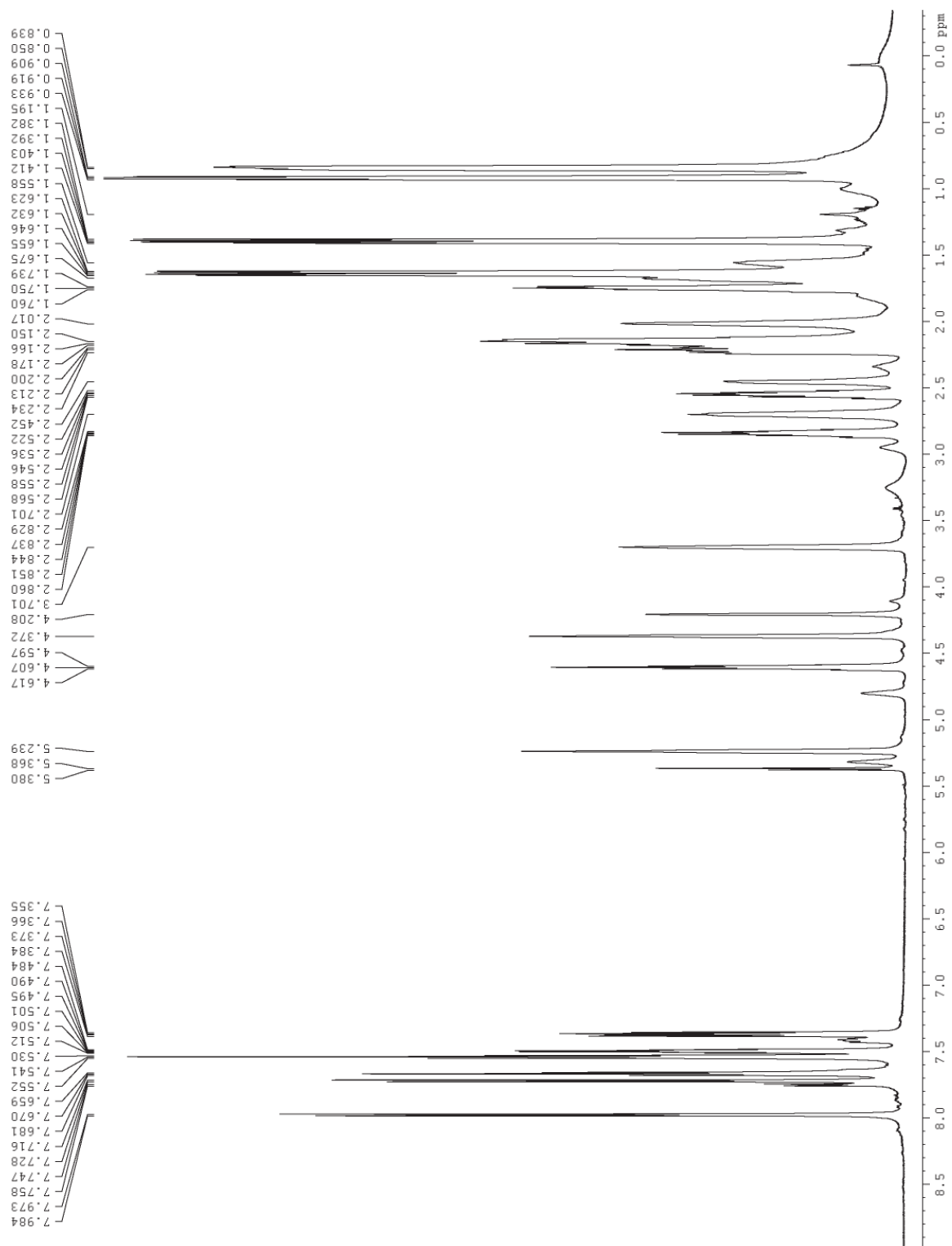


*<sup>31</sup>P-NMR Spectra VT Series*

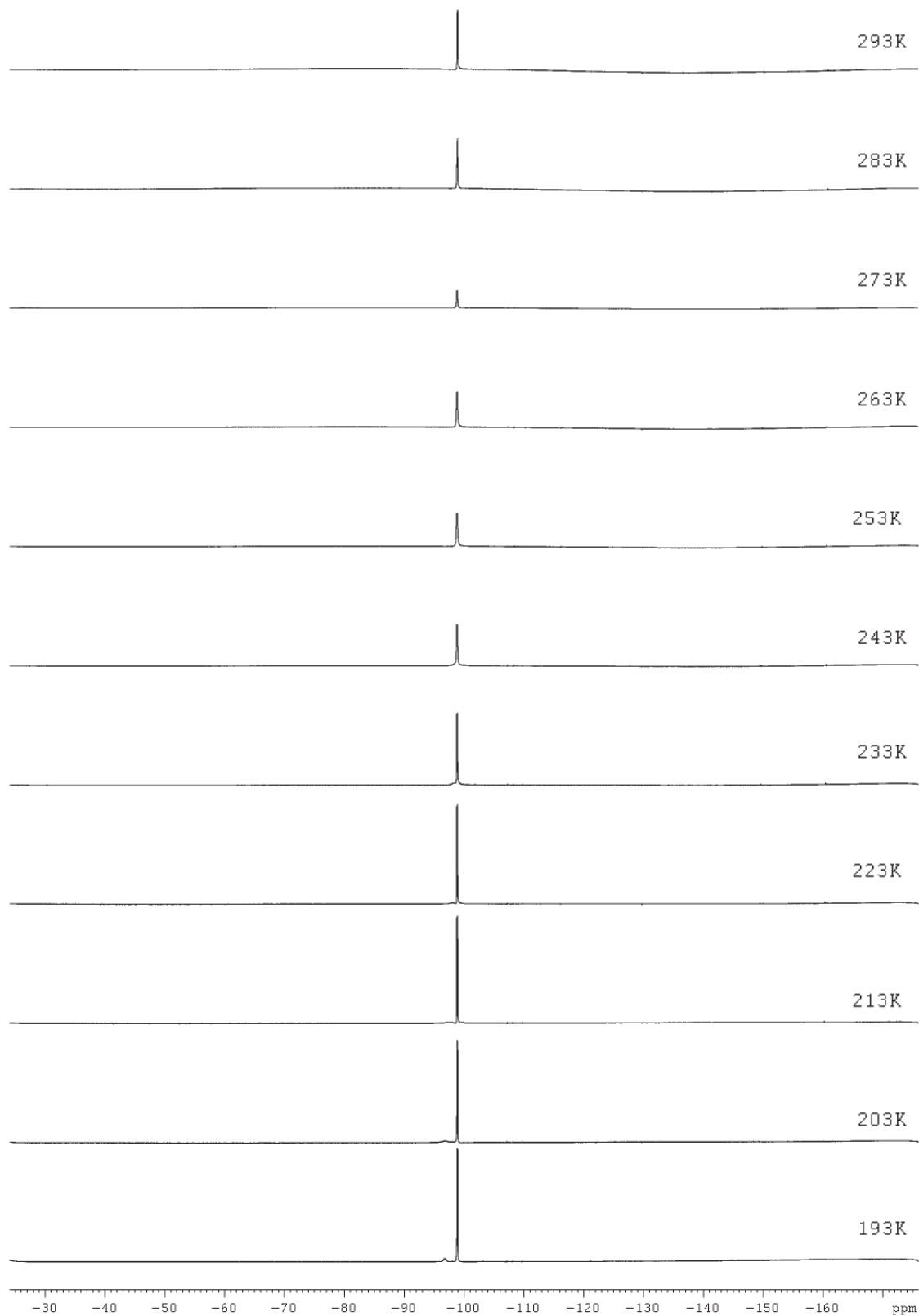


### 7.2.4 Rh-3

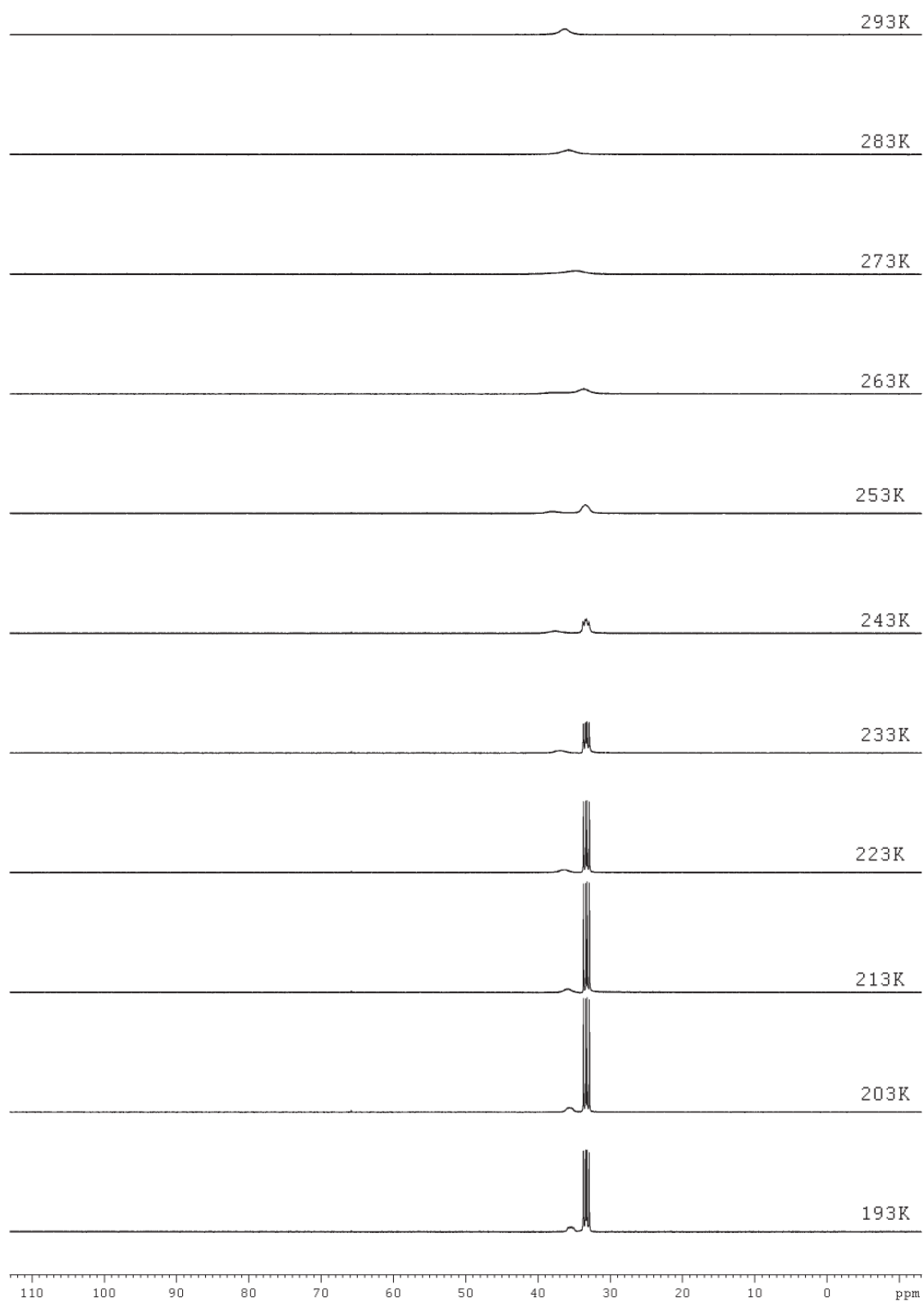
<sup>1</sup>H-NMR Spectrum at 203 K



*<sup>19</sup>F-NMR Spectra VT Series*

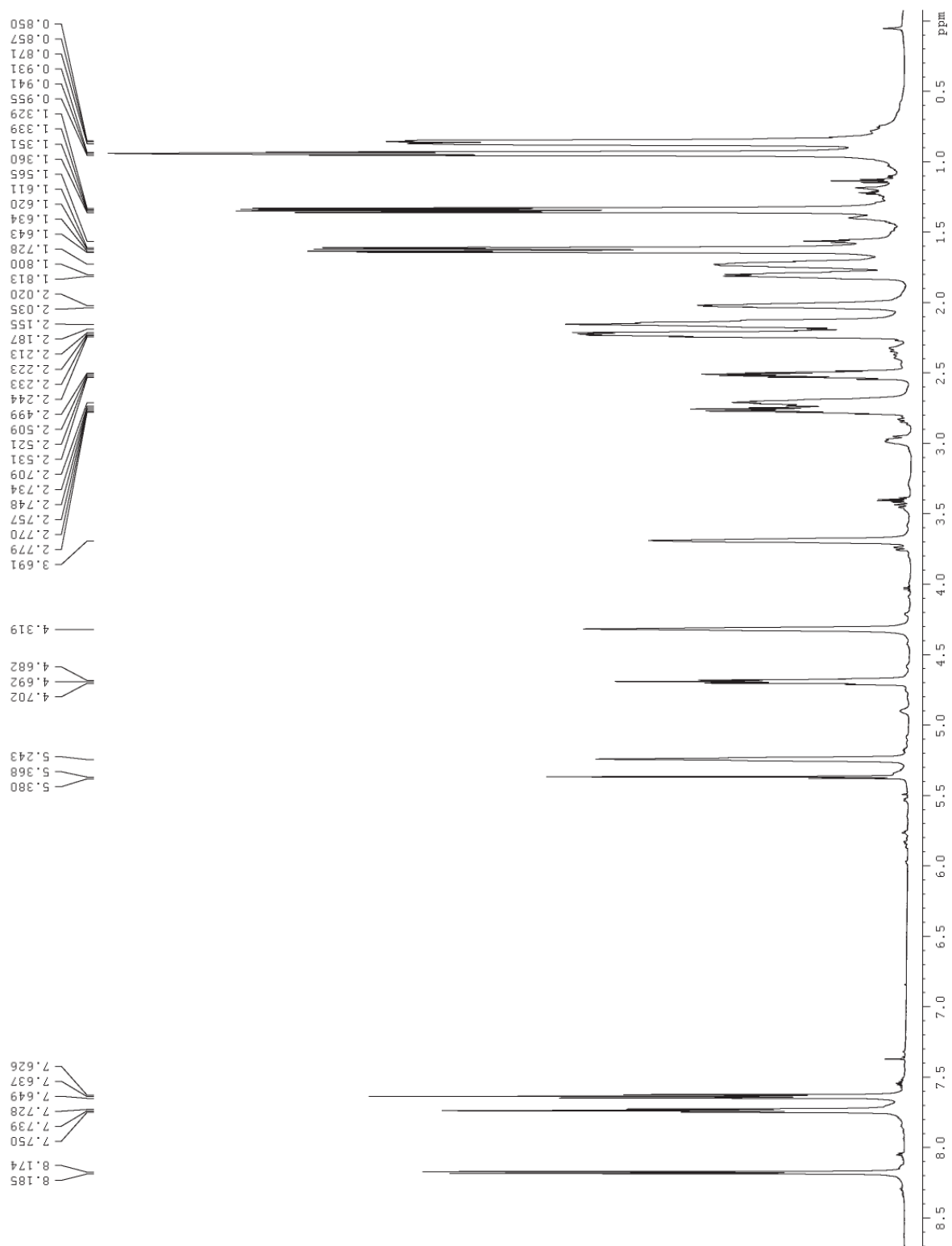


*<sup>31</sup>P-NMR Spectra VT Series*



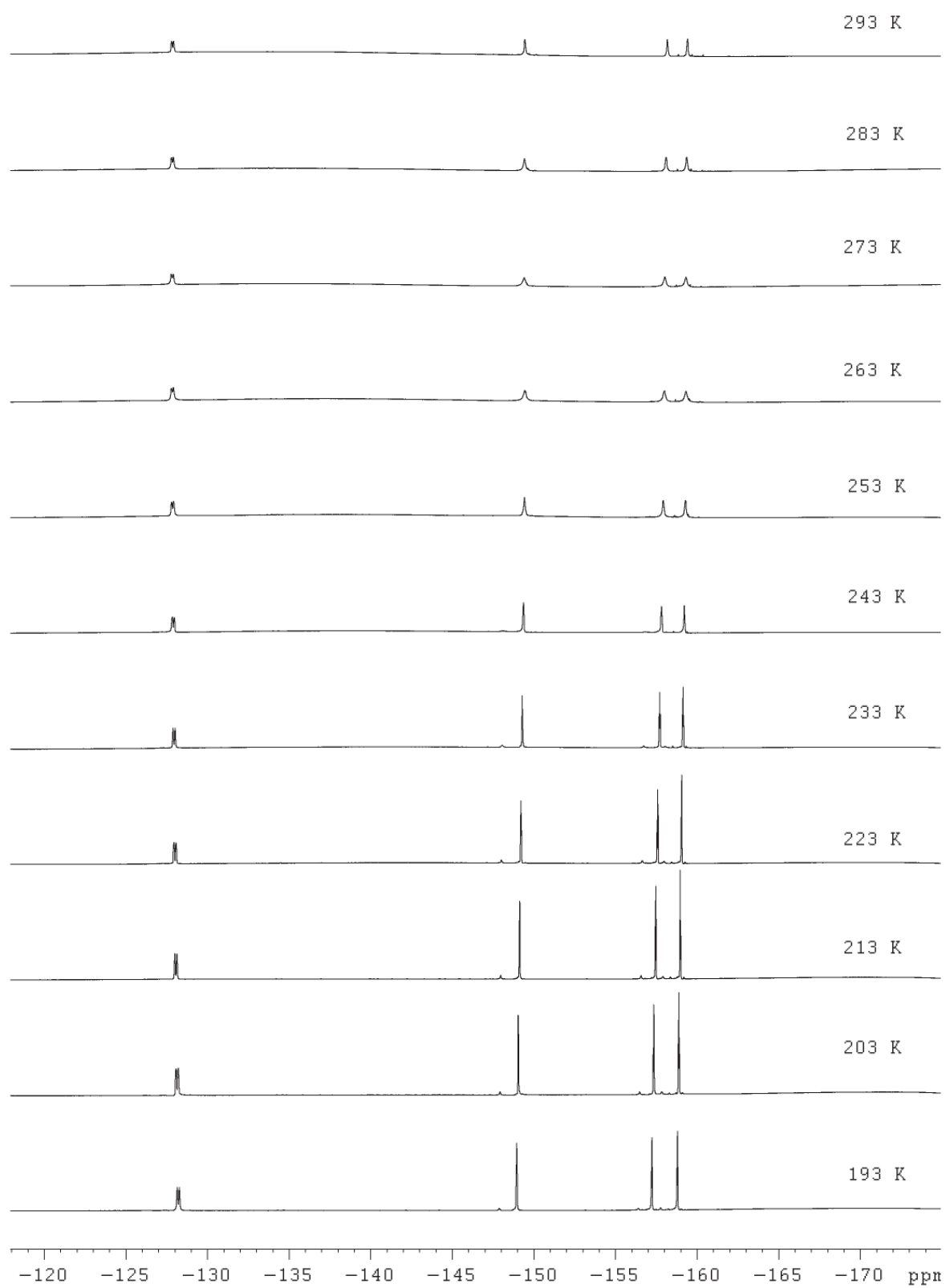
## 7.2.5 Rh-4

<sup>1</sup>H-NMR Spectrum at 203 K

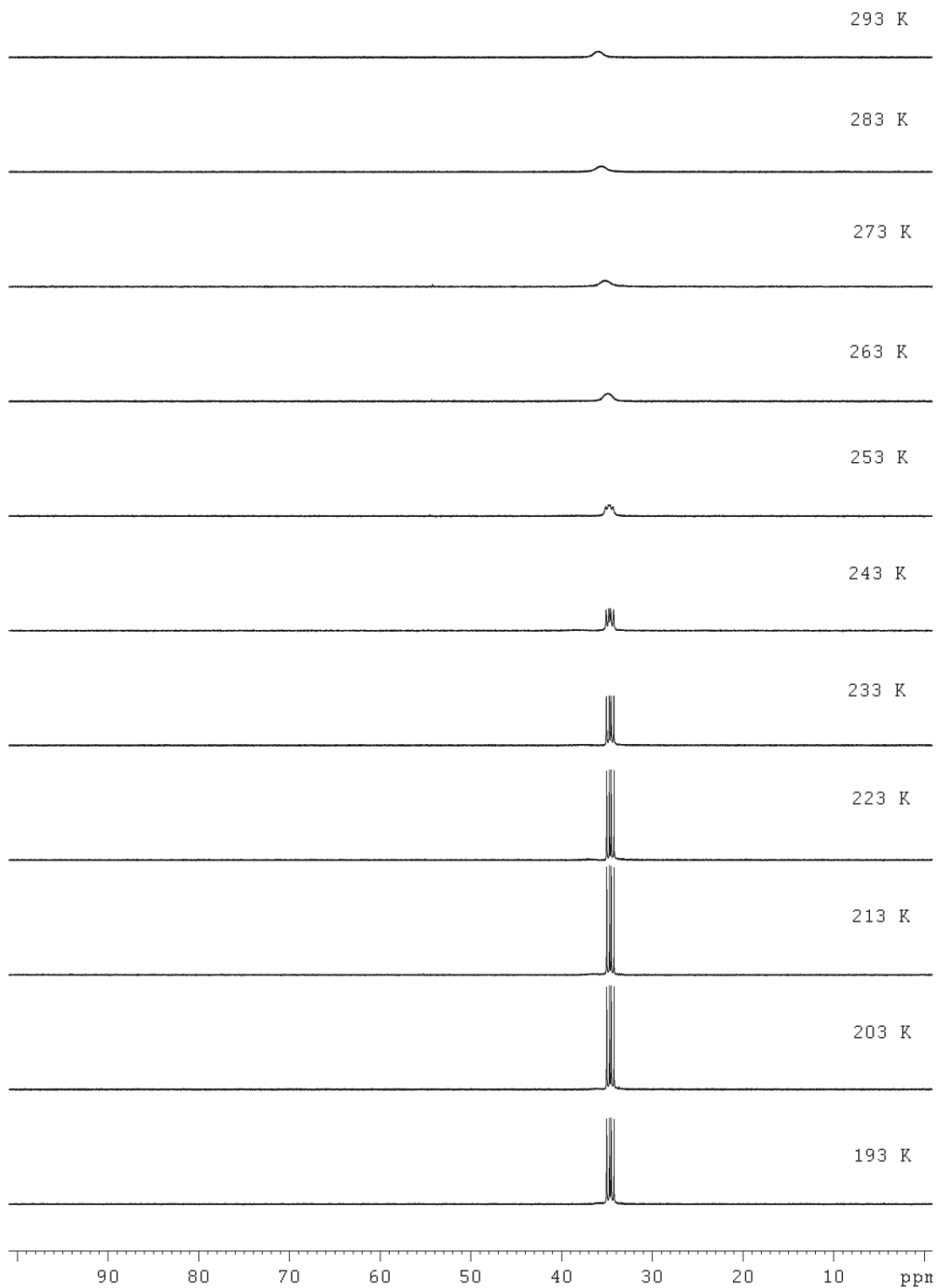




*<sup>19</sup>F-NMR SpectraVT Series*

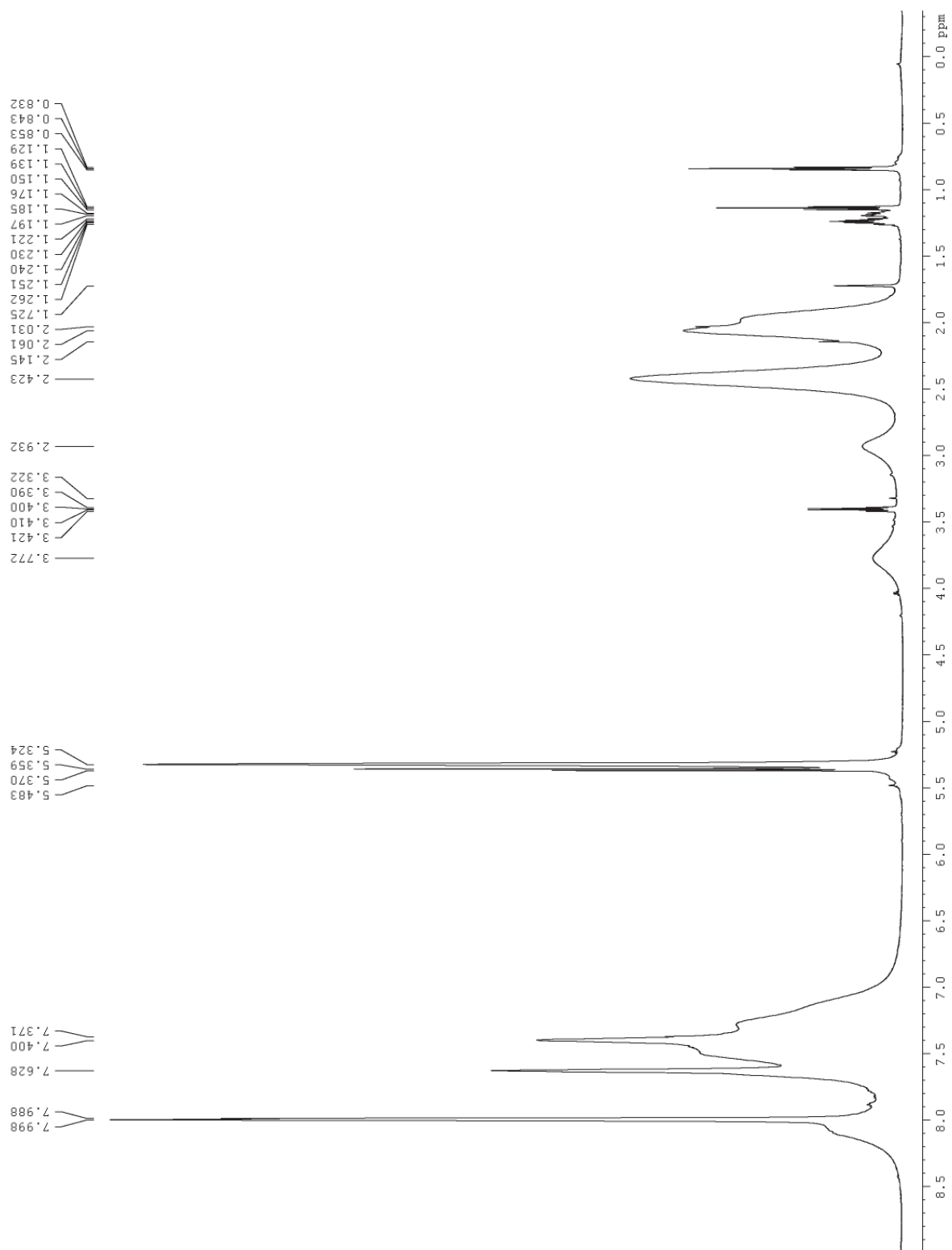


*<sup>31</sup>P-NMR Spectra VT Series*

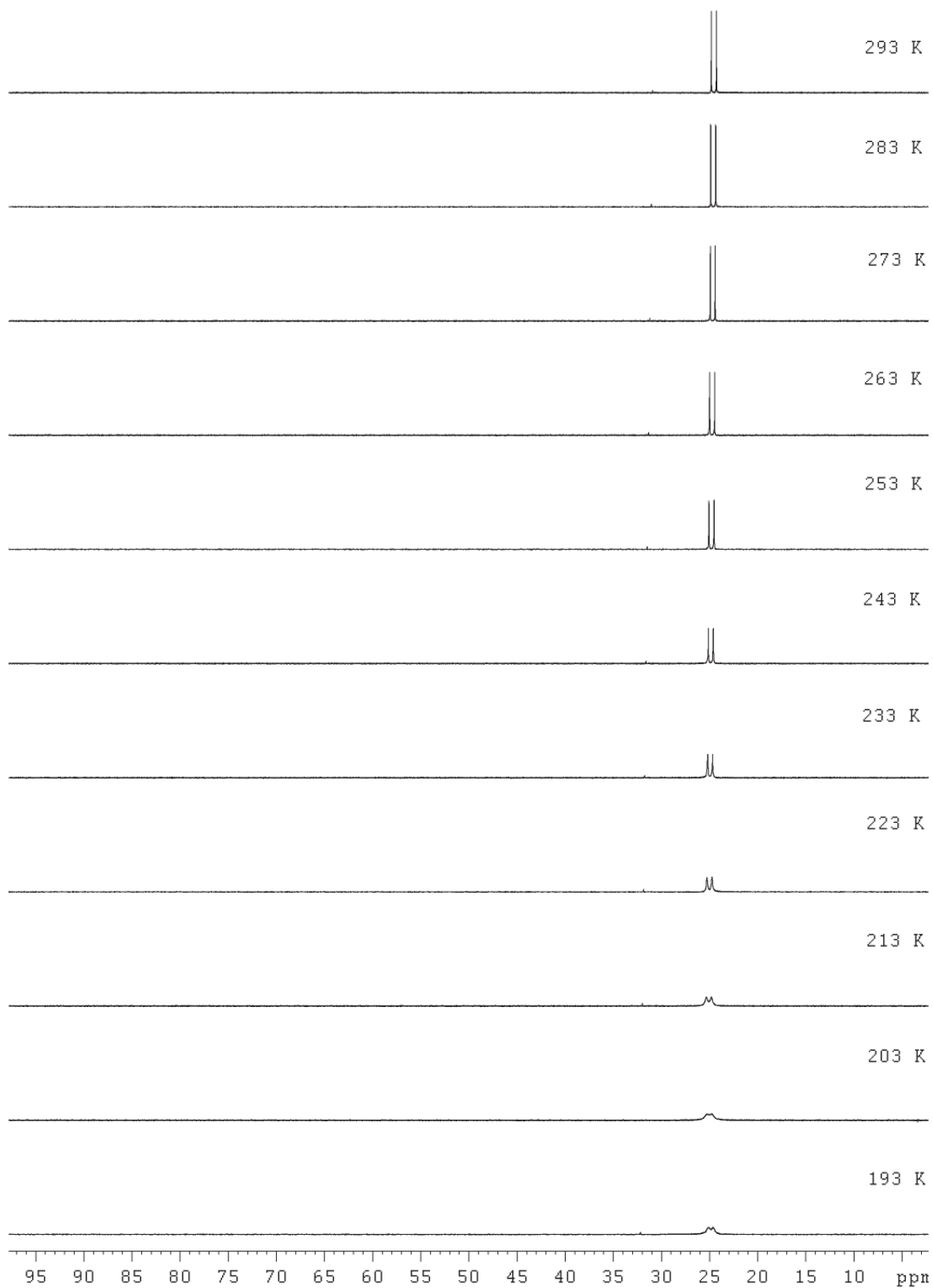


## 7.2.6 Rh-8

<sup>1</sup>H-NMR Spectrum at 203 K

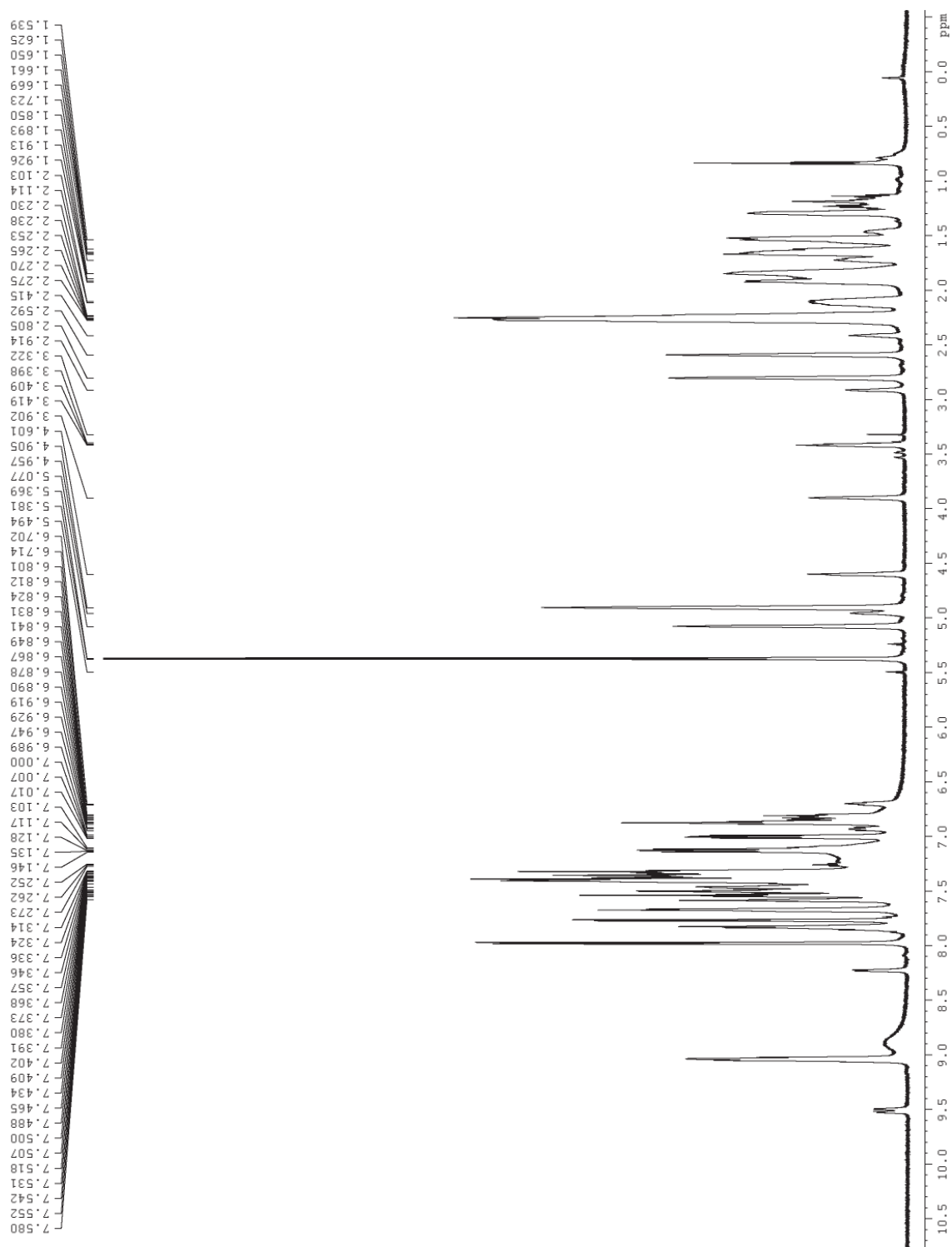


*<sup>31</sup>P-NMR Spectra VT Series*

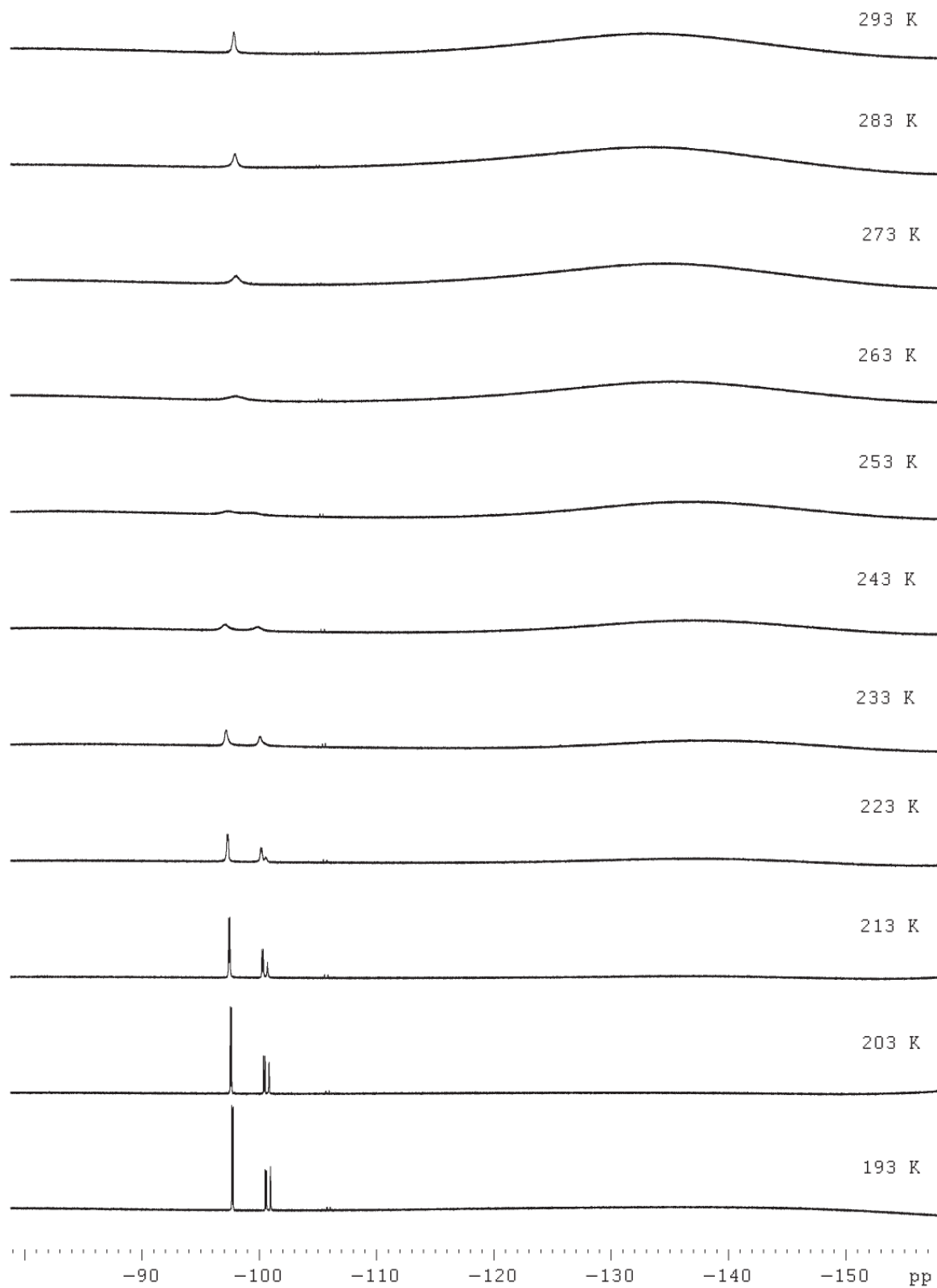


### 7.2.7 Ir-1

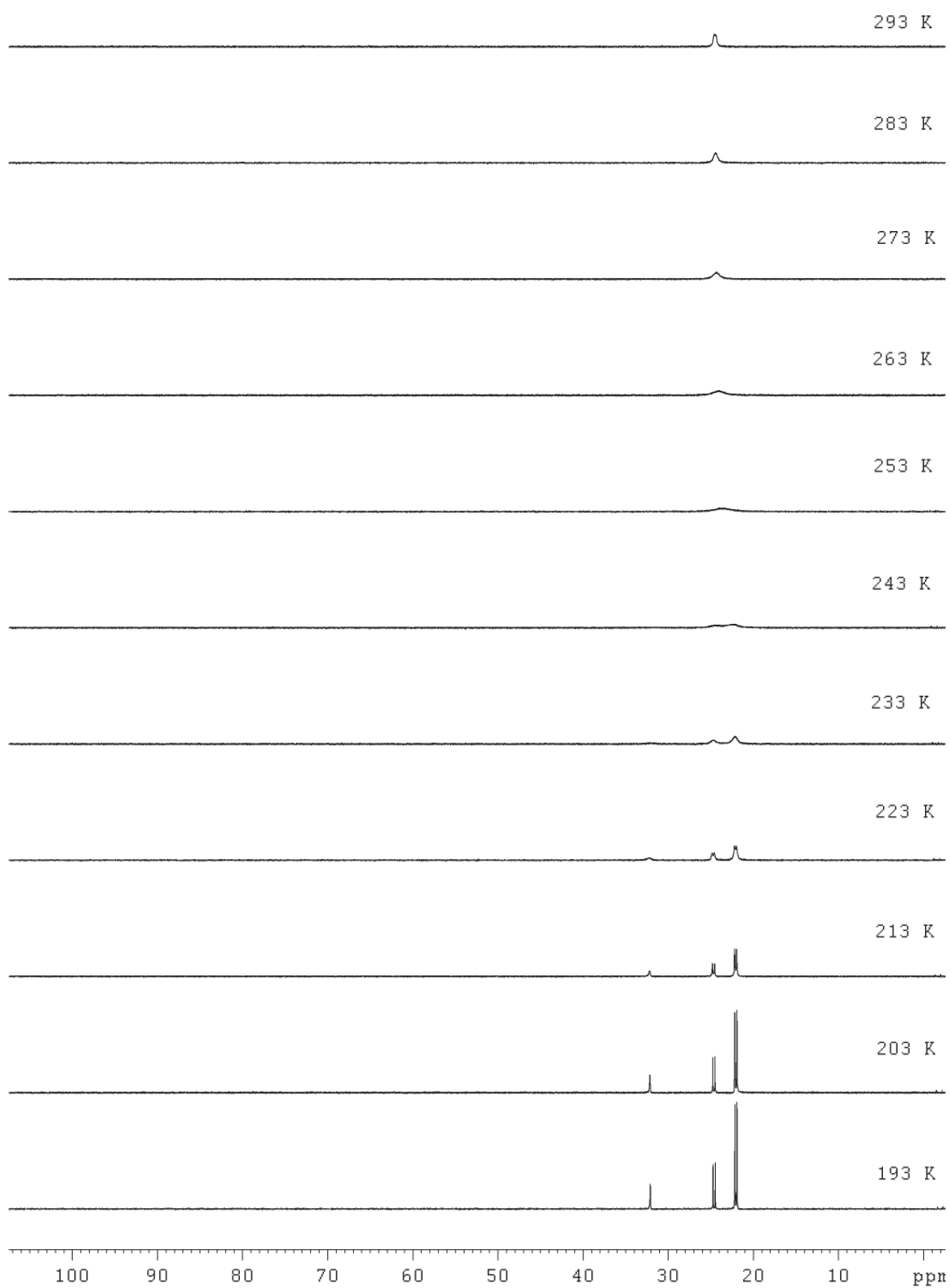
<sup>1</sup>H-NMR Spectrum at 203 K



*<sup>19</sup>F-NMR SpectraVT Series*



*<sup>31</sup>P-NMR Spectra VT Series*



## 7.3 Crystallographic Data

### 7.3.1 Chloro(1,5-cyclooctadiene)(diphenyl(8-fluoronaphthalen-1-yl)phosphine)rhodium(I) (Rh-1)

Empirical Formula	C <sub>30</sub> H <sub>28</sub> ClFPRh	
Formula Weight	576.85 g/mol	
Temperature	100(2) K	
Wavelength	0.71073 Å	
Crystal system, space group	Monoclinic, P2 <sub>1</sub> /n	
Unit cell dimensions	$a = 13.915(3)$ Å $b = 11.326(2)$ Å $c = 15.931(3)$ Å	$\alpha = 90^\circ$ $\beta = 104.780(4)^\circ$ $\gamma = 90^\circ$
Volume	2427.9(8) Å <sup>3</sup>	
Z	4	
$\rho_{\text{calc}}$	1.578 g/cm <sup>3</sup>	
Absorption coefficient	0.905 mm <sup>-1</sup>	
$F(000)$	1176	
Crystal size	0.24 × 0.19 × 0.10 mm	
Data collection	Siemens SMART PLATFORM with CCD Detector Graphite monochromator	
Detector distance	50 mm	
Method	Omega-scans	
Exposure time per frame	$t = 2$ s	
Solution by	Direct methods	
Refinement method	Full-matrix least-squares on $F^2$ , SHELXTL	
$\theta$ range for data collection	1.74 – 28.37°	
Limiting indices	$-18 \leq h \leq 18$ $-15 \leq k \leq 15$ $-21 \leq l \leq 21$	
Reflections collected	24237	
Unique Reflections	6053	
R(int)	0.0653	
Completeness to $\theta = 28.37$	99.8%	
Absorption correction	Empirical	
Max. and min. transmission	0.9174 and 0.8121	
Refinement method	Full-matrix least-squares on $F^2$	
Data	6053	
Restraint	0	
Parameters	307	
Goodness-of-fit on $F^2$	1.091	
Final R indices [ $I > 2\sigma(I)$ ]	R1 = 0.0527	wR2 = 0.0966
R indices (all data)	R1 = 0.0698	wR2 = 0.1023
Largest diff. peak and hole	0.747 and -1.086 e/Å <sup>3</sup>	



	x	y	z	U(eq)
Rh(1)	5483(1)	1632(1)	2191(1)	12(1)
Cl(1)	4428(1)	3298 (1)	2050(1)	22(1)
P(1)	4105(1)	398(1)	2148(1)	12(1)
F(1)	4435(2)	-325(2)	561(1)	18(1)
C(1)	4353(3)	-1211(3)	2249(2)	14(1)
C(2)	4339(3)	-1767(3)	3008(2)	17(1)
C(3)	4561(3)	-2979(3)	3154(3)	19(1)
C(4)	4794(3)	-3644(3)	2523(2)	17(1)
C(5)	4820(3)	-3131(3)	1718(2)	14(1)
C(6)	5067(3)	-3837(3)	1071(2)	18(1)
C(7)	5122(3)	-3352(3)	294(2)	18(1)
C(8)	4915(3)	-2149(3)	132(2)	17(1)
C(9)	4655(3)	-1480(3)	749(2)	16(1)
C(10)	4602(3)	-1904(3)	1572(2)	13(1)
C(11)	3700(3)	707(3)	3135(2)	14(1)
C(12)	2776(3)	363(4)	3230(3)	21(1)
C(13)	2538(3)	535(4)	4019(3)	25(1)
C(14)	3220(3)	1050(4)	4709(3)	24(1)
C(15)	4140(3)	1392(3)	4613(3)	25(1)
C(16)	4381(3)	1227(3)	3830(2)	18(1)
C(17)	2946(3)	475(3)	1275(2)	14(1)
C(18)	2352(3)	-527(4)	1037(3)	21(1)
C(19)	1500(3)	-461(4)	356(3)	27(1)
C(20)	1221(3)	581(4)	-76(3)	24(1)
C(21)	1793(3)	1574(4)	167(3)	25(1)
C(22)	2660(3)	1530(4)	841(3)	21(1)
C(23)	6473(3)	356(3)	2904(2)	16(1)
C(24)	7244(3)	929(3)	3634(2)	19(1)
C(25)	7574(3)	2144(3)	3392(2)	19(1)
C(26)	6742(3)	2799(3)	2766(3)	17(1)
C(27)	6630(3)	2777(3)	1889(2)	18(1)
C(28)	7293(3)	2079(4)	1448(2)	19(1)
C(29)	7387(3)	767(3)	1720(3)	19(1)
C(30)	6508(3)	299(3)	2034(2)	15(1)

### 7.3.2 Chloro(1,5-cyclooctadiene)(diphenyl(5,6,7,8-tetrafluoronaphthalen-1-yl)phosphine)rhodium(I) (Rh-2)

Empirical Formula	C <sub>30</sub> H <sub>25</sub> ClF <sub>4</sub> PRh	
Formula Weight	630.83g/mol	
Temperature	100(2) K	
Wavelength	0.71073 Å	
Crystal system, space group	Monoclinic, P2 <sub>1</sub> /c	
Unit cell dimensions	$a = 11.6216(7)$ Å	$\alpha = 90^\circ$
	$b = 14.2972(9)$ Å	$\beta = 100.768(2)^\circ$
	$c = 15.6137(10)$ Å	$\gamma = 90^\circ$
Volume	2548.6(3) Å <sup>3</sup>	
Z	4	
$\rho_{\text{calc}}$	1.644 g/cm <sup>3</sup>	
Absorption coefficient	0.886 mm <sup>-1</sup>	
$F(000)$	1272	
Crystal size	0.30 × 0.27 × 0.14 mm	
Data collection	Siemens SMART PLATFORM with CCD Detector Graphite monochromator	
Detector distance	50 mm	
Method	Omega-scans	
Exposure time per frame	$t(28) = 1$ s, $t(55) = 3$ s	
Solution by	Direct methods	
Refinement method	Full-matrix least-squares on $F^2$ , SHELXTL	
$\theta$ range for data collection	178 – 38.58°	
Limiting indices	$-20 \leq h \leq 20$	
	$-24 \leq k \leq 25$	
	$-27 \leq l \leq 27$	
Reflections collected	112456	
Unique Reflections	14407	
R(int)	0.0546	
Completeness to $\theta = 38.58$	100.0%	
Absorption correction	Empirical	
Max. and min. transmission	0.8830 and 0.7770	
Refinement method	Full-matrix least-squares on $F^2$	
Data	14407	
Restraint	0	
Parameters	334	
Goodness-of-fit on $F^2$	1.097	
Final R indices [ $I > 2\sigma(I)$ ]	R1 = 0.0364	wR2 = 0.0829
R indices (all data)	R1 = 0.0437	wR2 = 0.0862
Largest diff. peak and hole	1.724 and -0.479 e/Å <sup>3</sup>	

	<b>x</b>	<b>y</b>	<b>z</b>	<b>U(eq)</b>
Rh(1)	2519(1)	5318(1)	2460(1)	13(1)
Cl(1)	3174(1)	4699(1)	1227(1)	21(1)
P(1)	2571(1)	6801(1)	1838(1)	12(1)
F(1)	4567(1)	6646(1)	3215(1)	17(1)
F(2)	6773(1)	6372(1)	3974(1)	25(1)
F(3)	8518(1)	6356(1)	3044(1)	30(1)
F(4)	8023(1)	6653(1)	1307(1)	26(1)
C(1)	3871(1)	6922(1)	1328(1)	13(1)
C(2)	3700(1)	7061(1)	438(1)	18(1)
C(3)	4633(1)	7060(1)	-24(1)	22(1)
C(4)	5758(1)	6917(1)	397(1)	20(1)
C(5)	5988(1)	6781(1)	1314(1)	15(1)
C(6)	7148(1)	6644(1)	1757(1)	18(1)
C(7)	7413(1)	6497(1)	2634(1)	20(1)
C(8)	6511(1)	6500(1)	3112(1)	17(1)
C(9)	5374(1)	6640(1)	2702(1)	14(1)
C(10)	5051(1)	6781(1)	1793(1)	13(1)
C(11)	1316(1)	6981(1)	962(1)	15(1)
C(12)	562(1)	6228(1)	718(1)	17(1)
C(13)	-427(1)	6332(1)	65(1)	20(1)
C(14)	-663(1)	7186(1)	-348(1)	22(1)
C(15)	84(1)	7943(1)	-111(1)	23(1)
C(16)	1063(1)	7847(1)	548(1)	20(1)
C(17)	2577(1)	7873(1)	2483(1)	14(1)
C(18)	1666(1)	8025(1)	2939(1)	18(1)
C(19)	1699(1)	8778(1)	3506(1)	23(1)
C(20)	2637(1)	9394(1)	3625(1)	23(1)
C(21)	3527(1)	9275(1)	3150(1)	21(1)
C(22)	3494(1)	8519(1)	2581(1)	18(1)
C(23)	2224(1)	3884(1)	2898(1)	22(1)
C(24)	3365(1)	4158(1)	3227(1)	21(1)
C(25)	3828(1)	4515(1)	4138(1)	25(1)
C(26)	3005(1)	5220(1)	4458(1)	24(1)
C(27)	2365(1)	5829(1)	3721(1)	17(1)
C(28)	1251(1)	5615(1)	3233(1)	17(1)
C(29)	542(1)	4749(1)	3349(1)	25(1)
C(30)	1264(1)	3845(1)	3434(1)	26(1)

### 7.3.3 Chloro(norbornadiene)(diphenyl(8-fluoronaphthalen-1-yl)phosphine)rhodium(I) (nbd-Rh-1)

Empirical Formula	$C_{30}H_{26}Cl_3FPRh$	
Formula Weight	645.74 g/mol	
Temperature	100(2) K	
Wavelength	0.71073 Å	
Crystal system, space group	Monoclinic, $P2_1/c$	
Unit cell dimensions	$a = 10.2405(6)$ Å	$\alpha = 90^\circ$
	$b = 12.1316(7)$ Å	$\beta = 115.451(2)^\circ$
	$c = 23.5042(12)$ Å	$\gamma = 90^\circ$
Volume	2636.6 (3) Å <sup>3</sup>	
Z	4	
$\rho_{\text{calc}}$	1.627 g/cm <sup>3</sup>	
Absorption coefficient	1.039 mm <sup>-1</sup>	
$F(000)$	1304	
Crystal size	0.34 × 0.21 × 0.19 mm	
Data collection	Siemens SMART PLATFORM with CCD Detector Graphite monochromator	
Detector distance	50 mm	
Method	Omega-scans	
Exposure time per frame	$\tau = 2$ s	
Solution by	Direct methods	
Refinement method	Full-matrix least-squares on $F^2$ , SHELXTL	
$\theta$ range for data collection	1.92 – 28.33°	
Limiting indices	$-13 \leq h \leq 13$	
	$-16 \leq k \leq 16$	
	$-31 \leq l \leq 31$	
Reflections collected	26836	
Unique Reflections	6557	
R(int)	0.0516	
Completeness to $\theta = 28.33$	99.7%	
Absorption correction	None	
Refinement method	Full-matrix least-squares on $F^2$	
Data	6557	
Restraint	0	
Parameters	325	
Goodness-of-fit on $F^2$	0.947	
Final R indices [ $I > 2\sigma(I)$ ]	R1 = 0.0317	wR2 = 0.0655
R indices (all data)	R1 = 0.0416	wR2 = 0.0679
Largest diff. peak and hole	0.882 and -0.633 e/Å <sup>3</sup>	

	x	y	z	U(eq)
Rh(1)	6113(1)	7615(1)	1039(1)	14(1)
Cl(1)	6977(1)	7419(1)	2141(1)	23(1)
P(1)	3732(1)	7280(1)	853(1)	13(1)
F(1)	3932(1)	5496(1)	121(1)	18(1)
C(1)	2339(2)	7513(2)	39(1)	13(1)
C(2)	1445(2)	8414(2)	-77(1)	16(1)
C(3)	415(2)	8692(2)	-688(1)	18(1)
C(4)	285(2)	8071(2)	-1190(1)	17(1)
C(5)	1152(2)	7125(2)	-1109(1)	15(1)
C(6)	972(2)	6465(2)	-1632(1)	18(1)
C(7)	1783(2)	5543(2)	-1561(1)	19(1)
C(8)	2797(2)	5226(2)	-960(1)	18(1)
C(9)	2958(2)	5845(2)	-456(1)	15(1)
C(10)	2193(2)	6829(2)	-487(1)	13(1)
C(11)	3208(2)	8262(2)	1308(1)	14(1)
C(12)	3688(2)	9348(2)	1352(1)	18(1)
C(13)	3318(2)	10126(2)	1687(1)	20(1)
C(14)	2474(2)	9824(2)	1994(1)	20(1)
C(15)	1996(2)	8752(2)	1953(1)	21(1)
C(16)	2349(2)	7968(2)	1609(1)	19(1)
C(17)	3236(2)	5957(2)	1075(1)	14(1)
C(18)	4279(2)	5310(2)	1528(1)	18(1)
C(19)	3909(3)	4304(2)	1702(1)	24(1)
C(20)	2493(3)	3941(2)	1419(1)	27(1)
C(21)	1447(3)	4582(2)	962(1)	26(1)
C(22)	1811(2)	5583(2)	789(1)	20(1)
C(23)	5718(3)	8496(2)	214(1)	22(1)
C(24)	6026(3)	7406(2)	131(1)	20(1)
C(25)	7670(3)	7363(2)	323(1)	23(1)
C(26)	8262(2)	7555(2)	1038(1)	20(1)
C(27)	7953(2)	8632(2)	1114(1)	22(1)
C(28)	7161(3)	9123(2)	454(1)	25(1)
C(29)	7913(3)	8514(2)	101(1)	28(1)
Cl(5)	6139(1)	1460(1)	1423(1)	36(1)
Cl(6)	8830(1)	928(1)	2506(1)	33(1)
C(30)	6938(3)	753(2)	2147(1)	31(1)

### 7.3.4 Chloro(cyclooctadiene)(diisopropyl(5,6,7,8-tetrafluoronaphthalen-1-yl)phosphine)rhodium(I) (Rh-4)

Empirical Formula	C <sub>30</sub> H <sub>29</sub> ClF <sub>4</sub> PRh	
Formula Weight	562.80 g/mol	
Temperature	100(2) K	
Wavelength	0.71073 Å	
Crystal system, space group	Monoclinic, P2 <sub>1</sub> /c	
Unit cell dimensions	$a = 10.3287(5)$ Å	$\alpha = 90^\circ$
	$b = 12.1316(6)$ Å	$\beta = 103.2790(10)^\circ$
	$c = 18.2038(9)$ Å	$\gamma = 90^\circ$
Volume	2253.08(19) Å <sup>3</sup>	
Z	4	
$\rho_{\text{calc}}$	1.659 g/cm <sup>3</sup>	
Absorption coefficient	0.990 mm <sup>-1</sup>	
$F(000)$	1144	
Crystal size	0.50 × 0.48 × 0.26 mm	
Data collection	Siemens SMART PLATFORM with CCD Detector Graphite monochromator	
Detector distance	50 mm	
Method	Omega-scans	
Exposure time per frame	$\tau = 0.5$ s	
Solution by	Direct methods	
Refinement method	Full-matrix least-squares on $F^2$ , SHELXTL	
$\theta$ range for data collection	2.01 – 28.36°	
Limiting indices	-13 ≤ h ≤ 13	
	-16 ≤ k ≤ 16	
	-24 ≤ l ≤ 24	
Reflections collected	22974	
Unique Reflections	5638	
R(int)	0.0309	
Completeness to $\theta = 28.33$	99.9%	
Absorption correction	Empirical	
Max. and min. transmission	0.7856 and 0.6368	
Refinement method	Full-matrix least-squares on $F^2$	
Data	5638	
Restraint	0	
Parameters	284	
Goodness-of-fit on $F^2$	1.051	
Final R indices [ $I > 2\sigma(I)$ ]	R1 = 0.0265	wR2 = 0.0638
R indices (all data)	R1 = 0.0300	wR2 = 0.0654
Largest diff. peak and hole	0.796 and -0.428 e/Å <sup>3</sup>	

	x	y	z	U(eq)
Rh(1)	3521(1)	8288(1)	8258(1)	12(1)
Cl(1)	2272(1)	6999(1)	7417(1)	19(1)
P(1)	1953(1)	8162(1)	8995(1)	11(1)
F(1)	3951(1)	6421(1)	9167(1)	18(1)
F(2)	4913(1)	4460(1)	9204(1)	22(1)
F(3)	3350(1)	2674(1)	9157(1)	29(1)
F(4)	718(1)	2925(1)	9085(1)	29(1)
C(1)	1076(2)	6849(2)	9018(1)	14(1)
C(2)	-265(2)	6877(2)	9005(1)	17(1)
C(3)	-1042(2)	5938(2)	9003(1)	18(1)
C(4)	-479(2)	4936(2)	9018(1)	19(1)
C(5)	902(2)	4845(2)	9054(1)	16(1)
C(6)	1488(2)	3806(2)	9087(1)	19(1)
C(7)	2805(2)	3668(2)	9125(1)	21(1)
C(8)	3601(2)	4586(2)	9138(1)	17(1)
C(9)	3073(2)	5600(2)	9111(1)	14(1)
C(10)	1701(2)	5795(2)	9055(1)	14(1)
C(11)	597(2)	9140(2)	8597(1)	16(1)
C(12)	-91(2)	8865(2)	7784(1)	22(1)
C(13)	1136(2)	10304(2)	8631(1)	21(1)
C(14)	2454(2)	8502(2)	10022(1)	14(1)
C(15)	1313(2)	8905(2)	10357(1)	19(1)
C(16)	3137(2)	7536(2)	10486(1)	17(1)
C(17)	5082(2)	8282(2)	7608(1)	16(1)
C(18)	4155(2)	9075(2)	7331(1)	18(1)
C(19)	4322(2)	10276(2)	7495(1)	21(1)
C(20)	4878(2)	10520(2)	8334(1)	19(1)
C(21)	4436(2)	9693(2)	8849(1)	15(1)
C(22)	5142(2)	8752(2)	9131(1)	16(1)
C(23)	6431(2)	8376(2)	8953(1)	23(1)
C(24)	6447(2)	8495(2)	8115(1)	22(1)

## 7.4 Data for the Simulation

### 7.4.1 Program Code

```
/* AB_NMEx.cc *****-c++-*/
**
**          Mutual Exchange Example Program
**
** This program generates a series of 1D NMR spectrum for a system that
** is involved in mutual exchange. It is built to read an external file
** for the input system. It then loops over a series of exchange rates.
**
** The reader may readily make this program general with some simple
** modifications. Here are some aspects that make it not general:
**
** 1.) It is homomolear, detection & pulse is system wide.
** 3.) The spectral range is specific from [0, 75] Hz.
** 4.) The output is set for gnuplot to screen & FrameMaker.
** 5.) An additional, specific, linewidth was added to all transitions.
** 6.) No relaxation has been included from the spin system.
**
** Although these are trivial limitations, fixing them would add a few
** more lines and further complicate what is intended to be a tutorial
** example.
**
** Author:      Scott A. Smith
** Date:        Can't Recall
** Last Update: November 6, 2001
** GAMMA Version: 4.0.6
** Copyright:   Scott A. Smith
**
** This program may be freely modified in any manner for personal use.
** However it given to others it must be in its present form and with
** the associated ASCII input file AB.pset. This code originated
** from the GAMMA WWW site tour page
**
**          http://gamma.magnet.fsu.edu/info/tour/exchange/
**
** Assuming the user has compiled to program to produce either a.exe
** or a.out, as well as has Gnuplot properly installed, a spectrum
** should appear on screen with the command
**
**          ./a AB_NMEx.pset
**
*****/

# include <gamma.h>

int main(int argc, char* argv[], int argn)
{
    int qn = 1;
    double p_low = 0.0;           // Lower plot limit in Hz
    double p_high = 75.0;        // Upper plot limit in Hz
    double f_low = 0.0;          // Lower plot limit in Hz
    double f_high = 75.0;        // Upper plot limit in Hz
    double lb=1.0;
    multi_sys sys;               // An empty spin system
    sys.ask_read(argc, argv, qn++); // Read in the system
    std::cout << sys;             // Look at the system
    if(sys.heteronuclear())      // Insure this is homonuc.
    {
        std::cout << "\n\n\tSystem Must Be Homnuclear!\n\n";
        std::cout << "\n\n\tSorry...\n\n";
        exit(-1);
    }
    query_parameter(argc, argv, qn++, "\n\tSpectrum lower Freq (ppm)? ", p_low); // system was input
    query_parameter(argc, argv, qn++, "\n\tSpectrum upper Freq (ppm)? ", p_high); // system was input
    query_parameter(argc, argv, qn++, "\n\tLine Broadening (Hz)? ", lb); // system was input
    f_low = p_low*sys.Omega("1H");
    f_high = p_high*sys.Omega("1H");

    gen_op H = Ho(sys);           // Isotropic Hamiltonian
    gen_op D = Fm(sys, "1H");     // Detect F-, all nuclei
    gen_op sigma0 = sigma_eq(sys); // System at equilibrium
    gen_op sigma = Iypuls(sys, sigma0, 90.0); // Apply 90y pulse ideal
    H.set_EBR();                 // Put H in its eigenbase
    std::cout << "\nHoi 1\n";     // Look at the system
    // D.Op_base(H);             // Put D in H eigenbase
    std::cout << "\nHoi 2\n";     // Look at the system
    // sigma.Op_base(H);         // Put sigma in H e.b.
    std::cout << "\nHoi 3\n";     // Look at the system
    // super_op L0 = complexi*Hsuper(H); // Isotropic Hamiltonian
    super_op L0 = -complexi*Lo(sys); // Isotropic Hamiltonian
    std::cout << "\nHoi 4\n";     // Look at the system
    super_op L;                  // Full Liouvilian
    std::cout << "\nHoi 5\n";     // Look at the system

    int nK = 1;                  // This many rates
    // double Ks[10] = {0, 5, 10, 60, 100, 120, // Here they are in 1/sec
    //                  140, 400, 650, 1950};
    // double Ks[10] = {0, 10, 40, 80, 100, 120, // Here they are in 1/sec
    //                  140, 200, 400, 650};
    row_vector data, vxs[1];     // Arrays for the output
    matrix dmx(1, 4096);         // Data matrix

    int npts = 4096;             // For the block size
    std::string fname = "AB.asc"; // Spectrum data file
    TTable1D TT;                 // A transitions table

    for(int i=0; i<nK; i++)      // Loop over the rates
    {
```



```

// sys.Kex(Ks[i], 0); // Set the rate
L = L0 + Xnm(sys); // Add in exchange
acquire1D ACQ(D,L,1.e-3); // Set up acquisition
TT = ACQ.table(sigma); // Transitions table (no lb)
TT.broaden(lb, 1); // Add 1/2 Hz line broadening
data = TT.F(npts,f_low,f_high); // Frequency acquisition
vx[s[i]] = data;
dmx.put_block(i, 0, data);
}
GP_stack(fname,dmx,0,0,650,p_low,p_high); // Write in gnuplot format (ASCII)
// GP_stackplot("AB.gnu", fname); // Plot to screen with gnuplot
FM_lDm("AB.mif", nK, vx[s]); // Output to Adobe FrameMaker
std::cout << "\n\n"; // Keep the screen nice
}

```

## 7.4.2 Example Input File

This file contains parameters which define a multiple spin system in the GAMMA magnetic resonance simulation platform. In particular, it is used as input into the program AB.cc which simulates a two spins in different systems in non-mutual exchange. Although I set an exchange process up in the system, the program will loop over a series of exchange rates.

```

MSysName (2) : AB - Name of the Spin System
NComp (0) : 3 - Number of components in multi system
Popul(0) (1) : 1.0 - Population of component 0
Popul(1) (1) : 8.86 - Population of component 1
Popul(2) (1) : 2.31 - Population of component 2
Exch(0) (2) : (0<=>1) - Non-mutual exchange scheme
Exch(1) (2) : (1<=>2) - Non-mutual exchange scheme
Exch(2) (2) : (0<=>2) - Non-mutual exchange scheme
Smap(0,0) (2) : (0)0(1)0 - Cmp 0 0th spin <-> Cmp 1 0th spin
Smap(0,1) (2) : (0)1(1)1 - Cmp 0 1st spin <-> Cmp 1 1st spin
Smap(0,2) (2) : (0)2(1)2 - Cmp 0 2nd spin <-> Cmp 1 2nd spin
Smap(1,0) (2) : (1)0(2)0 - Cmp 1 0th spin <-> Cmp 2 0th spin
Smap(1,1) (2) : (1)1(2)1 - Cmp 1 1st spin <-> Cmp 2 1st spin
Smap(1,2) (2) : (1)2(2)2 - Cmp 1 2nd spin <-> Cmp 2 2nd spin
Smap(2,0) (2) : (0)0(2)0 - Cmp 0 0th spin <-> Cmp 2 0th spin
Smap(2,1) (2) : (0)1(2)1 - Cmp 0 1st spin <-> Cmp 2 1st spin
Smap(2,2) (2) : (0)2(2)2 - Cmp 0 2nd spin <-> Cmp 2 2nd spin
Kex_nm(0) (1) : 3000 - Exchange rate (1/sec)
Kex_nm(1) (1) : 1500 - Exchange rate (1/sec)
Kex_nm(2) (1) : 3200 - Exchange rate (1/sec)

[0]SysName (2) : A - Name of the Spin System
[0]NSpins (0) : 3 - Number of Spins in the System
[0]Iso(0) (2) : 1H - Spin Isotope Type A
[0]Iso(1) (2) : 1H - Spin Isotope Type A
[0]Iso(2) (2) : 1H - Spin Isotope Type A
[0]Omega (1) : 283.4 - Spect. Freq. in MHz (1H based)
[0]PPM(0) (1) : 42.24 - Chemical Shift (Hz)
[0]PPM(1) (1) : 1000.0 - Chemical Shift (Hz)
[0]PPM(2) (1) : 1000.0 - Chemical Shift (Hz)
[0]J(0,1) (1) : 0.0 - Coupling Constant
[0]J(0,2) (1) : 147.4 - Coupling Constant

[1]SysName (2) : B - Name of the Spin System
[1]NSpins (0) : 3 - Number of Spins in the System
[1]Iso(0) (2) : 1H - Spin Isotope Type B
[1]Iso(1) (2) : 1H - Spin Isotope Type B
[1]Iso(2) (2) : 1H - Spin Isotope Type B
[1]Omega (1) : 283.4 - Spect. Freq. in MHz (1H based)
[1]PPM(0) (1) : 33.23 - Chemical Shift (Hz)
[1]PPM(1) (1) : 1200.0 - Chemical Shift (Hz)
[1]PPM(2) (1) : 1200.0 - Chemical Shift (Hz)
[1]J(0,1) (1) : 86.5 - Coupling Constant
[1]J(0,2) (1) : 148.7 - Coupling Constant

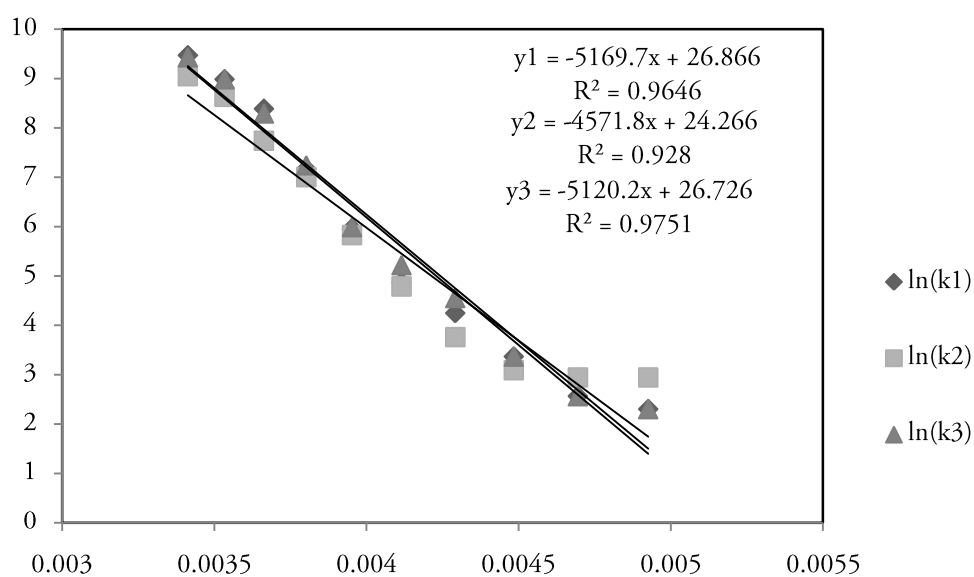
[2]SysName (2) : C - Name of the Spin System
[2]NSpins (0) : 3 - Number of Spins in the System
[2]Iso(0) (2) : 1H - Spin Isotope Type C
[2]Iso(1) (2) : 1H - Spin Isotope Type C
[2]Iso(2) (2) : 1H - Spin Isotope Type C

```

[2]Omega (1) : 283.4 - Spect. Freq. in MHz (1H based)  
 [2]PPM(0) (1) : 30.76 - Chemical Shift (Hz)  
 [2]PPM(1) (1) : 1400.0 - Chemical Shift (Hz)  
 [2]PPM(2) (1) : 1400.0 - Chemical Shift (Hz)  
 [2]J(0,1) (1) : 70.9 - Coupling Constant  
 [2]J(0,2) (1) : 152.6 - Coupling Constant

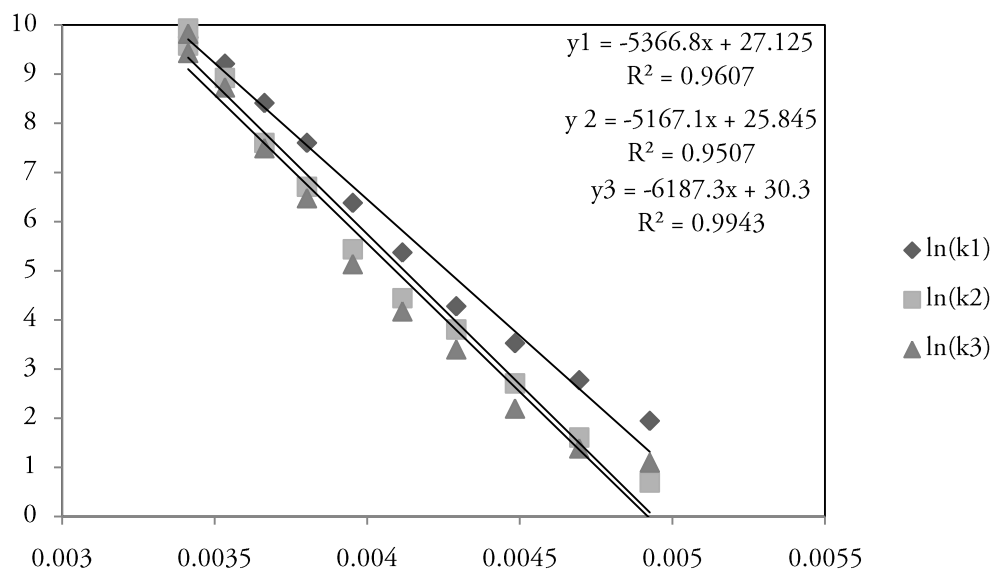
### 7.4.3 Results for Rh-1

T	k <sub>1</sub>	k <sub>2</sub>	k <sub>3</sub>
203	10	19	10
213	13	19	13
223	29	22	29
233	70	43	95
243	130	120	185
253	390	340	400
263	1300	1100	1400
273	4400	2300	4000
283	8000	5600	8000
293	13000	8500	12500



#### 7.4.4 Results for Rh-2

T	k <sub>1</sub>	k <sub>2</sub>	k <sub>3</sub>
193	7	2	3
203	16	5	4
213	34	15	9
223	72	45	30
233	215	85	65
243	590	230	170
253	2000	820	650
263	4500	2000	1800
273	10000	7500	6200
283	17000	14500	12500
293	25000	20500	18500



#### 7.4.5 Results for Ir-1

T	k <sub>1</sub>	k <sub>2</sub>	k <sub>3</sub>
193	6	4	1
203	7	6	3
213	12	10	14
223	35	17	42
233	85	45	100
243	220	150	310
253	700	520	800
263	3000	1500	3200
273	4200	2100	4100
283	6200	2800	6800
293	12500	9500	14000

